Evaluating Surface Concentrations of NO_2 and O_3 in Urban and Rural Regions by Combining Chemistry Transport Modelling with Surface Measurements

by

Zena Rebello

A thesis
presented to the University of Waterloo
in fulfillment of the
thesis requirement for the degree of
Master of Science
in
Earth Sciences

Waterloo, Ontario, Canada, 2010

AUTHOR'S DECLARATION

I hereby declare that I am the sole author of this thesis. This is a true copy of the thesis, including any required final revisions, as accepted by my examiners.

I understand that my thesis may be made electronically available to the public.

Abstract

A base case modelling investigation was conducted to explore the chemical and physical behaviour of ground-level ozone (O_3) and its precursor nitrogen dioxide (NO_2) in Ontario using the U.S. Environmental Protection Agency (EPA) Community Multiscale Air Quality (CMAQ) model. Two related studies were completed to evaluate the performance of CMAQ in reproducing the behaviour of these species in both rural and urban environments by comparing to surface measurements collected by the Ontario Ministry of the Environment (MOE) network of air quality stations. The first study was a winter examination and the second study was conducted for a period during the summer of the same year. The municipality of North Bay was used to represent a rural setting given its smaller population relative to the city of Ottawa which was the base of the urban site.

Statistical and graphical analyses were used to validate the model output. CMAQ was found to replicate the spatial variation of O_3 and NO_2 over the domain in both the winter and summer, but showed some difficulty in simulating the temporal allocation of the species. Validation statistics for North Bay and Ottawa showed overall O_3 mean biases (MB) of 3.35 ppb and 2.25 ppb, respectively, and overall NO_2 MB of -8.75 ppb and -4.37 ppb, respectively for the winter. Summer statistics generated O_3 MB of 4.66 ppb (North Bay) and 10.05 ppb (Ottawa) while both MB for NO_2 were between -2.20 ppb to -2.55 ppb. Graphical analysis showed that the model was not able to reproduce the lower levels of O_3, especially at night, or the higher levels of NO_2 during the day at the North Bay site for either season. This was expected since the comparisons were made between point measurements and 36 km grid-averaged model results. The presence of high amounts of NO_2 emissions local to the monitoring sites compared to the levels represented in the emissions inventory may also be a contributing factor. The simulations for Ottawa demonstrated better agreement between model results and measurements as CMAQ provided a more accurate reproduction of both

the higher and lower mixing ratios of O_3 and NO_2 during the winter and summer seasons. Results indicate that CMAQ is able to simulate urban environments better than rural ones.

Acknowledgements

My years here at Waterloo have been informative and interesting. The friendships and professional relationships I have developed with colleagues, group mates and professors have helped shape me as a person and as a scientist. As such, there are many people whom I'd like to thank for their support throughout my studies here. Firstly, I would like to thank my supervisor, Dr. James Sloan, for providing me with the opportunity to develop my knowledge in air quality modelling, as well as for scientific and financial support throughout the duration of this thesis. Air quality modelling was a new field for me when I started at Waterloo, and Dr. Sloan showed much patience as I progressed along the learning curve. His encouragement was indispensable as this thesis could not have been completed without it.

I would also like to express my sincerest gratitude to my committee members, Dr. Hind Al-Abadleh, Dr. John Lin and Dr. Walter Illman, who provided me with thoughtful guidance and reassurance throughout my research. I am very appreciative of the input they provided me with for the final copy of my thesis.

Special thanks is extended to Dr. Sunny Wong and Dr. Andrei Chtcherbakov at the Ministry of the Environment who, over the past year, took time out of their very busy schedules to help me work through generating spatial surrogates and running my emissions model. Despite my persistent questions and emails over the past many months, they continued to offer their assistance and expertise on the issues. When I ended up not using the surrogates or emissions model they provided me with all of the meteorology and emissions I needed to complete my thesis.

I would like to thank Sue Fisher and all those in the Department of Earth Sciences who have helped me with the administrative aspect of my graduate studies from my initial admissions application to my thesis submission. I am also grateful to everyone in Dr. Sloan's modelling

group - past and present - for their invaluable help with understanding and operating the air quality and emissions models. I am particularly grateful to Dr. Zhuanshi He who never hesitated to provide me with assistance whenever I needed it even on the weekends and late at night. I deeply value the friendships that have been formed with the graduate students whom I've worked with over these past few years. Whether it was a casual greeting in the morning, a 'what's up' email, or going out for sushi on the weekends, these interactions all enriched my graduate experience.

Most importantly, I would like to thank my family who have supported me throughout my Master's degree and did whatever they could to make my time in Waterloo easier. Thanks to my mum, dad and siblings who would bring me groceries and cooked food whenever I was under a lot of stress so that I would not have to worry about anything and could focus all my time on my thesis. They would also pick me up and drop me back to Waterloo whenever I wanted to come home for the weekend, which saved me a lot of time and hassle. My aunts Winnie and Letty who would accompany my mum whenever she came to Waterloo, and my aunt Collette who would send shrimps and homemade cake for me to snack on.

Lastly, I want to say thank you to my boyfriend Phil for being so patient and understanding over these last few months. Though I have had to put all my focus into my thesis lately, Phil's support and love have been exactly what I needed to get through my degree.

Dedication

I dedicate this thesis to my Gizmo whose big eyes and white paw put a smile on my face every morning!

Table of Contents

List of Figures

List of Tables

Chapter 1

Introduction

1.1 Objectives and Motivation

Air pollution in Ontario is a major concern due to its harmful effects on public health and ecosystems. In 2005, the Ontario Medical Association attributed 5 800 premature deaths in the province to poor air quality, as well as over 16 000 hospital admissions and 60 000 emergency room visits in 2005 (Ontario Medical Association, 2007). Though these figures remain a topic of debate, they do point to a growing threat the province faces. The government of Ontario currently implements a variety of programs and regulations which aim to educate the public and reduce the economic and health impacts of air pollution on society. For example, Ontario's Clean Air Action Plan sets targets for pollution reductions, while the Air Quality Index (AQI) reports the levels of several pollutants such as ground-level ozone (O_3) and nitrogen dioxide (NO_2) which are both major contributors to photochemical smog. To create, implement and monitor such programs air quality models (AQMs) are relied upon to provide current and future predictions of the chemical and physical behaviours of the pollutants of interest and related species.

The objective of this study was to assess the performance of the Models-3/Community Multiscale Air Quality (CMAQ) Model, and its ability to simulate accurate summer and winter levels of NO_2 and O_3 in 2005 over select municipalities. This year was chosen as the base case modelling period because it was a particularly bad year for air quality in Ontario, as the number of smog advisories issued by the province was the highest to date since 1995. Fifteen advisories were issued in 2005 compared to thirteen in 2007, and two in the first half 2010. These fifteen advisories covered a period of fifty-three days in total, the most since 1995, and the majority were issued from June to August (Ontario Ministry of the Environment, 2010) which are the prime ozone producing months in Canada and the United States (H. Wang et al., 2009).

This study provides direction for future air quality simulations by imparting a better understanding of the distribution and concentration of smog-producing species in Ontario. This was achieved by comparing the model output against surface measurements taken from the Ministry of the Environment's (MOE) network of AQI measuring stations located within the cities of Ottawa and North Bay. The purpose of selecting these two municipalities was to evaluate the performance of the model under urban and rural conditions. Though North Bay's monitoring site is listed as an urban site by the MOE due to its location within the region, it was chosen to represent rural conditions for multiple reasons. Firstly, NO_2 measurements were not available for any of the MOEs designated rural sites for 2005. Secondly, Ottawa is a large urban centre with a population of over 1 million people (Urquizo, Spitzer, Pugsley, & Robinson, 2009) and a population growth rate of 6.9 percent (Air & Energy Initiatives Environmental Management Division, 2004). It is located within the Windsor-Quebec corridor and is subject to pollution from local sources as well as from long-range transport from Southern Ontario and the United States.

During the winter, from November to May, prevailing winds are from the northwest {{117 Air & Energy Initiatives Environmental Management Division 2004}}. Most of the air pollution in Ottawa at this time is locally generated from idling, transportation and wood burning. Conversely, from June to October the prevailing winds originate in the south western United States {{117 Air & Energy Initiatives Environmental Management Division 2004}}, carrying polluted air masses from cities like Detroit, Cleveland and Chicago by advection into Southern Ontario and then through the Ottawa region. Because these summertime winds are often slow-moving or stagnant, pollutants have enough time to collect, mix together and react. Conversely, North Bay's population is just over fifty-three thousand people and does not experience the same effects of long-range transport from the Unites States that Ottawa experiences (Government of Ontario, 2010). Both sites have similar seasonal temperatures and are relatively flat, although at the north end of Ottawa, the

Gatineau Hills rise about 250 meters above the city and can impede the flow of air by preventing natural dispersion from occurring {{117 Air & Energy Initiatives Environmental Management Division 2004}}. Many CMAQ studies exist for urban areas or rural areas alone (Sokhi et al., 2006), but direct studies comparing two such regions are not very common (D. Tong & Mauzerall, 2006). Additionally, the majority of O_3 and NO_2 studies take place over the summer (Appel, Gilliland, Sarwar, & Gilliam, 2007) when the conditions for ozone production are optimal. By examining CMAQ simulations under ideal and non-ideal ozone producing conditions, the seasonality of the O_3 cycle can be observed.

Because CMAQ was developed by the U.S. Environmental Protection Agency (EPA) as a regulatory tool, the majority of CMAQ studies with a North American perspective focus on the continental United States, or specific areas within the U.S.A. like the northeast or the south where significant populations reside (Appel et al., 2007; Appel, Bhave, Gilliland, Sarwar, & Roselle, 2008a; Byun, Kim, & Kim, 2007; Eder & Yu, 2006; C. Hogrefe et al., 2006; J. Lin, Youn, Liang, & Wuebbles, 2008; S. C. Smyth, Jiang, Yin, Roth, & Giroux, 2006; D. Tong & Mauzerall, 2006). There are also a number of studies that concentrate on – or include – parts of Central Canada (Brankov et al., 2003; Brulfert, Galvez, Yang, & Sloan, 2007; Galvez, 2007); though none are specific for Ottawa or North Bay.

Examining O_3 and NO_2 concentrations in multiple regions is important because the concentrations of these species vary spatially and temporally from one region to the next. Morning and evening rush traffic hours in urban centres release large concentrations of NO_2 into the atmosphere. During the daytime NOx ($NOx = NO_2 + NO$) photolysis generates O_3 which can persist for many hours in the troposphere. This allows for O_3 to accumulate in urban air masses as it is transported downwind of major cities into neighbouring regions (Sillman, 1993). Conversely, NO_2 has a lifetime of approximately one minute, thus its peak concentrations are measured close to its source of production. Local emissions such as these are responsible for half of Ontario's air pollution (Ontario Ministry of the Environment,

2010). The other half originates from sources in the United States such as the Ohio River Valley. According to the Ministry of the Environment (2010), enough pollutants are carried by transboundary flow to warrant smog advisories even if all local sources were turned off. This is of great concern to the province as it is home to approximately 13 million people, 85 percent of whom live in urban centres around the Great Lakes Basin.

1.2 Overview

The remaining content of this thesis is organized into 6 additional chapters:

Chapter 2 explains the chemistry of the troposphere as it relates to O_3 and NO_2. Their nonlinear relationship is illustrated through the discussion of the null cycle and net ozone production. The sources and sinks of O_3 and NO_2, as well as their intermediate and final products are detailed. A brief discussion on the health effects of these species is also presented.

In Chapter 3, a background description of the CMAQ model and all of its modelling components is provided. I first describe the various types of air quality models available to the modelling community, followed by my rational for choosing CMAQ for in this study. I then move on to provide a detailed description of the internal components of CMAQ, as well as concise descriptions of the external models needed to supply input for a simulation.

Chapter 4 presents modelling exercises that were conducted to learn and understand the working of CMAQ, its inputs and outputs. These exercises included installing and compiling various models in addition to CMAQ, such as the emissions model and meteorological interface model. CMAQ benchmark cases were conducted to insure the compilations were successful. Aspects like nesting, data extraction, spin-up methodology, the effects of

emissions, creating vertical profiles, as well as the visualization and manipulation of output were all performed.

Presented in Chapter 5 and Chapter 6 are two comprehensive evaluations of CMAQs ability to reproduce ground-level O_3 and NO_2 in the winter and summer, respectively. The methodology employed in this study and all modelling parameters in both the wintertime and summertime modelling periods are provided. The domain for both episodes was the same, covering southern Ontario and Quebec as well as the north eastern United States. Graphical analysis like time series plots and diurnal cycles are employed to explain how accurately CMAQ reproduces the spatial and temporal variation of these species compared to surface measurements, as well as the causes for bias and discrepancies in the modelling results. The winter modelling period extends from the beginning of January to the end of March, while the summer period covers months of June, July and August. Statistical measures employed to supplement the graphical analysis in order to fully examine the model's performance and to determine any bias that may exist.

The concluding remarks and future outlook of this thesis are contained in Chapter 7. The main findings of this work are summarized along with their implications to the municipalities of Ottawa and North Bay. The results of this study also have relevance in the modelling community as whole as well as other urban and rural cities as this thesis applicable to them. The chapter concludes with recommendations for improvements for future investigations. For example, I suggest updating the emissions inventories and including other species like volatile organic compounds (VOCs) and meteorological factors like temperature and cloud cover in the modelling analysis is important to get a more inclusive outlook on the behaviour of O_3 and NO_2 systems in the troposphere.

Chapter 2

Tropospheric Chemistry

2.1 Ozone and Nitrogen Dioxide

Despite government efforts, ozone continues to exceed the Canada-Wide Standard 8-hour average of 65 ppb (Geddes, Murphy, & Wang, 2009), and NO_2 levels still remain high despite indications that government abetment policies are working. These species have strong implications on humans and ecosystems because they not only impact the atmosphere, but the aquatic and terrestrial environments as well. Such effects include smog, secondary particulate matter and acid deposition among others. Additionally, because they are green house gases, they also affect climate change through altering the levels of other trace gases in the troposphere. Chronic and acute exposure to either trace gas can have adverse health effects on humans. Acute doses to both O_3 and NO_2 can result in minor bronchitis and a dry cough (Mohsenin, 1994), while prolonged/chronic exposure is associated with asthma, shortness of breath, pulmonary disease and premature death among other illnesses (Bell et al., 2007; Ebi & McGregor, 2008; Environmental Monitoring and Reporting Branch of the Ontario Ministry of the Environment, 2009); In fact, increases in ambient ozone concentrations were correlated with increases in hospitalizations due to reduced lung functions and other respiratory infections (Peel et al., 2005). The risk of such effects are increased for children, the elderly (Buchdahl, Willems, Vander, & Babiker, 2000; Ontario Medical Association, 2007; White, Etzel, Wilcox, & Lloyd, 1994; A. M. Wilson, Salloway, Wake, & Kelly, 2004) and those with existing health conditions like asthma (Mudway & Kelly, 2000). Evidence also exists to suggest a strong relationship between plant and agricultural crop exposure to air pollution and growth reductions or visible injury (Cape, 2008). Given these health and environmental consequences, controlling levels of O_3 and NO_2 are very important.

2.2 The Null Cycle

The main daytime reaction that governs the O_3-NO_2 chemistry in the lower troposphere is the catalytic cycling of NO_2 and NO. In the clean troposphere, when NO_2 photolyzes, it breaks down into NO and atomic oxygen which subsequently reacts with molecular oxygen and a third body molecule to form ozone (R. Atkinson, 2000)

$$NO_2 + h\nu \rightarrow NO + O(^3P) \qquad (\lambda < 430 \text{ nm}) \qquad (1)$$

$$O(^3P) + O_2 + M \rightarrow O_3 + M \qquad (M = N_2, O_2) \qquad (2)$$

However, the NO formed in Reaction 1 reacts almost instantaneously with the newly generated O_3 molecule to reform NO_2 on the timescale of minutes.

$$NO + O_3 \rightarrow NO_2 + O_2 \qquad (3)$$

This dinural cycling between NO and NO_2 is a (quasi) steady-state cycle called the null cycle which establishes an equilibrium between O_3, NO and NO_2 in the absence of additional pathways (Cape, 2008; Finlayson-Pitts & Pitts, 2000). It is controlled by the NO_2 photolysis rate constant and the $[NO_2]/[NO]$ ratio (W. Carter, 1994).

The destruction of NO_2 occurs when it reacts with available O_3 that exists within the same air mass, forming nitrate radicals which are known NOx reservoirs. This property is attributed to their stability (R. Atkinson, 2000; Huie, 1994)

$$NO_2 + O_3 \rightarrow NO_3 + O_2 \qquad (4)$$

This reaction is the primary source of NO_3 in the troposphere (Jimenez, Baldasano, & Dabdub, 2003) and has a rate constant of $k_8 = 1.9 \times 10^4$ L mol^{-1} s^{-1} (Huie, 1994) which is significantly lower than that for the formation of NO_2 (Reaction 3). Nitrate radicals have a lifetime of about five seconds during the daytime when they photolyze rapidly, following two possible pathways whose relative yields of either NO or NO_2 depend on the wavelength of radiation (Table 1) (Jimenez et al., 2003). The photodissociation of NO_3 occurs over a wider absorption spectrum than does the photolysis of O_3 (R. Atkinson, 2000)

$$NO_3 + h\nu \rightarrow NO + O_2 \qquad (10\%) \qquad (5)$$

$$NO_3 + h\nu \rightarrow NO_2 + O(^3P) \qquad (90\%) \qquad (6)$$

These degradation reactions are typical of polluted atmospheres due to the abundance of available NOx. During the night, nitrate radicals react with NO and NO_2 by the following reactions

$$NO_3 + NO \rightarrow 2NO_2 \qquad (7)$$

$$NO_3 + NO_2 \rightarrow N_2O_5 \qquad (8)$$

N_2O_5 then reacts with water vapour to produce HNO_3 which is removed by deposition. While the diurnal nature of the OH radical allows it to dominate the daytime chemistry of the troposphere, at night time, NO_3 becomes the prevailing oxidizing agent and removes NO_2 from the ozone cycle by Reaction 8 (Jimenez et al., 2003).

Table 1 Absorption wavelengths for O_3, NO_2 and NO_3 photolysis

Reaction	Wavelength (nm)
$O_3 + h\nu \rightarrow O(^1D) + O_2(^1\Delta_g)$	< 335
$NO_2 + h\nu \rightarrow NO + O(^3P)$	250-400
$NO_3 + h\nu \rightarrow NO_2 + O(^3P)$	400-625
$NO_3 + h\nu \rightarrow NO + O_2$	585-625

Other reactions involving NO_2 and NO include reaction with OH radicals to form HONO and nitric acid via Reactions 9 and 10, respectively (Huie, 1994)

$$NO + OH \rightarrow HONO \qquad (M = N_2, O_2) \qquad (9)$$

$$NO_2 + OH \rightarrow HONO_2 \qquad (M = N_2, O_2) \qquad (10)$$

The $HONO_2$ acts as a sink for NOx, while the HONO can undergo photolysis to regenerate OH

$$\mathrm{HONO} + h\nu \rightarrow \mathrm{NO} + \mathrm{OH} \quad (11)$$

OH can also react with NO_2 to form HNO_3 which is the principal sink for NO_2 (J. Lin et al., 2008)

$$\mathrm{NO_2} + \mathrm{OH} \rightarrow \mathrm{HNO_3} \quad (12)$$

Given that nitric acid is another NO_2 sink, its subsequent chemical and physical reactions can affect the net concentration of O_3 in the troposphere. When a molecule of HNO_3 is removed by wet and dry deposition, it effectively eliminates a NO_2 molecule, an O_3 precursor, from the ozone cycle.

2.3 Net Ozone Production

The equilibrium created by the null cycle assumes that under idealized conditions, the following relationship should apply

$$\mathrm{O_3} = \frac{k5}{k7}\frac{[NO2]}{[NO]} \quad (13)$$

where k_5 and k_7 are the reaction rates for Reactions 5 and 7, respectively. While k_5 is dependent on the amount and energy of incoming solar radiation, k_7 has been determined experimentally to be 1.1×10^{-7} $L \cdot mol^{-1}s^{-1}$ (Huie, 1994). However, this equilibrium is often disturbed by fast changes in light intensity as well as changes in species concentrations (Altshuller, 1986) due to emissions from anthropogenic and biogenic sources into the troposphere.

According to observations by Madronich (1993), the concentration of O_3 is normally much higher than that of NO in the troposphere, indicating that an additional method of ozone production must exist where the NO-NO_2 conversion can take place without consuming ozone. These pathways do exist in the presence of reactive volatile organic compounds (VOCs) which either consume NO or become degraded to form organic peroxy radicals (RO_2), providing a route for NO to form NO_2 (Altshuller, 1986; R. Atkinson, 2000;

Finlayson-Pitts & Pitts, 2000). This process drives the equilibrium away from the steady-state conditions so that the null cycle cannot be completed.

$$OH + VOC \rightarrow RO_2 \qquad (R = C_nH_m) \qquad (14)$$

These VOCs consist of alkanes such as methane (CH_4) and biogenic non methane organic compounds (NMOCs) and originate from both anthropogenic and biogenic sources (R. Atkinson, 2000; Cape, 2008). These emitted species do not directly influence the production or destruction of ozone; instead they indirectly affect ozone by altering the NO-NO_2 ratio.

The relationship between O_3, NOx and VOCs can be described by initiation, propagation and termination reactions which result in an overall increase in ozone concentrations (R. Atkinson, 2000; Cape, 2008; X. Xie et al., 2008). The initiation reactions for O_3 production are those which generate intermediate OH, HO_2 or RO_2 free radicals, which are collectively known as HOx, through photolysis and ozonolysis. The photolysis of nitrous acid (HONO), formaldehyde (H_2CO) and hydrogen peroxide (H_2O_2), are all examples of HOx production. The photolysis of HONO and H_2O_2 are sources of HOx in polluted regions

$$HONO + h\nu \rightarrow OH + NO \qquad (15)$$

$$H_2CO + h\nu \rightarrow 2HO_2 \qquad (16)$$

$$H_2O_2 + h\nu \rightarrow HO_2 \qquad (17)$$

Once HOx radicals are formed, the propagation steps can proceed as OH oxidizes VOCs to the radical species RO_2 and HO_2 (Reaction 14) (X. Xie et al., 2008). In low NOx environments, RO_2 species react with themselves or with ozone, potentially decreasing ozone levels. In high NOx environments RO_2 almost solely reacts with NO which increases NO_2 concentrations.

$$RO_2 + NO \rightarrow NO_2 + HO_2 + \text{intermediate VOC} \qquad (18)$$

$$HO_2 + NO \rightarrow NO_2 + OH \qquad (19)$$

From here, NO_2 can photolyzes to generate O_3 completing the ozone cycle by Reactions 1 and 3, respectively. This shifts the NO-NO_2 equilibrium toward NO_2, (Cape, 2008; Finlayson-Pitts & Pitts, 2000) resulting in an overall increase in ozone formation.

In the termination steps, radicals are removed from the cycle through reactions with NOx or with other radicals. Some common examples are as follows

$$RO_2 + NO \rightarrow \text{Organic Nitrate} \quad (24)$$

$$CH_3CO_3 + NO_2 \rightarrow PAN \quad (25)$$

The reactions in this section demonstrate the importance of knowing the amount and distribution of NO and NO_2 present at a given time for accurate simulation of O_3 by an air quality model. Nitrogen oxides directly and indirectly influence the chemistry of the troposphere through participation in a multitude of chemical reactions, all of which yield species that bare their own consequences on the atmosphere. The photolysis of NO_2 leading to the formation of ozone is particularly important due to its direct impact on air quality, as well as the intricate nature of the relationship since the concentration of ozone depends on that of NO_2. The sensitivity of O_3 to NOx in general, depends heavily on the NOx-VOC ratio in a given region and production can be limited by either precursor species. This means that a decline in the concentration of the limiting precursor would cause a subsequent decrease in ozone production rate. An example of a NOx-limited scenario is a forested rural region which generates large amounts of biogenic VOCs. Here, the production rate of O_3 would decrease as NOx levels declined. Conversely, VOC-limited ozone production is most often observed in urban areas where the abundance of NOx from motor vehicles works to scavenge the O_3 from the atmosphere. Reducing NOx emissions would then result in less ozone being consumed. To properly replicate NOx and O_3 levels over a given region, it is necessary for an AQM to be able to calculate all of the major chemical reactions involving these species, in addition to the governing transport mechanisms. This is why CMAQ was employed, as it is capable of calculating all these important factors. Further details about CMAQ and its internal processors and external components will be provided in Chapter 3.

Chapter 3

CMAQ Modelling System

3.1 Introduction

The concentration of pollutants in the troposphere is affected by many different processes including, but not exclusive to, chemical transformations, meteorology, wet and dry deposition and emissions. Understanding these complex relationships is made easier by the use of air quality models (AQMs) whose goals are to assess the spatial and temporal distribution and evolution of tropospheric pollutant concentrations generated from both local emissions and long range transport. They do this by establishing (numerical) relationships between meteorology and transport processes, emissions, chemical deposition and chemical transformations (Jacob, 1999). There are three basic types of air quality models. The first type is called a box model which represents the area of interest as a stationary box where transport moves species X, in and out of the box. The production of X inside the box includes contributions from emissions and chemical production, while the loss of X is due to deposition and chemical loss (Jacob, 1999). The spatial distribution of X in the box is not resolved because it is assumed that the box is well mixed. The second type of air quality model is a Lagrangian or trajectory model where, in contrast to a box model, the selected domain (i.e. urban or country) is an air parcel that moves with the speed of the wind along the surface. Here too, the air parcel is taken to be well mixed. Lastly, the third type of model is a 3-dimensional Eulerian model which employs a fixed model grid, overlain with a series of three-dimensional grid cells in the horizontal and vertical directions. The advantages and disadvantages of each type of model are summarized in Table 2.

Table 2. The advantages and disadvantages of different types of air quality models.

	Box Model	Lagrangian Model	Eulerian Model
Advantages	▪ Easy to use, low complexity ▪ Often sufficient enough for most air quality issue	▪ Basis of conservation laws ▪ Equations are computationally simple to resolve	▪ Provides a more complete characterization of physical processes in the atmosphere compared to Lagrangian models ▪ Can predict species concentrations throughout the entire model domain
Disadvantages	▪ Chemistry is often oversimplified ▪ Does not resolve the concentration gradient of species 'X' inside the box (i.e. assumes the box is well-mixed)	▪ 3-D applications of the equations of motion are difficult to apply ▪ The physical processes it describes are somewhat incomplete	▪ Highly complex, requires extensive parameterizations

In these Eulerian models, coupled differential equations – the conservation equations – derived from the fundamental laws of physics, are used to calculate a mass balance within each grid cell by solving the transport across each cell boundary and chemical transformations within each cell during a specified period of time. The changes in concentration of pollutants in each grid cell are affected by the following processes: emissions from sources (Ec), horizontal and vertical advection (Adv) and diffusion (Diff), chemical transformations (Rc) and deposition/loss processes (Sc). Mathematically, they

relate to the concentration in each grid cell through the continuity equation (Russell & Dennis, 2000)

$$\frac{d\mathrm{ci}}{d\mathrm{t}} + \nabla \cdot \bar{\mathrm{U}}ci = \nabla\rho Di\nabla\left(\frac{\mathrm{c}i}{\rho}\right) + Ri(c1, c2 \ldots cn, T, t) + Si(x, t) \qquad (26)$$

where c_i is the concentration of species *i*, $\bar{U}$ is the wind velocity vector, ρ is the air density, D_i is the molecular diffusivity of species *i*, R*i* is the rate of concentration change of species *i* by chemical reaction, *n* is the number of predicted species and $S_i(x, t)$ is the source/sink of *i* at location *x*.

Because the chemical and physical processes of the atmosphere are so complex and variable, these equations cannot be solved exactly (Jacob, 1999; Pielke, 2002). Thus valid approximations and assumptions of the complex chemical and physical processes of the atmosphere must be made. It should be noted that the concept of assumptions is one major source of error in all air quality models. Because these equations are applicable to infinitesimal distances, they can relate to spatial scales close to approximately 1 cm and time scales of about 1 second in the atmosphere (Pielke, 2002). To apply them to synoptic or subsynoptic scale processes, they have to be integrated over the entire domain of the model. For the purpose of simplicity, the individual terms in the conservation equations are normally condensed in AQMs to make the equations easier to work with (Pielke, 2002).

3.2 Model Selection Rationale

In this study, the air quality model used for all simulations was the US EPAs Models-3 CMAQ Modelling System (Byun, Pleim, Tang, & Bourgeois, 1999). There were many reasons for choosing CMAQ over other air quality models, as it was purposely designed to account for, and improve upon the operational and scientific failures of early AQMs, as outlined in Dennis et al. (1996), and was to be used primarily by two different groups: policy makers and scientists. Policy makers need models which can make relatively rapid

predictions on numerous scenarios for comparison. In 2004, the provincial government used CMAQ to study the transboundary flow of ozone, particulate matter and their precursors, as part of the federal-provincial Canada Wide Standards initiative. The US EPA also routinely operates CMAQ to gauge the level of attainment of its own federal policies (Eder & Yu, 2006) and emission control strategies such as the National Ambient Air Quality Standards. Despite the availability of numerous AQMs, CMAQ has been increasingly chosen as the model of choice for government regulators and agencies.

The scientific community, however, is mostly interested in understanding the chemistry and physics of the atmosphere, such as how pollutants interact with each other, and how they are produced and removed from the system (Dennis et al., 1996). The favouring of CMAQ by the scientific community has been observed by its extensive use within academic institutions to study various facets of the atmosphere, from the fate of mercury in North America (Wen, 2006) and the evaluation of the deposition of acidifiying species on the air quality in East Asia (M. Lin et al., 2008), to the operation of CMAQ in forecasting systems in Europe (San José, Pérez, Morant, & González, 2008).

A sound air quality model must have the ability to be updated and tested as new scientific information is made available (Dennis et al., 1996). Since CMAQs release in 1998, it has been evaluated more extensively than any other chemistry transport model. Frequent scientific peer reviews of all atmospheric processes – chemical and physical – within the model (Arnold & Dennis, 2006; Byun & Schere, 2006; S. C. Smyth et al., 2006; Y. Zhang et al., 2006; Y. Zhang, Liu, Pun, & Seigneur, 2006a; Y. Zhang, Liu, Pun, & Seigneur, 2006b), in addition to the release of publicly available updates to ensure the model sensitivity and performance in modeling spatio-temporal processes are of the highest quality. For example, in 2008 CMAQ version 4.7 was publicly released. Thorough investigation led to changes to scientific algorithms based on laboratory, field and numerical studies being incorporated into the cloud and chemistry modules, emissions processing and dry deposition velocities (Foley

et al., 2010). These improvements were implemented sequentially followed by a diagnostic evaluation of each individual update so that the effects of each modification could be understood (Foley et al., 2010).

CMAQ also has the ability to address a multitude of air quality issues simultaneously on a variety of spatial and temporal scales making it a 'one atmosphere' model which is highly beneficial to the modelling community because it negates the need to use separate models for urban and regional simulations or for individual pollutant species (Byun & Schere, 2006; Dennis et al., 1996). CMAQs spatial scale ranges from local to hemispheric, and its temporal flexibility can be used to evaluate short term transport from localized sources (days to weeks) or longer term climatological changes (months to years) (US EPA, 2006). The 'one atmosphere' concept also applies to tropospheric air quality issues such as, but not exclusive to, acid deposition, relative humidity and temperature. Multi-pollutant capabilities also allow for the simultaneous examination of an array of pollutant species such as ozone, particulate matter (of various components and sizes), toxics and trace gases to name a few. This is in contrast to early 3-dimensional AQMs which treated air quality issue separately. For example, the Regional Oxidant model (ROM) was used to explicitly simulate ozone, whereas the purpose of the Sulphur Transport and Emissions model (STEM/STEM II) and the Regional Acid Deposition model (RADM) were to investigate acid deposition (Byun & Schere, 2006). Because the chemical and physical processes which occur in the atmosphere are all interconnected with one another, they cannot be dealt with on an individual basis. These aspects of the model allow it to be easily adapted to meet the needs of many users in the air quality community, from research and regulatory modellers, to science module developers to air quality forecasters and policy makers.

Modularity is an additional feature which adds to the strength of CMAQ, giving users the ability to choose between multiple configurations when running the model. Because the user is not responsible for changing the code or declaring variables within the program modules,

possible errors relating to these matters are greatly reduced. Additionally, its open source code allows any user with internet access to download and compile the model making it widely available and inexpensive.

While some may argue that these aforementioned benefits are applicable to many AQ models, direct comparison of CMAQ with other regional models have provided convincing evidence of the benefits of using CMAQ for numerous species under a variety of scenarios. When modelling long term scenarios for sulphate aerosols CMAQs performance was superior to the Regional Modeling System for aerosols and Deposition (REMSAD), though both models performed equally well for nitrate aerosols. When compared to other models like the Comprehensive Air Quality Model with Extension (CMAx) which is also broadly used, it was found that the models performed moderately well though CMAx generates higher ozone levels overall than CMAQ possible due to the more up-to-date dry deposition science in CMAQ, or its more robust vertical transport (Liang, Martien, Soong, & Tanrikulu, 2001).

Despite its usefulness, CMAQ is not without its drawbacks. Its grid-based structure causes it to be much more computationally intensive compared to box models and Lagrangian models (Russell & Dennis, 2000). Similar to all scientific analysis, CMAQ is subject to the limits and drawbacks of the numerical algorithms on which its operation is based. For example, the issue of numerical instability of the transport equations has been investigated within the model. It has been found that studies which analyze the influence of small changes in emissions on particulate matter can be subject to great numerical instability, such as severe over prediction in remote or far downwind regions (D. Tong & Mauzerall, 2005). Though more recent updates to the aerosol and transport modules in the CCTM have helped to limit these issues, they are still matters that need further attention.

3.3 Model Descriptions

3.3.1 **CMAQ**

CMAQ employs three main types of components to operate, namely a meteorological modelling system which describes the physical states and motions of the atmosphere, an emissions model which processes anthropogenic and biogenic emissions, and a chemistry-transport model (CTM) which is responsible for simulating the chemical reactions, transformations and transport processes of the atmosphere. Because the CMAQ CTM (CCTM) requires a great deal of input data from multiple sources to function correctly, CMAQ contains four internal processors to prepare, convert and provide the necessary data to the CCTM. These processors link the meteorology, emissions and chemistry transport components of a simulation (Byun & Schere, 2006). The clear sky photolysis rate calculator (JPROC) computes the photolysis rates used when simulating photochemical reactions in the CCTM, and the initial conditions (ICON) and boundary conditions (BCON) processors were used to generate the initial and boundary conditions for a CCTM simulation, respectively. The last program to be run is the CMAQ chemistry transport model (CCTM) which receives all the information generated from the other models and processors to replicate each of the atmospheric processes that affect the transport, transformation and deposition of participating pollutants. Several internal process modules also aid in the simulation. These include: horizontal and vertical diffusion and advection including mass-conservation adjustments for advection processes, aerosol dynamics and size distributions, aerosol deposition velocity estimation, aqueous-phase reactions and cloud mixing, gas-phase chemical reaction solver and process analysis. A schematic diagram of the internal and external components needed for the correct operation of CMAQ, as well as the flow of data between them, can be seen in Figure 1. Each of these components will be discussed in further detail in the following sections starting with the internal processors of CMAQ followed by the external models.

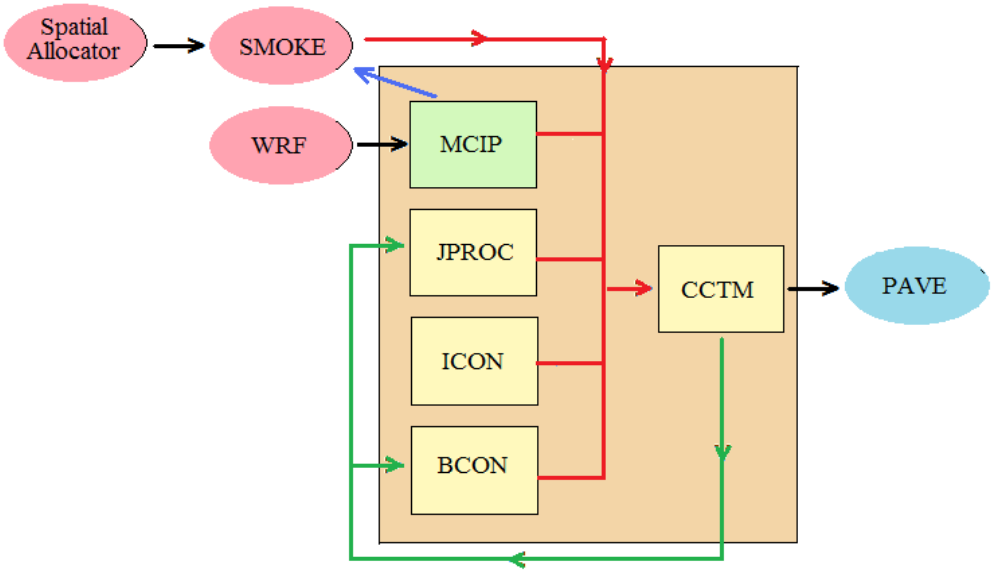

Figure 1. The internal and external components of the CMAQ modelling system. Red arrows illustrate the flow of data from the CMAQ pre-processor to the CCTM. Green arrows show the data feedback from the CCTM is used to create initial and boundary conditions for nested simulations. Black arrows indicate the external data flow, while the blue arrow shows that the output from MCIP is used to drive the emissions model, SMOKE.

3.3.2 **MCIP**

The Meteorology-Chemistry Interface Processor (MCIP) evolved from the meteorology pre-processor of the Regional Acid Deposition Model (RADM). Its primary role in air quality modelling is to translate the meteorological parameters generated from the meteorology model into I/O API formatted files that are readable by the CMAQ chemistry modules (Byun et al., 1999; Byun & Schere, 2006; US EPA, 2006). This step in air quality simulations is essential because consistency must exist between the meteorological output and the way it is used in the CCTM. It has the added capability to switch coordinate systems and use generalized vertical coordinates; this allows MCIP to support either the MM5 or the Weather Research Forecast (WRF) model for a given simulation. Another responsibility of MCIP is to process and gap fill the meteorological data since many meteorology models often omit

some of the parameters required by the CCTM. Dry deposition velocities and radiation fields are calculated within MCIP, while the user can opt to recalculate the provided planetary boundary layer (PBL) heights as well (Byun et al., 1999).

3.3.3 **JPROC**

The Clear-Sky Photolysis Rate Calculator (JPROC) generates daily photolysis rates for all photochemical reactions based on physical properties of photoreactive molecules, at every 10 degrees in latitude for 10-60 degrees north. The accuracy of the calculated rates is vital to the accuracy of the CMAQ simulation because photolysis is the primary source of radicals in the troposphere. These rates are determined for a selected gas-phase photochemical mechanism at varying altitudes in meters, latitudes in degrees and zenith angles. Equation 27 is the equation for the photolysis rate for a given photochemical reaction

$$Ji = \int \mathrm{F}(\lambda)\sigma i(\lambda)\phi i(\lambda)\mathrm{d}\lambda \qquad (27)$$

where $J_i(\mathrm{min}^{-1})$ is the photolysis rate, $\mathrm{F}(\lambda)$ is the actinic flux (photons cm^{-2} $\mathrm{min}^{-1}\mathrm{nm}^{-1}$), $\sigma_i(\lambda)$ is the absorption cross section for a given photodissociating molecule, $\square_i(\lambda)$ is the quantum yield of the photolysis reaction (molecules photon^{-1}) and λ is the wavelength (nm) (Byun & Schere, 2006). All of these variables are required as input for each species defined in the selected gas-phase chemical mechanism.

Temperature profiles, optical depth and aerosol extinction coefficients are all included in the input in addition to molecular absorption cross-sections and quantum yield data for molecular oxygen and ozone, both as a function of wavelength. Ozone column measurements are derived from the NASA Total Ozone Mapping Spectrometer (TOMS) on the Nimbus satellite (Spak, 2009). The correct absorption cross-section and quantum yield data files for the selected chemical mechanism must be provided to ensure consistency. These values are also corrected to account for temperature and pressure effects by using seasonal vertical profiles of these parameters. This information as well as extraterrestrial radiation, Rayleigh

scattering in for clouds and surface albedo is then used to determine the actinic flux for clear sky conditions and photolysis rates (Byun & Schere, 2006).

3.3.4 **BCON and ICON**

The Initial Conditions (ICON) and Boundary Conditions (BCON) Processors provide the chemical concentration fields for individual species at the start of a simulation and for those that lie in the grid cells outside of the modelling domain. They are compulsory in a simulation, and both utilize either time-independent vertical concentration profiles which represent the clean atmosphere, or existing CCTM output to generate the initial and boundary conditions (ICs and BCs). With BCON, users have the additional option of utilizing a larger-scale (i.e. global-scale) output file from an external CTM. Whichever option is used, BCs influence surface-O_3 concentrations on the interior of the domain through transport and vertical advection (Tang et al., 2009), while the impact of the ICs is more prevalent in short term simulations. To minimize or eliminate their effects, a period called a 'start up' period is run prior to the simulation of interest so that errors can be averaged out over a longer period of time.

3.3.5 **CMAQ Chemistry Transport Model (CCTM)**

The last program to run in the CMAQ model is the CCTM which is the Eulerian component of CMAQ. It uses the output from the emissions and meteorological models as well as the other CMAQ programs and to address the chemistry and transport of pollutant species. It is where the simulation of all dynamical processes including advection, dispersion, deposition and reactions take place. Figure 2 shows the internal components of the CCTM.

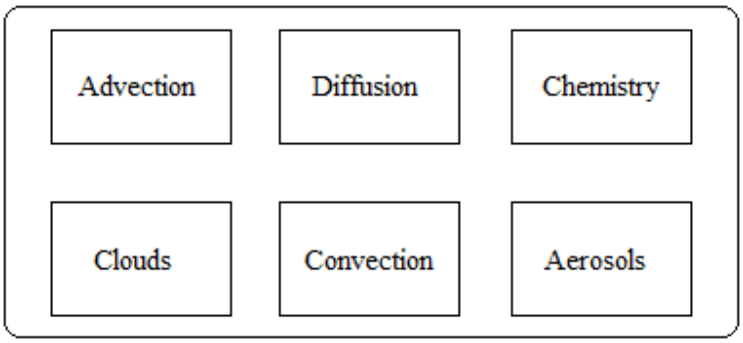

Figure 2. The internal modules of the CMAQ Chemistry Transport Model (CCTM).

In the CCTM, pollutants are transported by various physical processes such as **advection**, **diffusion** and **convection**, all of which are subject to the principal of mass conservation. Advection moves pollutants either vertically or horizontally, though mean atmospheric motion is predominantly in the horizontal direction. Movement in the vertical direction is largely referred to as convection which depends wholly on meteorological conditions. The CCTM uses a globally mass conserving scheme for horizontal motion, while the vertical velocity component is derived at each grid cell that satisfies teh mass continuity equation. Diffusion which occurs on a sub-grid scale results in quick mixing closer to the pollutant source which can produce large changes to pollutant concentrations. This is particularly important when individual sources are directly added to the grid as point sources since instantaneous mixing is assumed and thus must be corrected for using parameterizations (US EPA, 2006). The CCTM implements horizontal diffusion with a single eddy diffusion algorithm that is dependent on the model's grid size and is based on local wind deformation. The diffuseness is assumed to be uniform but is higher for higher resolutions.

Aerosols are calculated by the CCTM through the CMAQ aerosol module. There are two different versions of the module, aero3 and aero4. The difference between the two versions is that aero4 includes calculations of sea salt aerosols which are speciated into sodium, chloride and sulphate and are distributed by size. The CCTM is capable of simulating both

fine and coarse particles which generally follow different production mechanisms and chemical characteristics (Binkowski, 1999), and includes both primary emissions and secondary species. Particle sizes are equal to or less than 2.5 microns in diameter (PM2.5), greater than 2.5 microns and equal to or less than 10 microns in diameter (coarse particulate matter) as well as those of size equal to 10 microns in diameter or less (PM10), where PM10 is the sum of PM2.5 and coarse particulate matter. The fine group (PM2.5) are sulphates, nitrates, ammonium, water, and organic and elemental carbon among others. They are divided into two subgroups, Aitken and accumulation modes, and are generated by one of three processes: nucleation, combustion processes or condensation upon existing particles. The coarse particulate matter (PM10) is represented by wind-blown dust and generic anthropogenic species mostly associated with industrial processes. All **cloud and aqueous-phase chemistry** are modelled by the cloud and aqueous chemistry modules, and include processes such as wet deposition, the vertical redistribution of pollutants for sub-grid clouds and the calculation of in-cloud scavenging via precipitation. Cloud droplets themselves, are formed by heterogeneous nucleation on aerosols, and grow via collision, condensation and coalescence. The cloud module is divided into sub-grid and resolved cloud modules which are employed according to the grid size. Horizontal grid resolutions of 12 km or more require the sub-grid module because the size of a convective cloud is assumed to be smaller than the grid cell and must be parameterized. Depending on whether the meteorological model indicates the occurrence of convective precipitation, the sub-grid module in CMAQ will simulate either precipitating or non-precipitating clouds accordingly. The resolved cloud module however, is used in CMAQ for grid cells of 4 km or less for clouds that are resolved by the meteorological model and occupy the entire grid cell (Roselle & Binkowski, 1999). The simulated clouds can include stratus, cumulus or cirrus clouds.

3.3.6 **Photochemical Gas-Phase Chemical Mechanisms**

Photochemical gas-phase chemical mechanisms mathematically describe photochemical processes through simplified sets of chemical reactions involving both primary and secondary compounds; whereby primary pollutants interact to form secondary pollutants. The species represented in chemical mechanisms are inorganic compounds such as NOx, Ox, HOx and SOx, as well as organic compounds which consist primarily of VOCs (Dodge, 2000). Because the number of represented inorganic species is limited and their kinetic parameters are generally well understood, they are characterized in a similar manner in all mechanisms, with explicit representation. Conversely, the organic species in a mechanism are simplified (condensed) because it would be computationally impractical to represent the complete chemistry of the (polluted) atmosphere (R. Atkinson, 2000), as this would require over twenty thousand different reactions, several thousand species and their reaction products, and the integration of all the rate equations (W. Carter, 2000b; Dodge, 2000; Russell & DennisOn assignment to the Atmospheric Research and Exposure Assessment Laboratory, U.S. Environmental Protection Agency, Research Triangle Park,NC 27711., Robin, 2000). Condensed mechanisms are particularly necessary for grid based AQMs which call for chemical concentrations to be calculated over every grid point (Dodge, 2000; Jimenez et al., 2003).

Condensing these compounds and their reactions can be accomplished by several different methods. Some of the more frequently employed methods are as follows: The first type is the 'lumped structure' approach which groups (organic) compounds according to the types of carbon bonds in each species. Secondly, the' lumped molecule' approach groups organic compounds, specifically VOCs, with species that have comparable chemical structures and each group is represented by a generalized – or surrogate – species (W. Carter, 2000b; Faraji, Kimura, McDonald-Buller, & Allen, 2008)(W. Carter, 2000b; Faraji et al., 2008). A third approach is called the' variable lumped parameter condensation' groups VOCs having similar rate constants with a surrogate; the kinetic and product yield parameters of the

surrogates are weighted averages of the mixture of VOCs they represent (W. Carter, 2000b)(W. Carter, 2000b). Lastly, the 'morphecule' approach has also been developed where the composition, concentration and rate of reaction for surrogate species called morphecules, is updated after every time step in the simulation (Dodge, 2000). Examples of gas-phase chemical mechanisms that include each type of lumping are Carbon Bond-IV (CB4), State-wide Air Pollution Center (SAPRC-99), Regional Acid Deposition Model 2 (RADM-2) and Morphecule mechanism (MM), respectively.

3.3.6.1 *SAPRC-99*

To date, numerous chemical mechanisms have been developed for AQ modelling. SAPRC-99, the gas-phase chemical mechanism chosen for use in this study, was developed and modified by Carter et al. (1999) and is one of the most commonly utilized mechanisms for urban air quality modelling. It was specifically designed to assess VOC activity in more detail than other mechanism used in Eulerian modelling. It uses a lumped molecule approach to calculate chemical concentrations for 80 species in 214 reactions (W. Carter, 2000b; Jimenez et al., 2003; Luecken, Phillips, Sarwar, & Jang, 2008)(W. Carter, 2000b; Jimenez et al., 2003). A list of the reactions in the mechanism can be found in Appendix B. For base case and ambient simulations, the hydrocarbons are lumped into five alkane groups (ALK1-5), two aromatic groups (ARO1 and 2), two alkene groups (OLE1 and 2) and 1 group for terpenes (TRP1) (W. Carter, 2000b). The main building block of SAPRC-99 is the base mechanism which contains the reactions of generic VOCs as well as inorganic species, common organic products and the intermediate radicals these products produce. Other key components include the estimation methods used to determine which VOC reactions are not in the base mechanism and the lumping procedures which characterize the mixtures or VOCs for which no estimations are available (W. Carter, 2000b). The reactions of VOCs can be added to the mechanism for individual VOCs or for lumped (surrogate) species, depending on the application. The addition of such species or classes of species would be necessary if, for example, the model predictions of a particular species that would otherwise be lumped

with similar compounds needed to be compared with experimental measurements (W. Carter, 2000b). For example, isobutene, which is normally represented by the alkene surrogate, OLE2, can instead be represented by four different chemical reactions with HO, O_3, NO_3 and $O(^3P)$.

Like all chemical mechanisms, SAPRC-99 has been extensively peer-reviewed (Stockwell, 1999) and updated to represent the most recent advances in atmospheric chemistry. It has been evaluated against approximately 1700 environmental smog chamber experiments carried out at the University of California at Riverside (W. Carter, 2008; Dodge, 2000) to assess how accurately it represents ambient conditions. Smog chambers are used for analysis because they are closed systems and so are not influenced by factors like meteorology, making analysis easier (Faraji et al., 2008); though smog chambers are not, themselves, without error. Changes to the original base mechanism centred on evaluations by IUPAC and NASA in the late 1990s and led to revised absorption cross sections, quantum yields, reaction mechanisms and rate constants for various reactions including a 20 percent change in the rate constant for the reaction of OH with NO_2 (W. Carter, 2008). Updates to the kinetic parameters for ARO1 and AEO2 lumped species were more recently added to the mechanism; the treatment of low-NOx conditions was also addressed. Since the report by Carter (2000b), a total of 19 additional compounds were added to SAPRC-99 including highly branched alkanes ($C \geq 11$) and several oxygenated compounds (W. Carter, 2000a).

Comprehensive reviews comparing SAPRC-99 with other commonly employed gas-phase chemical mechanisms for a variety of chemical species and conditions are also available (Luecken et al., 2008). An alternate mechanism which is commonly used to describe urban atmospheric chemistry is the carbon bond mechanism, of which two main versions exist, Carbon Bond IV (CB4) (Gery, Whitten, Killus, & Dodge, 1989)and the newer Carbon Bond V (CB05) (Yarwood, Rao, Yocke, & Whitten, 2005). The points of divergence among the three mechanisms centre on how they process unknown reaction rates and their dependence

on factors like time, temperature and pressure, as well as how they condense reactions and organic compounds (Luecken et al., 2008). A comparison of these condensed mechanisms with SAPRC-99 can be seen in Table 3. Many studies have compared SAPRC-99 with the CB mechanisms (Byun, 2002; Faraji et al., 2008; Luecken et al., 2008; Yarwood, Stoeckenius, Heiken, & Dunker, 2003). With respect to NOx, SAPRC-99 predictions are more similar to those of CB05 than the older CB4 mechanism. This is partly because SPARC-99 and CB05 include the recycling of short-lived, oxidized nitrogen species like NO, NO_2, HONO and N_2O_5, while CB4 does not. By including these recycling reactions, compounds which were treated as termination products in CB4, can regenerate reactive species. For example, HNO_3 which is a sink for NO_2 can photolyze, as can organic nitrate, to produce HOx and NO_2 , resulting in higher ozone levels (Byun, 2002; Faraji et al., 2008; Luecken et al., 2008). Urban areas and areas with a high NOx/VOC ratio provide the largest difference (Luecken et al., 2008). From this it is evident that changing the mechanism can have an impact on predictions of nitrogen containing compounds – and thus ozone – in urban and rural environments.

Table 3. A comparison of SAPRC-99, CB4 and CB05 chemical mechanisms as used by Luecken et al. (2008).

	CB4	**CB05**	**SAPRC-99**
Type of lumping	Lumped structure	Lumped structure	Lumped molecule
Total number of species	46	59	80
Number of organic species	30	41	64
Total number of reactions	96	156	214
Number of inorganic reactions	45	63	45

3.3.7 **Weather Research and Forecasting Model (WRF)**

The meteorological fields for the air quality simulations were generated by the Weather Research and Forecasting Model (WRF) which is a mesoscale numerical weather prediction system. WRF has scales ranging from a few meters to thousands of kilometres. Its framework supports non-hydrostatic conditions, but also has a hydrostatic option where the force of gravity balances out the atmosphere's pressure gradient, and uses terrain-following vertical pressure coordinates. Another commonly used meteorology model is the Fifth-generation NCAR/Penn State Mesoscale Model (MM5). Though MM5 has been more frequently used in past operational applications, recent improvements to WRF have made its performance is comparable to that of MM5. WRF not only has the same capabilities as MM5, it also includes updated physics schemes like those for the land-surface model (LSM), planetary boundary layer (PBL), cloud microphsyics and radiation in addition to high quality mass conservation characteristics (Appel, Roselle, Gilliam, & Pleim, 2009; Challa et al., 2007) .

3.3.8 **Emissions Model**

Emissions inventories are processed by the Sparse Matrix Operator Kernel Emissions (SMOKE) Modelling System which prepares them for input into the CMAQ chemistry transport model (CCTM). The SMOKE modelling system was developed by the MCNC Environmental Modelling Center in 1996 for emissions processing in both urban and regional applications. It continues to be reviewed and improved at the University of North Carolina at Chapel Hill's Carolina Environmental Program and is highly versatile in that it can create input for 3D and 2D AQMs. For use in CMAQ, the emissions must be speciated, temporalized and gridded for each individual or lumped species defined in the chemical mechanism. SMOKE does this by performing temporal allocation, spatial allocation, speciation and merging. **Temporal Allocation** uses factors based on source characteristics, such as temporal profiles, to transform the inventory data to the time scale required by the

AQM. These factors are listed by the US EPA (http://www.epa.gov/ttn/chief). **Spatial Allocation** is the process by which the emissions data are distributed over the simulation domain according to the grid specifications, from the geographical units which they are available. **Speciation** is employed to convert the classes of species reported in the inventory to those defined by the AQM photochemical mechanism by applying source specific mass or mole factors. Lastly, a single 3-D output file of the emissions is created for the AQM from all sources by **Merging**. The sources include point, area, mobile and biogenic sources.

3.3.8.1 *Emission Inventories*

Emission inventories are the main input files to SMOKE. They contain different data types called inventory pollutants which can be modified according to the application of the AQM. The different data types are criteria, particulate, toxics and activity data. Criteria inventories contain carbon monoxide (CO), NOx and VOCs or total organic gases (TOG), ammonia (NH_3) and sulphur dioxide (SO_2). Particulate inventories include particulate matter of size 10 microns or less (PM_{10}) and 2.5 microns or less ($PM_{2.5}$). The toxics inventories are obtained from the US National Emission Inventory (NEI) for hazardous air pollutants (HAPs), and are composed of several hundred compounds that represent pollutant groups like polycyclic organic matter (POM), cyanide compounds and metal compounds such as manganese and chromium, among others.

The emissions inventories are also divided into different source categories depending on their attributes and characteristics, and SMOKE processes these into four different types in order to account for the difference in temporal and spatial distribution of different emission sources: area (nonpoint and nonroad mobile sources), biogenic (biogenic land use data), mobile (on-road mobile) and point (point and wildfire sources). **Area Sources** include nonpoint/stationary sources as well as nonroad mobile sources. Stationary sources refer to those that are not movable, and are estimated over a particular area like a county or district because it is not possible to collect emissions data at each point of emission. Examples

include residential heating and mining operations. They may also include some sources like dry cleaning facilities which can be summed and treated as nonpoint sources because they are small and too abundant to account for individually. Nonroad mobile sources contain vehicular and movable sources with the exception of those that travel on roads. They are spread over an area during processing. Examples include trains, construction vehicles, boats and lawn and garden equipment. **Biogenic Sources** use land use data which is characterized by the type of vegetation within the domain. Emissions are estimated using Biogenic Emission Inventory System (BEIS) model based on the factors such as the distribution of vegetation, foliage density, temperature and solar radiation. Biogenic sources account for all natural emissions from vegetation, soils and lightning. **Mobile Sources** are vehicular sources that travel on roads such as gasoline and diesel vehicles. They are estimated with the internal MOBILE 6 model based on road type and vehicle classes, and are computed over a spatial extent. MOBILE 6 uses a special type of input called activity data which consists of vehicle miles traveled and can include vehicle speed. **Point Sources** are those which release emissions from isolated stacks or vents. They are largely industrial emissions, vertically distributed from sources such as electric generating utilities, refineries and chemical processing and manufacturing. They equal one tonne or more per year, and are identified by exact locations because they are regulated and their location are available in regulatory reports (Byun & Schere, 2006).

3.3.9 **Spatial Allocator - Surrogate and Vector Tools**

Spatial surrogate input files for SMOKE were developed with the Spatial Allocator version 3.6. The Spatial Allocator consists of the surrogate and vector tools, and was created from the Multimedia Integrated Modelling System (MIMS) Spatial Allocator. It is used to generate grid, E-Grid or polygon based spatial surrogates directly from shapefiles for use in SMOKE, where the input shapefiles are created using GIS software such as ArcGIS, and are available for the North American domain from the US EPA's ftp site (ftp://ftp.epa.gov/EmisInventory/emiss_shp2003). A spatial surrogate is a value greater than

zero and less than or equal to one. It specifies the fraction of emissions in a given area such as a county or province that is to be allocated to each grid cell that overlaps that particular area. This is an important part of air quality modelling because the accuracy of a simulation depends largely on its emission inputs. They are used to map county-level emissions data onto modelling domain by assigning a certain fraction of the emissions in an area, usually a county, to the individual grid cells that overlap that area. They are needed to provide data that is missing from the raw inventory files.

Chapter 4

Associated Exercises

4.1 Benchmark Case

Before an air quality model can be used for a simulation, it must be properly installed, compiled and tested for accuracy. These steps are essential to make sure the model is set up and running correctly. Before the benchmark case could be conducted, the system requirements for running CMAQ were addressed. First, the latest versions of the Current Versions System (CVS), Input/Output Applications Programming Interface (IOAPI) and Network Common Data Form (netCDF) libraries were installed, and then the CMAQ source code, scripts and benchmark data was unpacked and compiled. The Package for Analysis and Visualization for Environmental Data (PAVE) version 2.1 was also installed and compiled for viewing the information contained in CMAQ, SMOKE, MCIP and WRF output files. Once these installations were complete, the CMAQ version 4.2 benchmark case was run as outlined in the CMAQ 4.2 User's Guide, using nested domains over three days to test the setup of the model. The output was then compared with the dataset provided in the CMAQ distribution. After determining that the output matched, the following exercises were conducted to gain experience and knowledge in the process of air quality modelling.

4.2 Exercise 1: Bath Project

Although the benchmark case provided guidance on how to run CMAQ, it invoked only one specific configurations of the model. The model's actual setup can be modified in numerous ways depending on the objective of the simulation. Thus the main purpose of this exercise was to learn how to alter and run MCIP, SMOKE and CMAQ for my own specific modelling case. To do this, the MCIP, SMOKE and CMAQ models were employed to generate AQ data for the town of Bath with local emissions from the nearby Lafarge cement plant turned

off in order to provide a better understanding of the air quality impacts of the factory on the town of Bath. CMAQ output was created for the entire month of July 2007, with a three-day warm up period from June 27-June 30, 2007, for three domains (two nested). A Red Hat Linux platform was used with one node containing 4 CPU. Each CPU provided 1G of memory. This exercise involved installing and compiling MCIP version 3.1 which was the most current release of the model at the time. MCIP was used to prepare the meteorological fields for input into CMAQ as well as SMOKE version 2.1. The emissions dataset was generated from the US EPA's 1999 emissions inventory for the US and 1996 inventory for Canada. The output was compared against a reference set of CMAQ output that included the emissions from the Lafarge plant. This exercise was very useful as it provided experience in using MCIP and SMOKE, and helped to explain the processes involved in air quality modelling such as input generation and preparation for the CCTM. The practice and benefit of using nested domains was also investigated as three domains had to be run for each SMOKE, MCIP and CMAQ. Using nested domains allows for greater accuracy and higher spatial resolution locally (Mueller, Mao, & Mallard, 2010), and reduces the impacts of error propagation from the boundary conditions. Nesting however, is computationally intensive due to the increased number of grid cells involved in each successive domain. The wall-clock time required to produce a month's worth of data was also extensive because all models had to be run once for each domain, for each day. To run a single three-day simulation using two nested domains required approximately 10 hours of wall-clock time.

4.3 Exercise 2: A-MAPS Project

The second exercise conducted was to run CMAQ from December 1, 2007 to March 31, 2008 using a three day warm up period from November 28 to November 30, 2007. This is where the model was allowed to run prior to the modelling episode in order to smooth out any inaccuracies associated with the initial and boundary conditions. The MCIP, SMOKE and CMAQ scripts were altered according to the required specifications, and the model was

run for the same domains described in Section 4.2. After the first few weeks of the modelling episode were complete the CCTM was changed to run on multiple processors. This was a difficult task as the build and run scripts for the CTM had to be altered. A description of these changes can be found in Appendix A. After numerous trial runs in parallel mode, it was determined that the Parallel Virtual Machine (PVM3) version 3.4.5 library, which is used to support communication between multiple machines, was needed. Spending the time on this alteration was beneficial because running CMAQ on multiple processors significantly reduces the wall-clock time for each simulation. Each single-processor simulation for domains 1, 2 and 3 took 60 minutes, 2 hours and 7 hours, respectively, whereas the cluster simulations required approximately 2.5 hours in total to run all three domains. Once the parallel mode was established, simulations for the rest of the period were carried out and the final output was validated against concentration profiles and satellite measurements provided by A-Maps Environmental Inc. At a closer look of the results, I determined that this was because the data had been initialized every three days which kept setting the concentration of NO_2 to zero. This was an important realization because the ICs and BCs need approximately three days for their effects on the modelling episode to be minimized (C. J. Lin et al., 2005). Future simulations took this into account and the run scripts for the CCTM were altered accordingly.

4.4 Exercise 3: Model Updates

As new versions of air quality and supporting models are periodically released, it is beneficial for users to update their models to take advantage of the newest advances in tropospheric chemistry and transport. This exercise involved updating installing the latest releases of CMAQ, SMOKE and MCIP and the Spatial Allocator to simulate NO_2 for the year of 2007. The first step was to update CMAQ to version 4.7. This process was very time-consuming because version 4.7 had only been released a short time prior to this exercise, and had not yet been fully evaluated by the modelling community. Often model developers do not fully test and evaluate for bugs in the source code. Instead, they release

new versions and leave it up to users to discover and report back any problems which may exist in the chemistry or physical processes. After trying to compile CMAQ version 4.7 without success, I determined that it contained too many bugs which prompted me to move down a version to 4.6 which was still relatively new – as it had only been released in 2006 – but had been fully investigated and tested (Mueller et al., 2010). This proved to be a beneficial step because recent studies revealed that version 4.7 was seen to produce worse results in ozone studies (Foley et al., 2010). The same steps that were carried out in 4.1 were repeated with the updated versions of all libraries because each successive version of CMAQ usually requires a different release of libraries and supporting programs. That being said, the meteorological interface and emissions models needed to be updated as well in order for their output to be compatible with the new CMAQ.

Once the CMAQ benchmark case was successfully run according to the user's guide (US EPA, 2006), MCIP version 3.3 was installed. The output was fed into CMAQ along with emissions files from my old SMOKE model for a test run. The CMAQ run failed, and the errors suggested that the dry deposition of various pollutants were handled incorrectly. Further examination led to the conclusion that MCIP version 3.4 was the best adaptation to use with CMAQ version 4.6 because it was more 'robust' in its handling of dry deposition (Otte, 2009). After this change was made and the simulation was complete, SMOKE version 2.4 was installed and compiled. The 2005 U.S. emissions inventory was downloaded from the EPA's emissions inventory clearing house (2005 platform), and the 2006 Canada emissions inventory was provided by Dr. Sunny Wong from the Ontario Ministry of the Environment (MOE). The MOE's Canadian inventory was a more complete dataset than that provided by the EPA (Wong, 2010).

With the upgraded version of SMOKE, a new set of spatial surrogates needed to be created for compatibility with SMOKE. Surrogates are necessary to properly allocate pollutants over a given area. The Spatial Allocator version 3.6 was installed and a total of 68 surrogates

were created for three domains to supplement the inventories. These surrogates included land and water boundaries, population and housing information, road networks and land use among other categories. Processes such as weighting, filtering, merging and gapfilling were carried out to get the best spatial representation of the emissions.

After much work, time constraints dictated that updating the emissions model was not feasible, so the exercise was put to an end. Because SMOKE is a highly complex model, a great amount of time is required to fully understand the structure of the model and the interconnectedness of each file. File formats and inventories data are very specific and need to be individually chosen to suit each simulation. This exercise provided a great learning experience because it allowed me to become familiar with all the different aspects of air quality modelling, from the creation of the meteorology and emissions files, to the internal modules of CMAQ. Studying the set-up of each model and the work required to generate high quality CMAQ input provided the sound knowledge base required for my master's project in 3-dimensional air quality modelling

Chapter 5

Winter Study

5.1 Introduction

The troposphere – which extends from the Earth's surface to 10-18 km in altitude depending on the latitude and season – contains 85 percent of the atmosphere's mass (Jacob, 1999; Wallace & Hobbs, 2006) and its composition is influenced by transport processes in the planetary boundary layer (PBL) which is the lowest part of the troposphere (R. Atkinson, 2000; Wallace & Hobbs, 2006). Here, the atmosphere has direct contact with the Earth's surface; consequently it is within the PBL that pollutants are emitted into the atmosphere from anthropogenic and biogenic sources (Jacob, 1999; Wallace & Hobbs, 2006). Tropospheric NO_2 and O_3 are two such pollutants. The main supply of NO_2 is through conversion from NO when NOx is emitted into the lower atmosphere primarily through fossil fuel combustion from sources like road transport, power generation and industry (R. Atkinson, 2000; Environmental Monitoring and Reporting Branch of the Ontario Ministry of the Environment, 2009; van Noije et al., 2006). Ozone is a secondary pollutant generated through chemical reactions involving NOx and VOCs and is heavily dependent on meteorological conditions like sunlight and temperature such that O_3 episodes normally occur above 25°C (Sillman, 1993).

Despite the need for warm temperatures, O_3 episodes do still occur in the winter even though formation efficiency and solar radiation are limited. This aspect of O_3 differs from other pollutants like sulphur dioxide (SO_2) or carbon monoxide (CO) (Sillman, 1993; Tesche et al., 2006) which are more concentrated under cold weather conditions and sparse sunlight. Most O_3 investigations do not focus solely on the winter season (Eder & Yu, 2006), but some authors have examined these uncommon wintertime events to try to understand the seasonal cycle of O_3, its precursors as well as the photolysis reactions associated with their formation

and destruction. Zhang et al. (2006) reported that CMAQ was able to sufficiently simulate various pollutant species during the winter months in East Asia, though O_3 was overestimated and NO_2 values larger than 1.20 ppb were not easily reproduced. In North America, Chtcherbakov et al. (2002) found that modelled and measured NO_2 showed good correlation for a high O_3 conditions in the winter of 1998. In this chapter, the focus will be on O_3 and NO_2 simulations for the first three months of 2005 which experienced higher than normal O_3 levels.

5.2 Method

The spatial and temporal distributions of O_3 and NO_2 over the cities of Ottawa and North Bay were evaluated by pairing the model results with the measurements extracted from the MOE's Air Quality (AQ) network stations in those respective cities. The daily 1-h average and diurnal cycles, 8-h maximum and 8-h average values for O_3 and NO_2 were analyzed along with wind speed and wind direction. The urban AQ station was located at Rideau Street/Wurtemburg Street in downtown Ottawa at an elevation of 68 meters with an air intake height of 4 meters. The rural AQ station was found at Chippewa Street West at the Department of National Defence in North Bay, at an elevation of 219 meters with an air intake height of 4 meters. Though North Bay's station is close to human activity, its population is substantially lower relative to Ottawa's population which makes it suitable to representative the rural site. Ozone and NO_2 measurements at these sites were recorded every minute then averaged over one hour to produce an hourly datasets for each day of the year.

5.2.1 **Modelling Domain**

A modelling domain incorporates the area of interest which accounts for local emissions, as well as an external area that, based on wind patterns, can sufficiently account for the long range transport of pollutants into the area of interest. Figure 3 shows the CMAQ modelling domain which is centred at 45ºN and 90ºW and encompasses all of Southern and Central Ontario including the cities of Ottawa located at 45º25'N and 75º40'W and North Bay located at 46º19'N and 79º26W. The domain also incorporates the north eastern U.S around the Great Lakes basin in view of the fact that the air quality in Ontario is highly impacted by transport from the United States. It contains 79 x 71 grid cells with a horizontal resolution of 36 km and 19 vertical layers which extend from the surface to the height of 100 mb. The layers are measured in sigma coordinates which are defined as the ratio of the pressure at a given altitude to the pressure on the surface of the earth below.

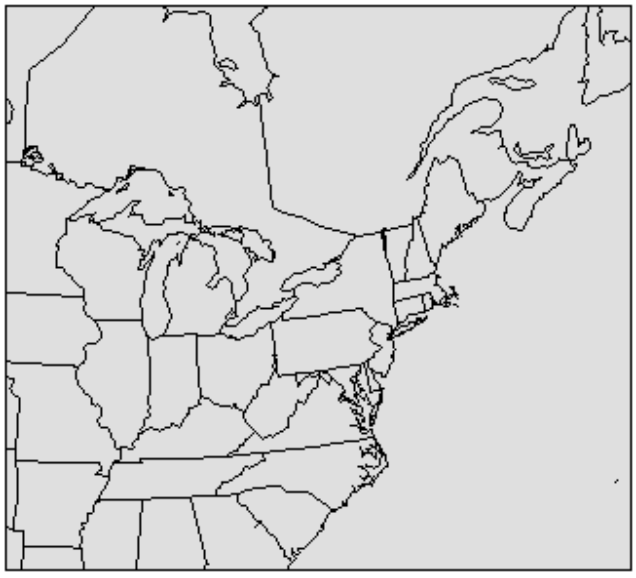

Figure 3. The CMAQ modelling domain used in this study with a resolution of 36 x 36 km.

Ozone and NO_2 were simulated using CMAQ version 4.6 (Byun & Schere, 2006) on a Red Hat Linux cluster containing 8 nodes. The SAPRC-99 gas phase chemical mechanism (W. Carter, 2000b), Euler backward interactive (EBI) solver (Hertel, Berkowicz, Christensen, &

Hov, 1993) and AERO3 aerosol module were used to simulate the transport and chemical transformations in the troposphere for the period of January 4 to March 31, 2005. The simulation was initiated assuming a clean atmosphere by using the background default profiles for the boundary and initial conditions that were provided with the CMAQ package. To minimize the propagation effects of these and establish a realistic atmosphere during the period of interest, a two day spin up period was allowed at the beginning of January (Jimenez, 2007; C. J. Lin et al., 2005; Wong, 2010). The CMAQ simulation options used in this study are listed in Table 4.

Table 4. CMAQ simulation options invoked for this study.

Parameters	Settings[a]
Mass consistency adjustments	Yamartino scheme for mass-conserving advection
Coupling-decoupling scheme	Generalized coordinate system
Horizontal advection	Piecewise Parabolic Method
Vertical advection	Piecewise Parabolic Method
Horizontal diffusion	Multiscale diffusion
Vertical diffusion	Eddy diffusivity theory
Photolysis	Photolytic rate constants
Plume in grid	Not invoked
Gas phase chemistry solver	Euler Backward Iterative solver for SAPRC-99 mechanism
Aerosol model	Aerosol solver 3
Aerosol deposition velocity	Aerosol deposition velocity routine
Cloud dynamics and aqueous chemistry	Asymmetric convective model based on Regional Acid Deposition Model

[a] A description of the settings can be found in Wang et al. (2004) and Skamarock et al. (2005).

5.2.2 **Meteorology and Emissions**

The 2-D and 3-D, gridded meteorology and emission fields were provided by Dr. Sunny Wong and Dr. Andrei Chtcherbakov from the Ontario Ministry of the Environment's Air Monitoring and Reporting Section. The meteorological data were created using the Weather Research and Forecasting (WRF) Model version 3.2, and were processed for CMAQ using MCIP version 3.4. The meteorological physics options, outlined in Table 5, were invoked according to findings by Challa et al. (2007). The U.S.A. O_3 and NOx emissions were based on the EPA's National Emission Inventory (NEI) 2005 based platform which takes into account the NO_2 emissions changes due to the EPAs NOx State Implementation Plan (SIP Call) and were processed by SMOKE version 2.4. The Canadian inventory was updated to include heat island effect to provide a more comprehensive output. The Spatial Allocator version 3.6 produced the spatial surrogates to supplement the emissions, while SMOKE used the Biogenic Emissions Inventory System version 3.14 (BEIS 3) and the MOBILE6 model to compute natural surface emissions and gridded motor vehicle emissions for the period, respectively.

Table 5. WRF physics options used in this study.

Parameters	Settings [a]
Grid Spacing	36 km x 36 km
PBL Scheme	YSU
Cumulus paramterization	Kain-Fritsch (new eta)
Microphysics	WSM 3-Class Simple Ice
Longwave Radiation	RRTM
Shortwave Radiation	Dudhia
Surface Layer Scheme	Monin-Obuk
Land-Surface Scheme	NOAH Land-Surface Model
Number of Layers	19

[a] A description of the settings can be found in Wang et al. (2004) and Skamarock et al. (2005).

5.2.3 **Statistical Analysis**

In the modelling community there is no universally accepted set of performance measures used to determine if the correlation between model predictions and ground measurements are satisfactory (Brulfert et al., 2007). Various forms of bias and error have been proposed in air quality studies (Appel et al., 2007; Chen, Stein, Zubrow, & Kotamarthi, 2006; Russell & Dennis, 2000; D. Tong & Mauzerall, 2006), all of which provide valuable insight into the accuracy of model predictions. In 1991, the US EPA created a comprehensive list of statistical measures that it recommended as a guideline for CMAQ users to follow when examining predicted ozone concentrations (US EPA, 1991). The following evaluation metrics – which have been applied extensively in past investigations (C. Hogrefe, Rao, Kasibhatla, Hao et al., 2001) – were used in this study to compare the similarity of the model O_3 results with measurements given the importance the EPA has place on them (D. Tong & Mauzerall, 2006). The measured data was extracted from the Ministry of the Environment's Ambient Air Quality Monitoring Network for North Bay, Chatham and Ottawa. At least 75 percent of the hours covering the modelling period were available for all three sites, as suggested by Tong et al., 2006.

Mean Normalized Bias Error (MNBE)

$$\text{MNBE} = \frac{1}{N} \sum_{i=1}^{N} \left[\frac{Cmod\,(i) - Cobs\,(i)}{Cobs\,(i)} \right] \times 100\% \tag{28}$$

Mean Normalized Gross Error (MNGE)

$$\text{MNGE} = \frac{1}{N} \sum_{i=1}^{N} \left[\frac{|Cmod\,(i) - Cobs\,(i)|}{Cobs\,(i)} \right] \times 100\% \tag{29}$$

Unpaired Peak Prediction Accuracy (UPA)

$$\text{UPA} = \frac{Cmod\,(i)\,max - Cobs\,(i)\,max}{Cobs\,(i)\,max} \times 100\% \tag{30}$$

Here N indicates the number of observation-model pairs, C*mod* and C*obs* indicate the modelled and observed O_3 concentrations at each site, respectively; and *max* refers to the maximum observed or modelled O_3 value for the period.

The MNBE represents the scale of the error for the modelled O_3 relative to the observed measurements at the specified site. The MNGE is used as an indicator of the model's precision as it calculates the mean unsigned error for the simulated O_3 and relates the error to the observed measurements. Both tests can be limited to cases where the observed concentrations are above a predetermined minimum, such that observation-prediction pairs are excluded from the analysis when the observations fall below the set minimum value. This cut-off value, which is normally set to the average background concentration of ozone in the region of interest, varies among studies (Brulfert et al., 2007; C. Hogrefe, Rao, Kasibhatla, Hao et al., 2001). For example, Tong et al. (2006) used a cut-off value of 40 ppb when evaluating summertime O_3 concentrations across the continental U.S., while Russell et al. (2000) set the cut-off value to 60 ppb. I chose not to impose any limits in my analysis because this study is interested in the total ozone emissions in Ottawa, Chatham and North Bay, and not just those values above the background levels.

The last parameter, the UPA, is used to compare the maximum predicted and observed values over all hours in the modelling period. The general ranges of acceptability for these tests are $\pm$5-15% for the MNBE, $\pm$30-35% for the MNGE and $\pm$15-20% for the UPA (US EPA, 1991); however, the EPA does suggest that these criteria alone should not be used as the determining factors for model accuracy. To supplement these calculations, a fourth measure was called the Mean Bias (MB) was used. This expresses model bias in actual (ppb) values (Eder & Yu, 2006; Eder, Kang, Mathur, Yu, & Schere, 2006), and was used to evaluate both O_3 and NO_2 in this study

Mean Bias (MB)

$$\text{MB} = \frac{1}{N} \sum_{i=1}^{N} Cmod\ (i) - Cobs\ (i) \qquad (31)$$

Though this particular calculation was not specified by the EPA in its report, it has been frequently employed in other O_3 and NOx investigations (M. Zhang et al., 2006). It is an important tool in air quality modelling because it provides a quantitatively allows one to assign an amount by which the modelled and measured datasets differ. Graphical examination should also be used to visually inspect the correlation between predicted and measured concentrations. The combination of all of the above techniques can provide a powerful analysis.

5.3 Results and Discussion

5.3.1 **Spatial Variability of Model Performance**

Figures 4 and 5 present simulated and measured daily 1-h average ozone and NO_2 mixing ratios, respectively, for February 5, 2005. This day was chosen at random to illustrate the winter diurnal, spatial patterns of O_3 and NO_2. A comparison of these figures shows that CMAQ is generally able to simulate the spatial distribution of surface O_3 throughout southern Ontario and the north eastern United States. Ozone follows a predictable intraday cycle where its concentration drops during the morning and evening rush traffic hours, but peaks between 11 am to 3 pm during what is typically the brightest, most photochemically active time of the day (Geddes et al., 2009). This diurnal cycle is represented qualitatively in Figure 4a and b which illustrate the morning rush hour at 7 am local time (12 UTC) and the peak ozone production hour at 1 pm local time (18 UTC), respectively. During the morning traffic which is approximately 7-9 am, it can be seen that ozone mixing ratios are low over the entire domain as expected due to the scavenging of O_3 by the sudden influx of NOx emissions from motor vehicles. The range of O_3 levels over most of Ontario in Figure 4a is roughly 25-34 ppb, which earlier studies (Yap, Ning, & Dong, 1988) have suggested to be just below the range of background ozone levels for the area (30-50 ppb hourly maximum) though most of these studies focus on the summer months.

In contrast to Figure 4a, Figure 4b displays O_3 during the prime ozone time of the day with the highest amount of photochemical radiation. At this time, the morning traffic has subsided, and the large mobile source NOx emissions have ceased. Here, CMAQ ozone mixing ratios are around 34 ppb in southern Ontario and reach 50 ppb in parts of the eastern and mid-western U.S. It should be noted however that while the maximum value on the scale is 50 ppb, ozone levels may have exceeded this value in these regions. Any exceedance is not shown though, due to the limits of the scale. The spatial distribution of ozone in these figures is in agreement with the distribution of NO_2 in Figures 5a and b which illustrate the peak NO_2 spatial distribution. This is a clear example of the O_3-NO_2 diurnal cycle because it shows that low O_3 mixing ratios due to titration by NOx at times when NO_2 is high. This is due to the non-linear chemical coupling of ozone and nitrogen dioxide (Mazzeo, Venegas, & Choren, 2005). In these figures, 'spots' of high concentrations of NO_2 can be seen over large urban centres in the domain such as Detroit-Windsor, Toronto, Ottawa, New York, parts of the Ohio River Valley as well as cities along the south-eastern seaboard. This is precisely what is expected due to the high volume of commuter traffic in cities. High ozone concentrations (30-35 ppb) can also be seen over the St. Lawrence River. Though this waterway experiences a great volume of shipping traffic which is provided for in the mobile emissions and surrogate files, the concentration shown is large enough to suggest that meteorological factors allow ozone to accumulate to appreciable levels. Because the St. Lawrence River Valley is at the east end of the Windsor-Quebec corridor, it is subject to the long range transport (LRT) of pollutants from Southern Ontario and the Midwestern U.S.A.

Figure 6a-c portray the wind direction in degrees for 6-20 UTC for February 5 2005. Figure 6d-f show the corresponding change in O_3 mixing ratios over the entire domain. As the wind direction slowly changes (decreasing in degree) over the fourteen hour period, the ozone levels surrounding the St. Lawrence River slowly decrease toward 31 ppb. At 12 UTC, the area around the St. Lawrence is predominantly green indicating ozone levels of about 34-40 ppb. The wind direction along the eastern United States at the same time is about 308-360

degrees (north-west to north directions) as indicated by the orange and red colours in Figure 6a. This north/north-west wind pushes along the U.S. coast and drags with it ozone and precursors from heavily polluted cities like New York and Philadelphia. Because ozone can persist in the troposphere for a few days, it has the potential to travel great distances (Yap et al., 1988) and accumulate within an air parcel. This explains why CMAQ generated high levels of O_3 over the St. Lawrence River.

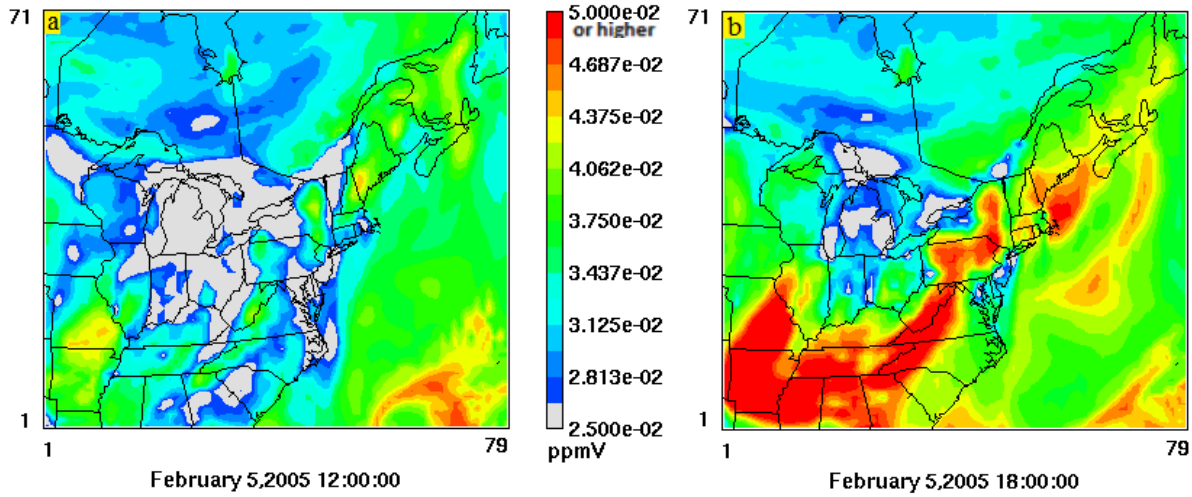

Figure 4. Surface mixing ratios of ozone (O_3) over Ontario and the north eastern U.S. for February 5 2005 during (a) the morning rush traffic hour at 7 am local time (12 UTC) and (b) the expected daytime high at 1 pm local time (18 UTC).

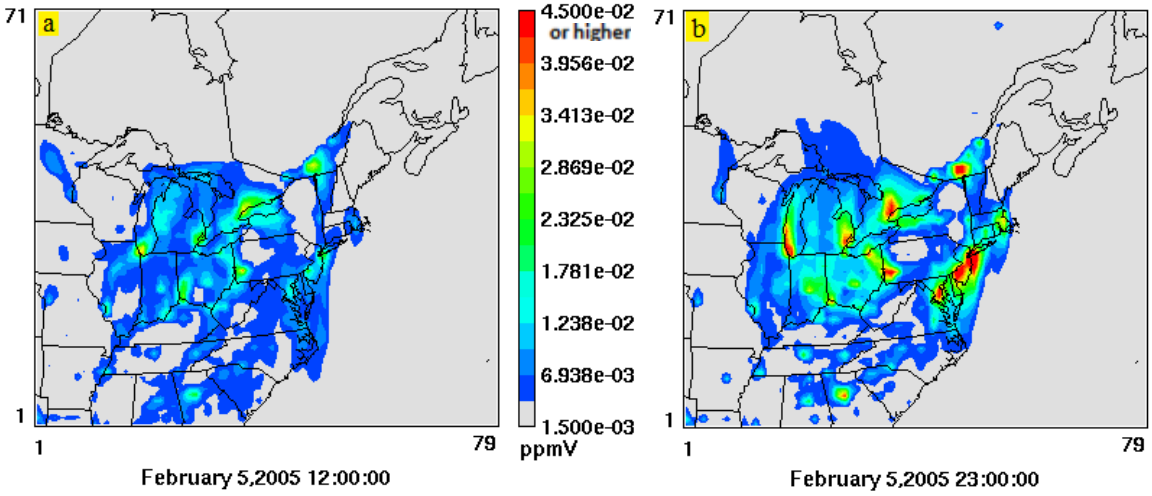

Figure 5. Nitrogen dioxide (NO_2) spatial distribution over southern Ontario and the north eastern U.S. for February 5 2005 during (a) the 7 am morning rush traffic hour and (b) the 6 pm evening rush traffic hour.

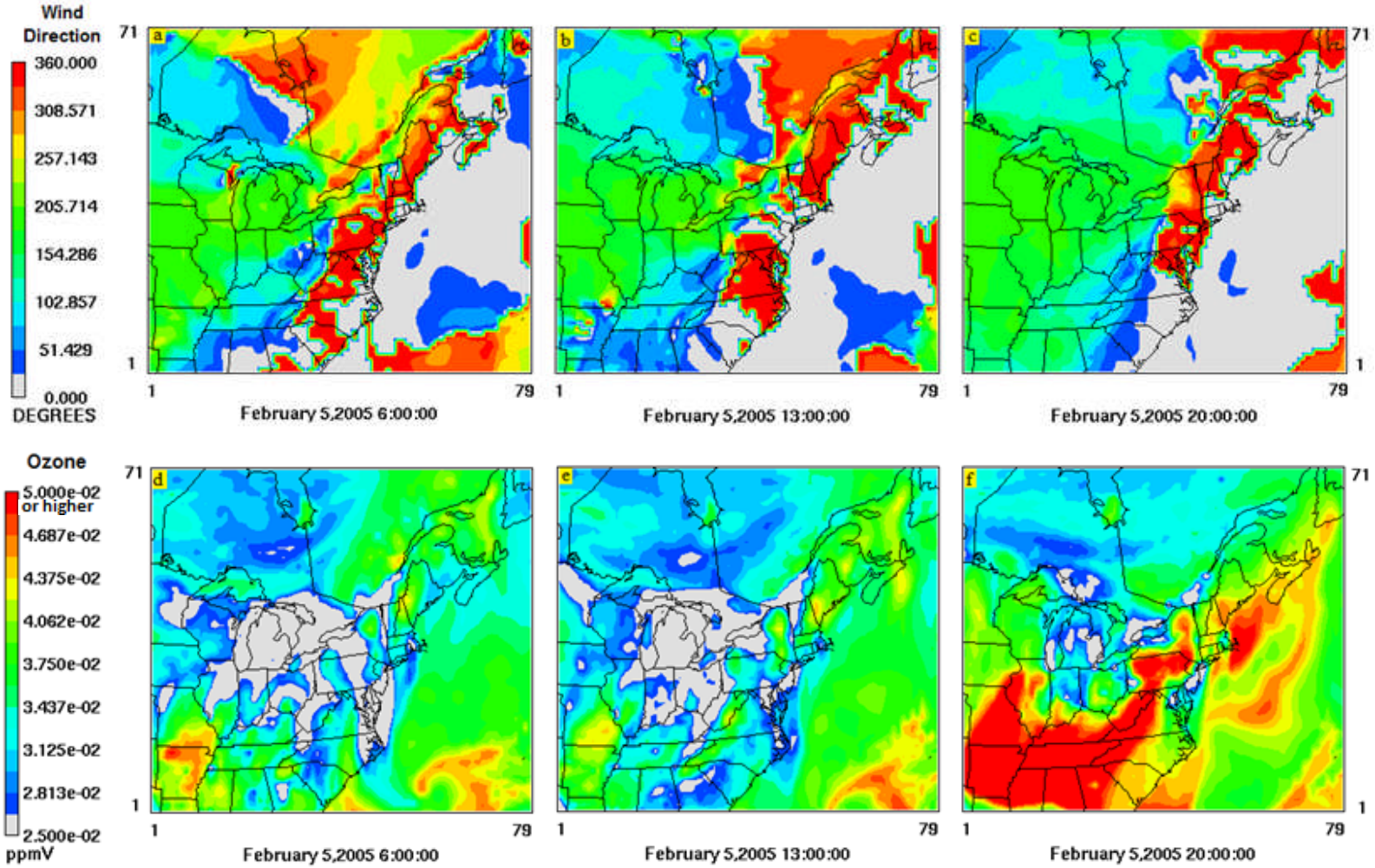

Figure 6. The wind direction over a representative fourteen hour period during the winter of 2005 (top panel), and the corresponding ozone (O_3) changes over the same period (bottom panel). North (348.75-11.25), east (78.75-101.25), south (168.75-191.25), west (258.75-281.25).

5.3.1.1 *Quantitative Analysis: Base Case*

Figure 7 compares the modelled 1-h average surface O_3 concentrations for North Bay and Ottawa with the O_3 concentrations from the MOE monitoring network stations in co-located grid cells. The entire domain is not shown in these plots. Instead, a close up image focusing on the three areas of interest in southern Ontario is seen. Here, the spatial allocation of ozone at each monitoring site based on the statistical parameters in Table 6 and Table 7 is visualized. Though CMAQ was able to capture the domain-wide spatial variation of O_3 and NO_2, quantitative analysis shows that it tends to over-predict ozone when its results are directly compared to both sites, but systematically under-predicts NO_2 at each site within the range of about -4 ppb to -8 ppb. The statistics for NO_2 show a much greater negative bias compared to those for O_3 because NO_2 is more sensitive to errors that exist in the emissions and meteorology data, especially under slow moving or stagnant wind conditions (Yu, Sokhi, Kitwiroon, Middleton, & Fisher, 2008). These results are not surprising because many ozone and NOx modelling studies have reported a systematic under-prediction of ozone precursors (Russell & DennisOn assignment to the Atmospheric Research and Exposure Assessment Laboratory, U.S. Environmental Protection Agency, Research Triangle Park,NC 27711., Robin, 2000). The over- and under-predictions of both species are connected to each other since the cycling of NO_2 and O_3 is governed by the null cycle (Equations 1-3).

Table 6. Model evaluation statistics for hourly ozone mixing ratios for January-March 2005.

City	Month	MB (ppb)	MNBE (%)	MNGE (%)	UPA (%)
North Bay	January	7.17	145	151	3
	February	3.07	115	127	-9
	March	0.13	122	149	-15
	Winter Total	3.35	128	143	- 15
Ottawa	January	5.84	128	137	34
	February	2.25	159	177	8
	March	-2.79	14	45	12
	Winter Total	1.56	91	111	12

Table 7. Mean Bias for hourly nitrogen dioxide (NO_2) concentrations for January-March 2005.

	January (ppb)	February (ppb)	March (ppb)	Winter Total
North Bay	-7.25	-8.39	-10.42	-8.75
Ottawa	-4.08	-7.50	-1.82	-4.37

Ozone spatial patterns in Figure 7 indicate that CMAQ performs adequately in estimating ozone in southern Ontario, given that the wintertime MB at both monitoring stations are relatively low (0 ppb $<$ MB $<$ 5 ppb). Conversely, consistent negative values for NO_2 across both sites denote that CMAQ under-predicts observed concentrations of up to 10 ppb for North Bay and up to 5 ppb for Ottawa. The MNBE values (Figure 7) however, reveal a positive bias for all sites that greatly surpasses the accepted range of 15 -20% thus illustrating the inability of the model to replicate ozone concentrations across southern Ontario. This over-estimation is also seen by the MNGE (Figure 7) which is well outside of its satisfactory range of 30-35%. The UPA pattern for North Bay was the only statistic that was within the EPA's recommended range ($\pm$15-20%) while the UPA for Ottawa was just outside this range at 12%. These statistics are not surprising because the amount of NOx present in urban centres due to motor vehicles almost always exceeds that which is accounted for in the mobile emissions inventories. The scavenging of O_3 by NOx, process which is more pronounced in the winter than in the summer, limits the daily concentration of ozone in city centres as well as areas along major roadways. Some studies have shown this reduction to be as high as 50% on average (McKendry, 1993).

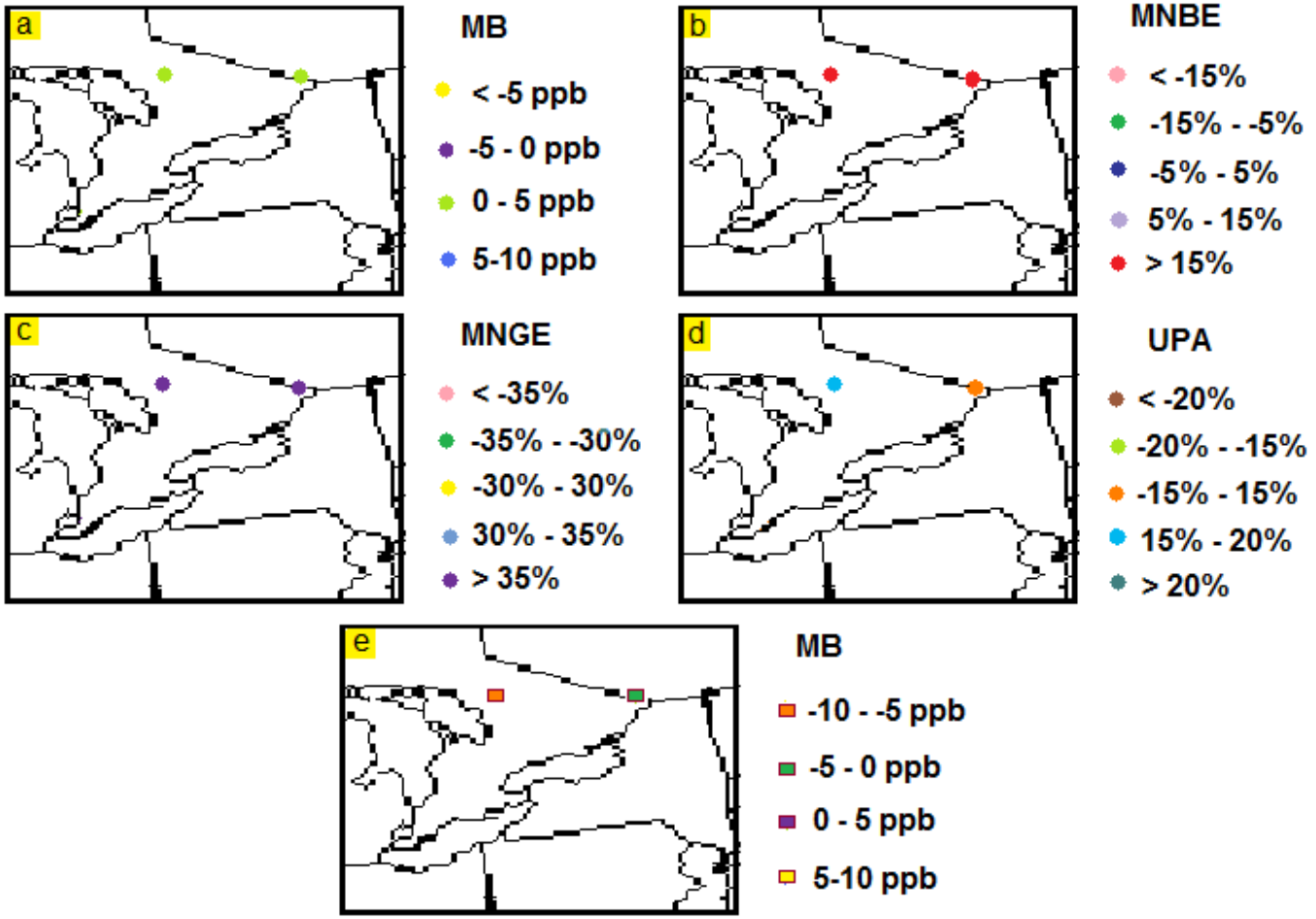

Figure 7. A statistical comparison of (a) mean bias, (b) mean normalized bias error, (c) mean normalized gross error and (d) the unpaired peak prediction accuracy for the 1-h average surface ozone (O_3) mixing ratios between CMAQ output and the individual monitoring stations at North Bay and Ottawa. Mean bias for (e) nitrogen dioxide (NO_2) 1-h average mixing ratios are also reported. Model predictions that did not have a corresponding measurement value were not included in the analysis.

5.3.1.2 *Quantitative Analysis: Cases 2 and 3*

To further evaluate the model's spatial performance, the statistical parameters outlined in Section 5.2.3were recalculated using the same datasets from the previous section – both AQI station measurements and CMAQ output – but with applied cut-off values of 30 ppb for Case 2 and 40 ppb for Case 3 (i.e. all data pairs containing measurements below the specified cut-off value were not used in the analysis). This method is similar to that outlined in Tong et al. (2006) where three different limits of 20 ppb, 40 ppb and 60 ppb were imposed on an ozone summertime experiment to assess the propensity toward positive or negative bias in CMAQ output. Tong et al. (2006) used 40 ppb as the initial cut-off value to eliminate the contributions of background O_3 levels, and then applied additional limits to further test the performance of CMAQ. While many ozone studies use 40 ppb as a cut-off value (Brulfert et al., 2007), in this project the limiting value of 30 ppb was chosen first for Case 2 because 40 ppb is often used as the cut-off in summertime ozone analysis (Brulfert et al., 2007), and so a lower level must be chosen for winter investigations to eliminate the background ozone contribution since ozone production in the winter is less efficient due to decreased solar radiation and temperatures (H. Wang et al., 2009). After this, the mixing ratio of 40 ppb was applied to the dataset to get a better understanding of CMAQ's performance as a function of O_3 concentration. The statistical analysis for each case is presented in Table 8 and Table 9, respectively. Only the overall winter totals were plotted for Case 2 and Case 3, as opposed to the monthly values as in the Base Case because the number of usable model-measurement pairs for each month became less than 75% of the hours in each month (D. Tong & Mauzerall, 2006; Yu et al., 2008) with each successive limit. For example, the number of data pairs for North Bay that met the 40 ppb limit in January was only 1% of all January measurements. This number was even smaller for Ottawa where no measurements above 39 ppb were recorded.

Table 8. Model evaluation statistics for hourly ozone (O_3) concentrations for January-March 2005 using a measurement cut-off value of 30 ppb.

	MB (ppb)	MNBE (%)	MNGE (%)	UPA (%)
North Bay	-4.95	-11	15	-15
Ottawa	-5.27	-15	18	12

Table 9. Model evaluation statistics for hourly ozone (O_3) concentrations for January-March 2005 using a measurement cut-off value of 40 ppb.

	MB (ppb)	MNBE (%)	MNGE (%)	UPA (%)
North Bay	-9.50	-21	21	24
Ottawa	-7.84	-19	23	12

These statistics show that the MB for North Bay and Ottawa are increasingly negative with a cut-off value of 30 ppb and 40 ppb, but positive when no cut-off value was used (Table 6), indicating that CMAQ overestimates surface ozone at low concentrations, but underestimates ozone levels above 30 ppb. This shift in model performance toward underestimation was also observed by Tong et al. (2006). Compared to the Base Case, CMAQ underestimates with a larger bias for both sites when the cut-off values were applied. This pattern is consistent with many other studies which have found CMAQ simulations to be negatively biased at higher O_3 levels (Appel et al., 2007). Evaluating Table 8 and Table 9 against the criteria outline by the EPA (section 5.2.3) one can see that the MNBE for Ottawa and North Bay both lie within the suggested range of $\pm$ 5-15% when 30 ppb is used as a cut-off, but fall outside that range with a 40 ppb limit. The MNBE in these cases are much smaller than the MNBE for the Base Case which had a very large positive bias in the absence of a cut-off. The MNGE for all sites still do not meet the $\pm$ 30-35 percent condition of accuracy, but the biases in Cases 2 and 3 are much smaller than in the Base Case. Lastly, the UPA for North

Bay with a 30 ppb cut-off was the only UPA value to meets the EPA's criteria ($\pm$15-20) for maximum ozone accuracy.

The discrepancies between the model output and measurements shown in this section are possibly caused by erroneous emissions input which greatly influence the spatial distribution of ozone and NO_2. This is illustrated by the systematic overestimation by CMAQ at both sites as revealed by the statistical calculations when no cut-off value was used. More likely the source of the error however was the comparison between point measurements and grid-averaged model concentrations. The quantitative analyses provided also make it evident that the tendency of CMAQ's simulations toward over- (under-) prediction is somewhat subjective depending on the criteria used for evaluation. Thus, to properly evaluate the model and determine the source of the inaccuracies, the temporal patterns of O_3 and NO_2 need to be analyzed

5.3.2 **Temporal Variability of Model Performance**

5.3.2.1 *North Bay*

In order to evaluate the model's ability to replicate the temporal distribution of O_3 and NO_2 in a rural setting, I compared the hourly modelled concentrations of these species to the observed levels obtained from the MOE's AQ monitoring network. Figure 8 illustrates the 1-hour O_3 time series comparisons for the months of January to March 2005 for North Bay. Time series are an important part of any performance analysis because they can expose bias within the modelled output (US EPA, 1991). By observing these graphs it can be seen that for the duration of the winter period, CMAQ was unable to correctly reproduce the lower concentrations of O_3. The general temporal pattern for the hourly data is similar between the model and measurements in terms of the timing of the ozone maxima and minima; however the amplitudes of the peaks showed a lot of bias. The ozone measurements are seen to decline to zero or close to zero from the evening into the early morning hours and do not

begin to rise again until after the morning traffic has ceased. Though one would not expect to observe traffic patterns at rural sites, the North Bay station does experience vehicular traffic do to its proximity to human activity; though North Bay does not experience the same intensity in traffic flow as downtown Ottawa. These extremely low O_3 levels can be attributed to extreme pollution due to slow moving or stagnant wind conditions – which allow for O_3 titration – combining with ground level inversions caused by a shallow planetary boundary layer (PBL) (Fraser, 2010), as will be discussed shortly. This event which can carry over into the mid-morning is more often associated with urban sites due to their abundance of NOx. Given the proximity of North Bay's monitoring station relative to the Jack Garland airport – 10 minutes south west – it is not surprising that high NOx conditions exist there. The modelling results, however, do not match these low mixing ratios. This is most likely because of the datasets being used in the comparison. The model results were created from concentrations averaged across a 36 km x 36 km grid cell while the measurements were hourly averages obtained from a single point located within the grid cell. The coarse 36 km-averaged concentrations are thus not quite representative of point measurements.

This was supported by the corresponding scatter plots (Figure 9) which had very poor correlations as seen by the correlation coefficient (R^2) values which are all below the acceptable minimum of 0.50. Scatter plots are necessary for an air quality analysis because they reveal the extent of the bias between the model-measurement pairs based on the arrangement of data points along the perfect correlation line. The more dispersed the points are from this line, the greater the error in the simulation (US EPA, 1991). Figure 9 shows great amounts of dispersion away from the perfect correlation line. Because of this poor correlation between the model results and measurements it is difficult to see any distinct pattern in the plots, though there is a slight underestimation of ozone mixing ratios toward the higher range of O_3 concentration in plots for February and March. These results are consistent with the hourly time series and are confirmed by referencing back to the statistical

metrics from Table 6. These statistics show that the winter UPA has a value of -15%. Though this falls within the acceptable range (±15-20%) it appears that CMAQ underestimates peak O_3 concentrations, suggesting that the reactivity of the ozone (production) chemistry in the CCTM is not sufficient. The hourly time series also shows that CMAQ is unable to replicate the lower levels of ozone which causes a systematic over-prediction resulting in an overall winter MB of 3.35 ppb. Though this value is not very large, the values for the MNBE, MNGE show poor model performance overall as they are all outside of the recommended ranges provided by the EPA. The only parameter within its acceptable range is the UPA which has a value of -15 and is used to determine the model's ability to reproduce the maximum ozone concentrations for the period. This statistic for North Bay matches the trend seen in the hourly CMAQ time series where CMAQ is able to replicate higher ozone values. As previously mentioned, these results are not surprising since the model results are hourly averaged concentrations, averaged over a 36 km x 36 km grid cell, whereas the measurements are taken at a single point within the grid cell.

The maximum and average 8-hour O_3 concentrations were also plotted to further determine how well CMAQ captures peak ozone levels during the winter (Figure 10), and their statistical metrics are displayed in Table 10Table 10 and Table 11. These time series are important from a regulatory point of view since the Canada Wide Standard of 65 ppb is based on an 8-h averaging time, and the US EPA uses an 80 ppb daily 8-h maximum as its health and monitoring guideline. Neither standard was exceeded during the modelling period, although Figure 8c reveals that the measured 8-hour maximum did reach as high as 64 ppb at the end of March. CMAQ was not able to match this value. The summary statistics show a gradual trend from overestimation to underestimation for the 8-hour maximum values, while the 8-hour average displays a decline in MB from about 7.5 ppb to less than 1 ppb. The UPA calculations span a broad range in both tables, but both have an overall negative winter total. The day to day variations in the CMAQ simulations in general replicate the observed data, although timing of the maxima are slightly out of phase and the amplitude of the peaks do

not match each other. On a handful of days CMAQ predicts high ozone levels relative to the measurements, while February and March show model under-predictions. Though these results are poor, they must be further compared to NO_2 time series and diurnal cycles to fully gauge the capability of the model.

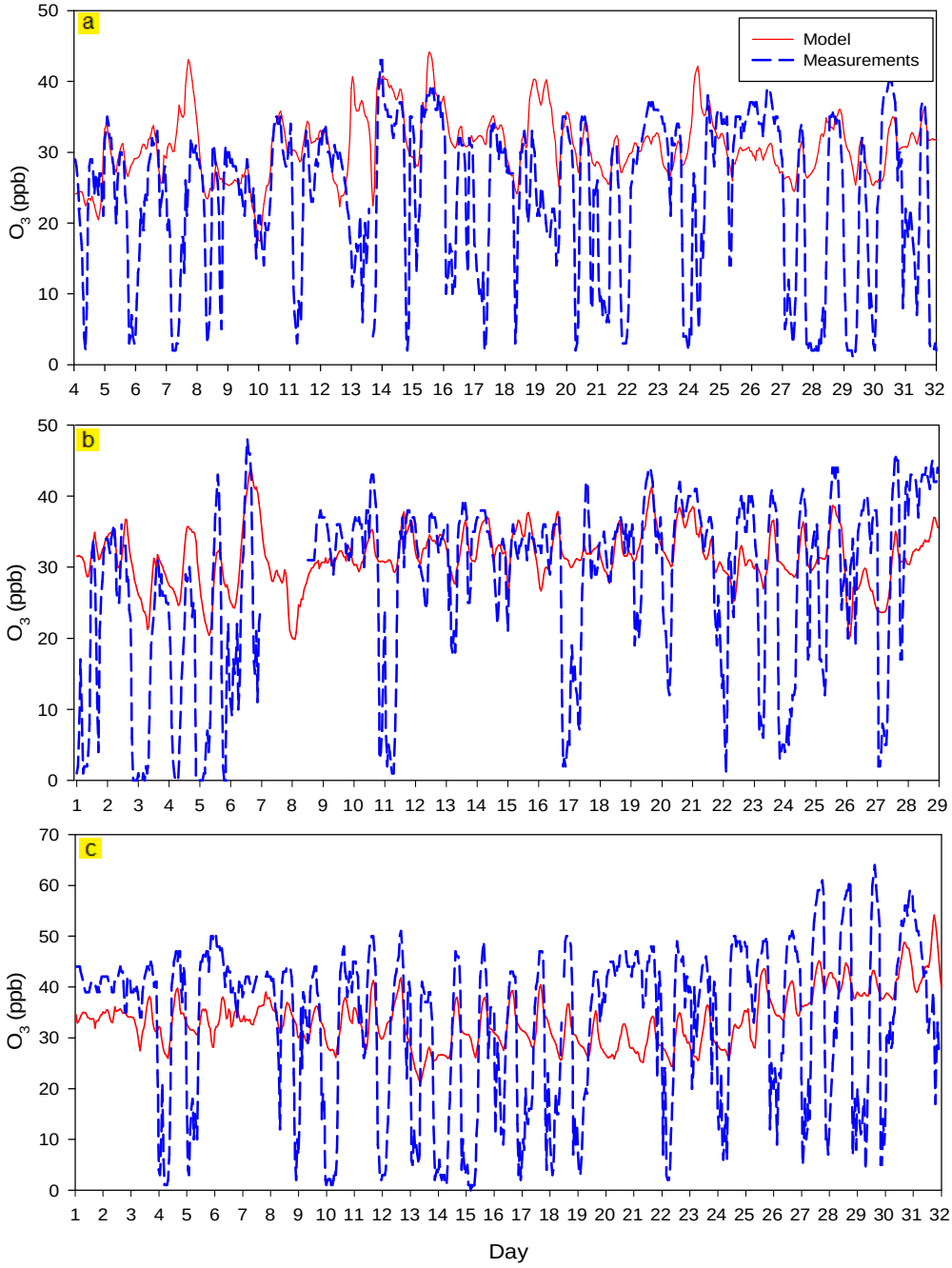

Figure 8. Comparisons of modelled (—) and measured (--) 1-h averaged surface ozone (O_3) mixing ratios for North Bay during (a) January, (b) February and (c) March 2005.

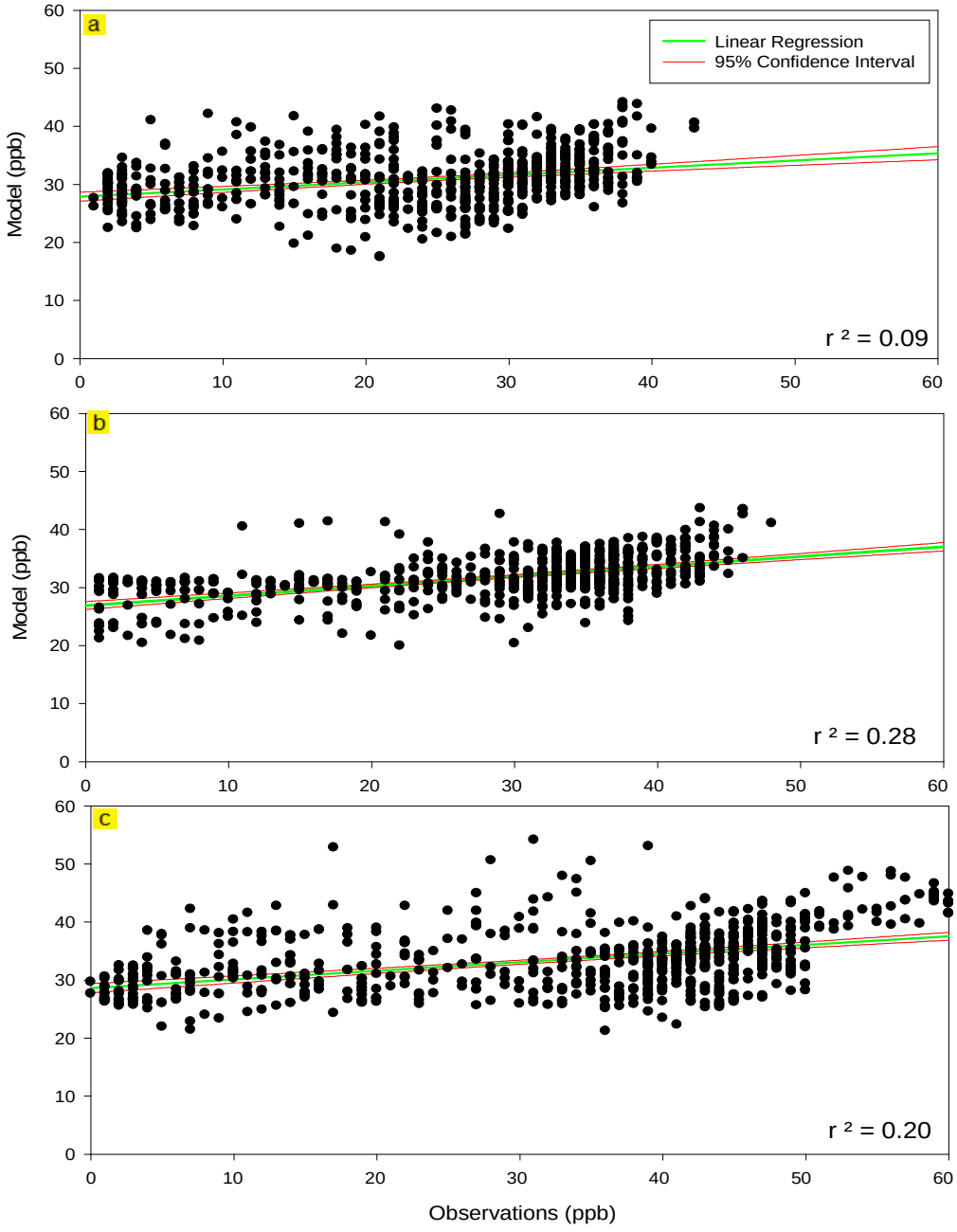

Figure 9. The 1-h averaged ozone (O_3) scatter plots of model results plotted against measurements taken from the provincial monitoring station for North Bay during (a) January, (b) February and (c) March 2005.

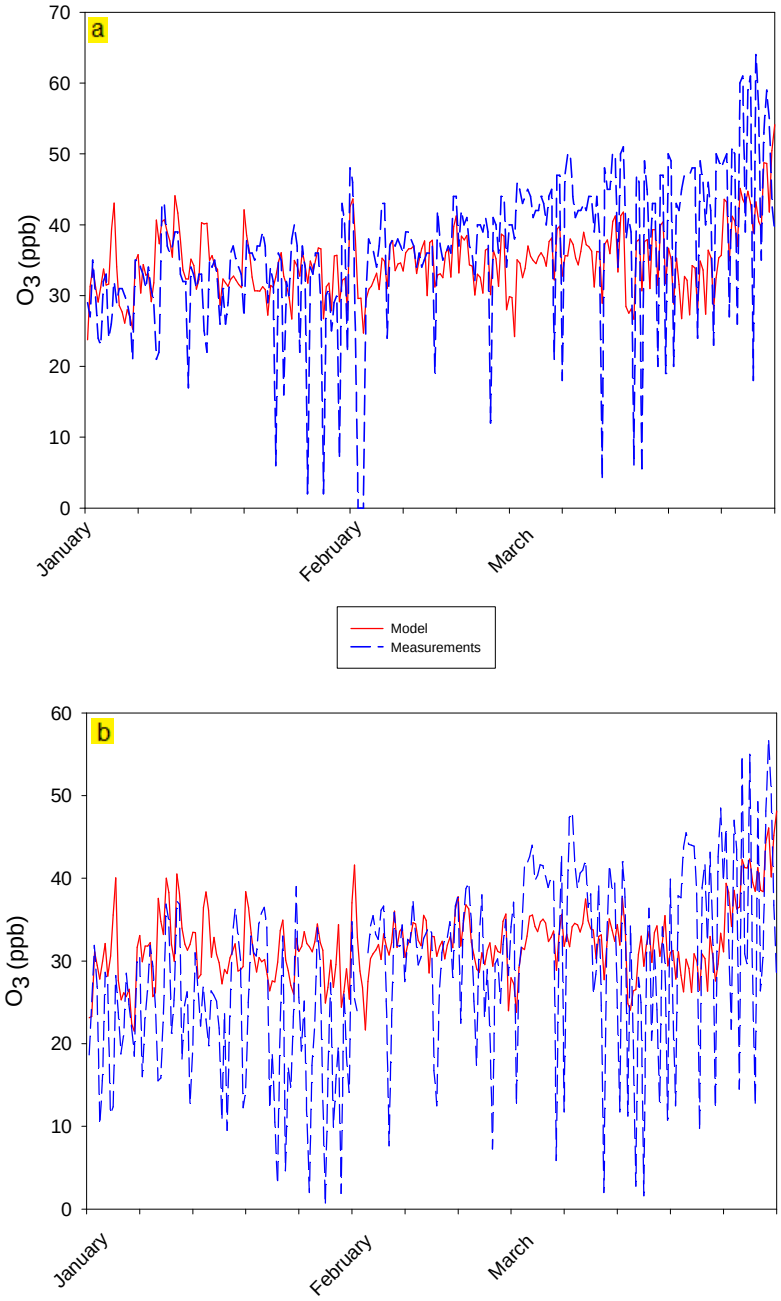

Figure 10. Comparisons of modelled (—) and measured (--) 8-h maximum and 8-average ozone (O_3) mixing ratios for North Bay during (a) January (b) February and (c) March 2005.

Table 10. Model evaluation statistics for 8-hour maximum ozone (O_3) mixing ratios for January to March 2005.

Month	MB (ppb)	MNBE (%)	MNGE (%)	UPA (%)
January	2.22	31	39	3
February	-0.87	15	33	-9
March	-5.70	6	40	3
Summer Total	-1.57	17	37	-15

Table 11. Model evaluation statistics for 8-hour average ozone (O_3) mixing ratios for January to March 2005.

Month	MB (ppb)	MNBE (%)	MNGE (%)	UPA (%)
January	7.45	77	80	4
February	4.22	97	104	-5
March	0.30	60	83	-15
Summer Total	3.86	77	88	-15

Comparing Figure 8 and the NO_2 time series (Figure 11) an anti-correlation between O_3 and NO_2 can be seen. This follows the same cycling as described in Equations 1 and 2 which shows that as NO_2 is consumed, O_3 is produced. The spikes in NO_2 levels in Figure 11occur over during the morning and evening rush traffic hours when NOx is emitted in large amounts. Though the majority of NOx is emitted as NO, nitrogen dioxide is created when NO reacts with O_3. This is what causes the spikes and dips in O_3 and NO_2 concentrations in the hourly measurements.

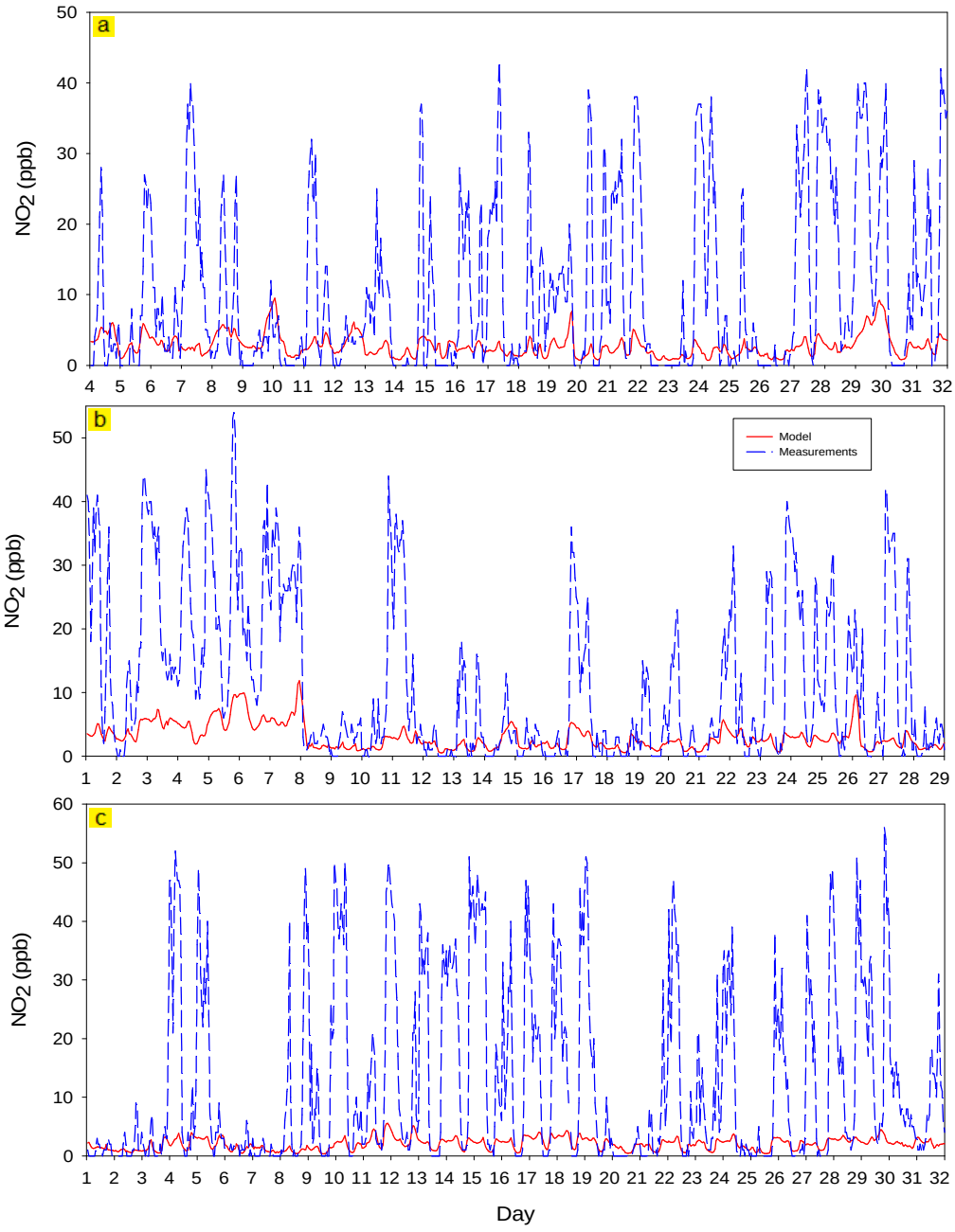

Figure 11. Comparisons of modelled (—) and measured (--) 1-h averaged surface nitrogen dioxide (NO_2) mixing ratios for North Bay during 2005 (a) January (b) February and (c) March 2005.

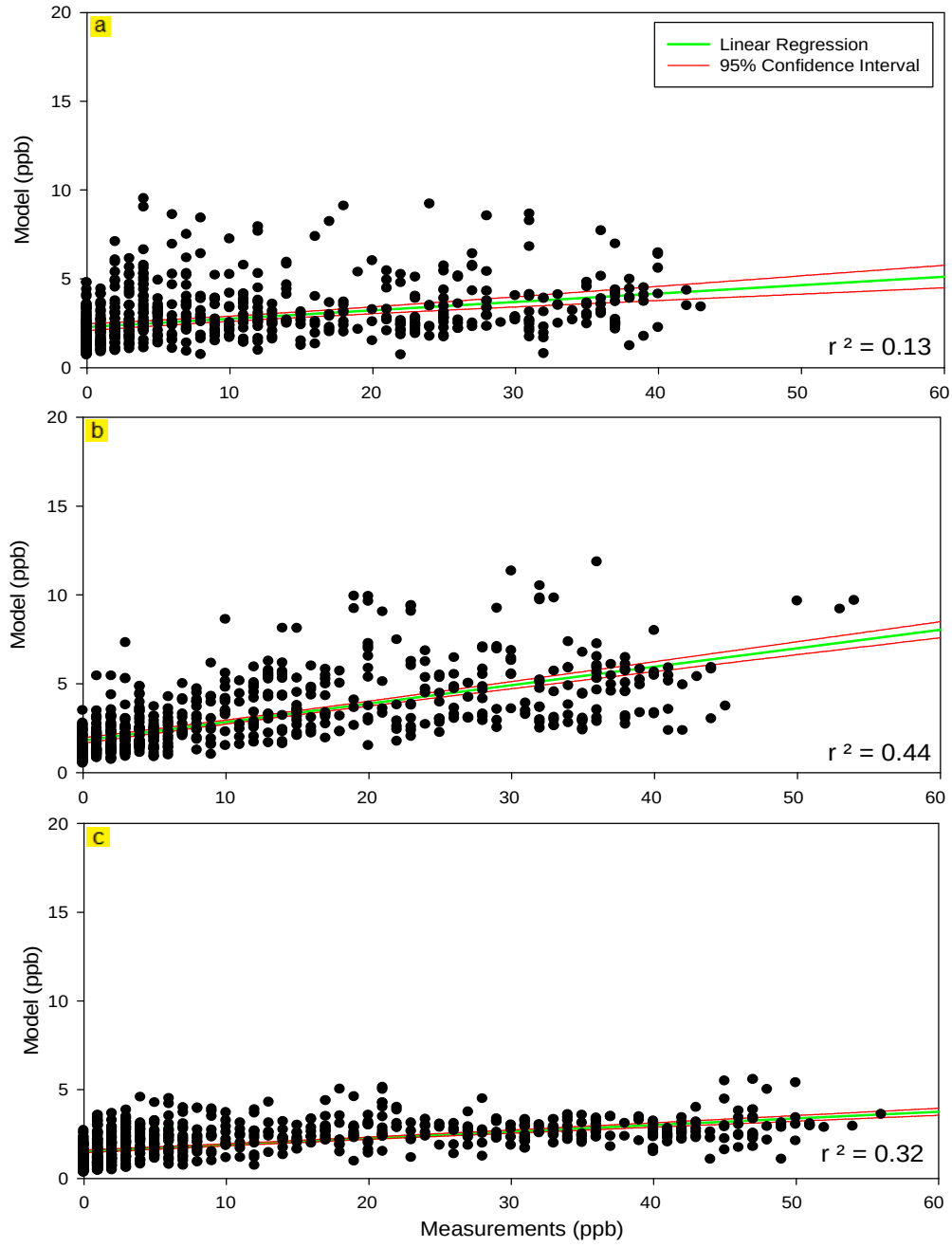

Figure 12. The nitrogen dioxide (NO_2) 1-h averaged scatter plots of model results plotted against measurements taken from provincial monitoring stations for North Bay during (a) January, (b) February and (c) March 2005.

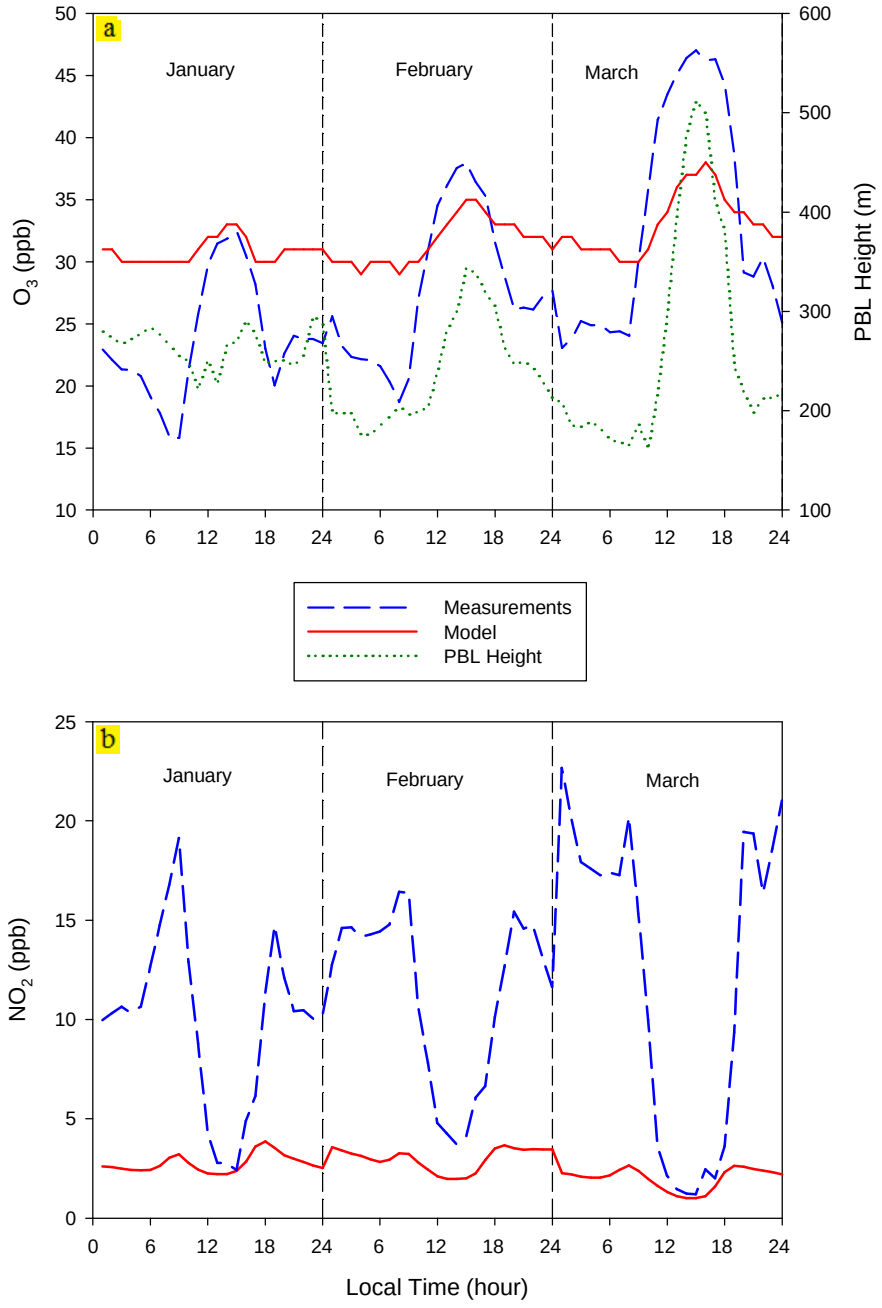

Figure 13. The 2005 wintertime diurnal cycles of (a) ozone (O_3) and the planetary boundary layer (PBL) and (b) nitrogen dioxide (NO_2) for North Bay. Model (—), Measurements (--), simulated PBL height (···).

The diurnal cycles of O_3 and NO_2 were then studied to test whether CMAQ could capture their intraday variation. This method has been used as a gauge in many ozone investigations (J. Lin et al., 2008) to assess the capability and efficiency of the model during the day because these species have very specific daily peak production patterns. The diurnal cycles in Figure 13 illustrate the correlation between the model and measurements for O_3 and NO_2 over the entire modelling period for North Bay. The simulated PBL diurnal cycle is also displayed in Figure 13.

The measured and modelled diurnal patterns for ozone presented in Figure 13. They are seen to follow the same temporal distribution where ozone maximizes in the afternoon around 2 pm and minimizes around 8 am, though some notable differences are apparent. For example, the timings of the maximum values in both datasets have a phase shift of about 1 hour and the amplitudes of the peaks are much more prominent in the measurements. The measurements begin to drop around 7 am each month and hit a minimum at 8 am. The curve then starts to rise from around 10 am to a maximum at 2-3 pm followed by another decline. Ozone destruction at this time occurs rapidly in the measurements but is very gradual in the modelling results. Lin et al. (2008) suggest that this is due to the simulated PBL being too strong which results in a more robust upward transport of NOx and a more forceful downward transport of O_3 from the upper PBL. The result is a greater accumulation of simulated O_3 at the surface and weaker NOx titration. The rise of a small, secondary peak in Figure 13 is seen to occur overnight which other investigators (McKendry, 1993) have attributed to a reduction in wind speed and a lowering of the planetary boundary layer (PBL). Ozone mixing ratios begin to drop again around sunrise due to loss processes like dry deposition and NOx titration. Ozone concentrations fluctuate in response to the hourly PBL heights. Figure 13 illustrates the ability of CMAQ to simulate these important diurnal cycles. When the PBL rises, O_3 is transported upward. This reduces the concentrations of ground-level O_3. The maximum PBL heights are approximately 270 m, 350 m and 500 m for January to March and drop as low as 160 m at night. Simultaneously, the NO_2 diurnal cycle

(Figure 13) drops and rises in opposition to ozone levels. This dimodal curve shows two peaks around 8 am and 7 pm and a minimum at 2 pm which is in agreement with the O_3 diurnal cycle. The ability of CMAQ to adequately simulate the diurnal cycles shows that the model is working well. To further test the source of the errors, comparison between the modelled and measured Ox ($Ox= NO_2 + O_3$) must be examined to determine whether the emissions inventory contained any significant errors which would have cause the hourly time series comparisons to be inaccurate.

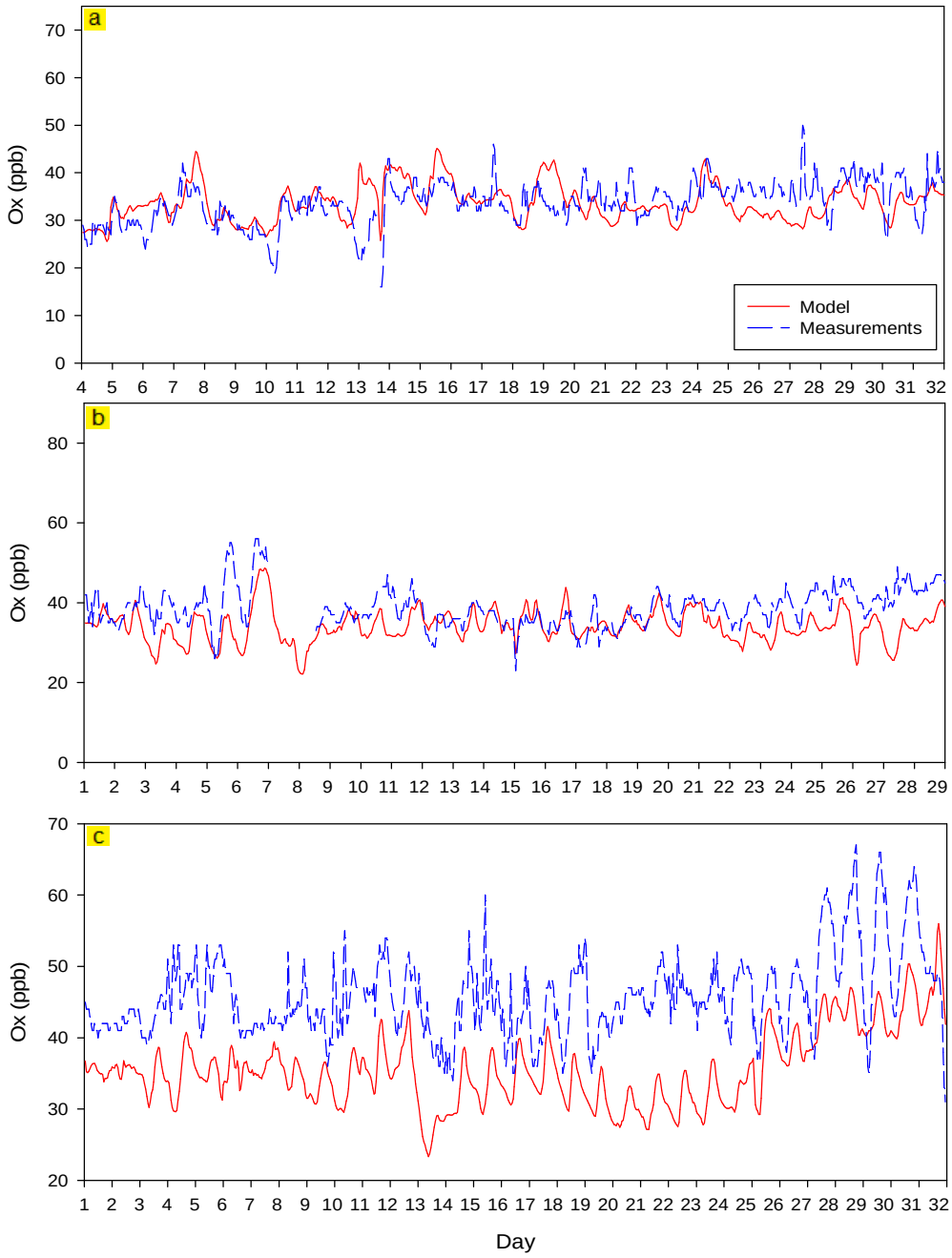

Figure 14. Comparison of 1-h averaged Ox mixing ratios for the modelling results (—) and measurements (--) for January 2005 in North Bay.

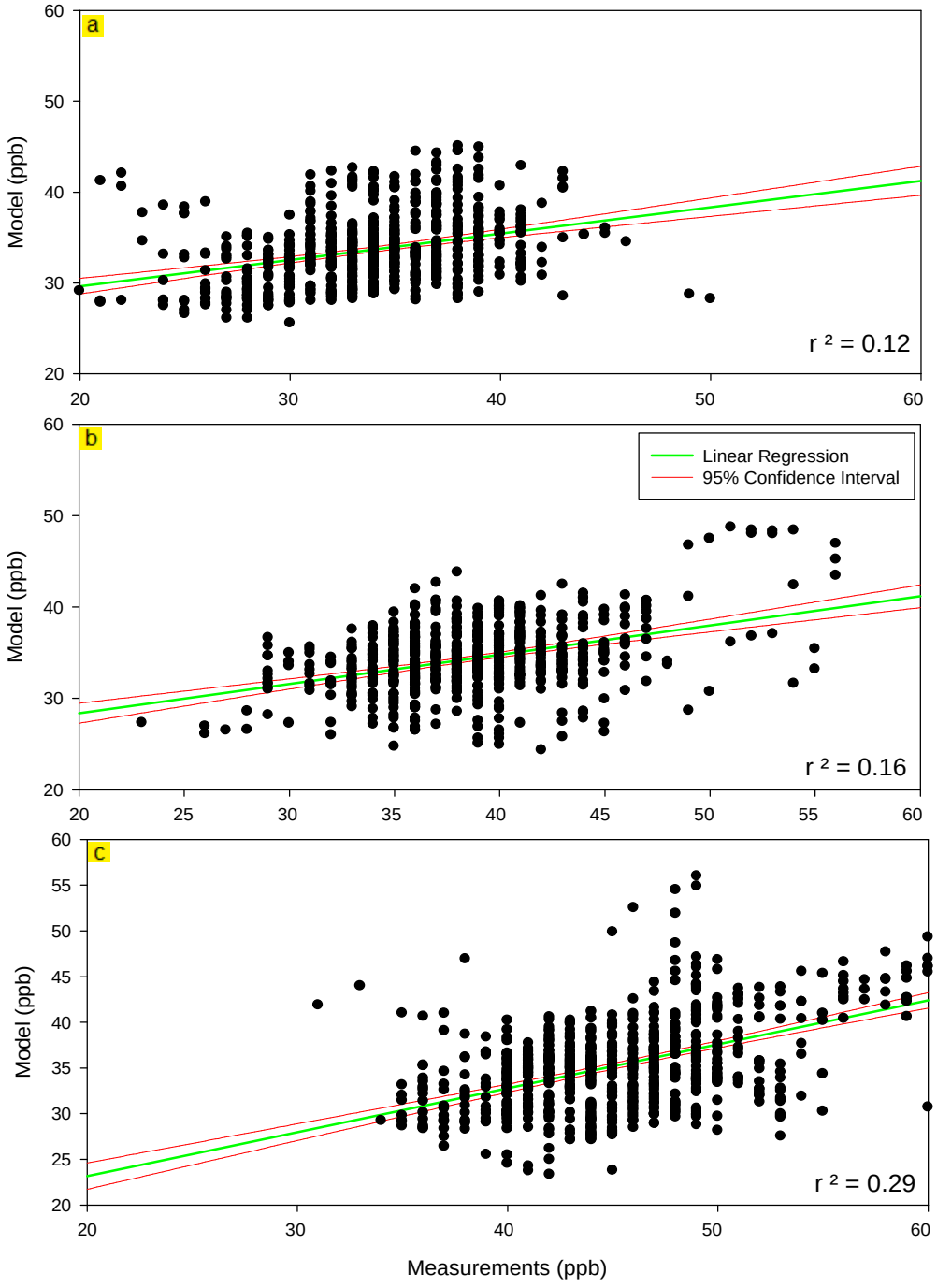

Figure 15. The oxidant (Ox) 1-h averaged scatter plots for North Bay for (a) January, (b) February and (c) March 2005.

The Ox hourly time series imply that the emissions inventories do not contain any large errors since the peaks and troughs of the measurement and model curves for January and February follow a very similar pattern. Though the scatter plots all fall under the acceptable range of R^2= 0.5, there are no significant differences between the simulations and measurements except during March where the model underestimated Ox mixing ratios relative to the measurements. This indicates that the emissions are not erroneous, and that the coarse grid resolution plays n important role in the overestimation of O_3 and underestimation of NO_2. Further investigation of O_3 and NO_2 in urban areas was then conducted to test how well CMAQ can estimate the two species in urban settings.

5.3.2.2 *Ottawa*

After analyzing CMAQs ability to simulate O_3 and NO_2 for a rural region, I examined how well the model could reproduce these surface species in urban areas. The 1-h ozone time series and scatter plots for Ottawa are given in Figure 16. The time series show that the temporal distribution of O_3 between the modelled and measured data seems to vary by month. The amplitudes however show a gradual trend from overestimation to underestimation through the winter period which is supported by the MB statistics reported in Table 6 for January (5.84 ppb), February (2.25 ppb) and March (-2.79 ppb). CMAQ does show an overall positive MB for the winter (1.56 ppb). The model is not able to capture lower ozone concentrations toward the beginning of the winter period, and is unable to replicate higher ozone values near the end of the winter.

In January the correlation between CMAQ output and measurements is less than satisfactory, giving an R^2 value of 0.27. The timings of the daily O_3 peaks in the February time series (Figure 16b) appear to match each other well. This can also be seen in the corresponding scatter plot whose R^2 value of 0.52 is within an adequate range. It should be noted though, that a large portion of the AQ station measurements for the month of February were either

unavailable or deemed unreliable by the MOE, thus were not used in any statistical evaluation. In March, the agreement between the datasets in the hourly ozone time series is very poor. The scatter plot for the month confirms this as the R^2 value is only 0.27 which indicates almost no correlation between the datasets. The graph does confirm the MB statistics given that the majority of points between 20-40 ppb fall below the perfect correlation line meaning that the model is under-predicting ozone. Overall, the graphical and statistical analyses do not display good agreement between the model output and measurements.

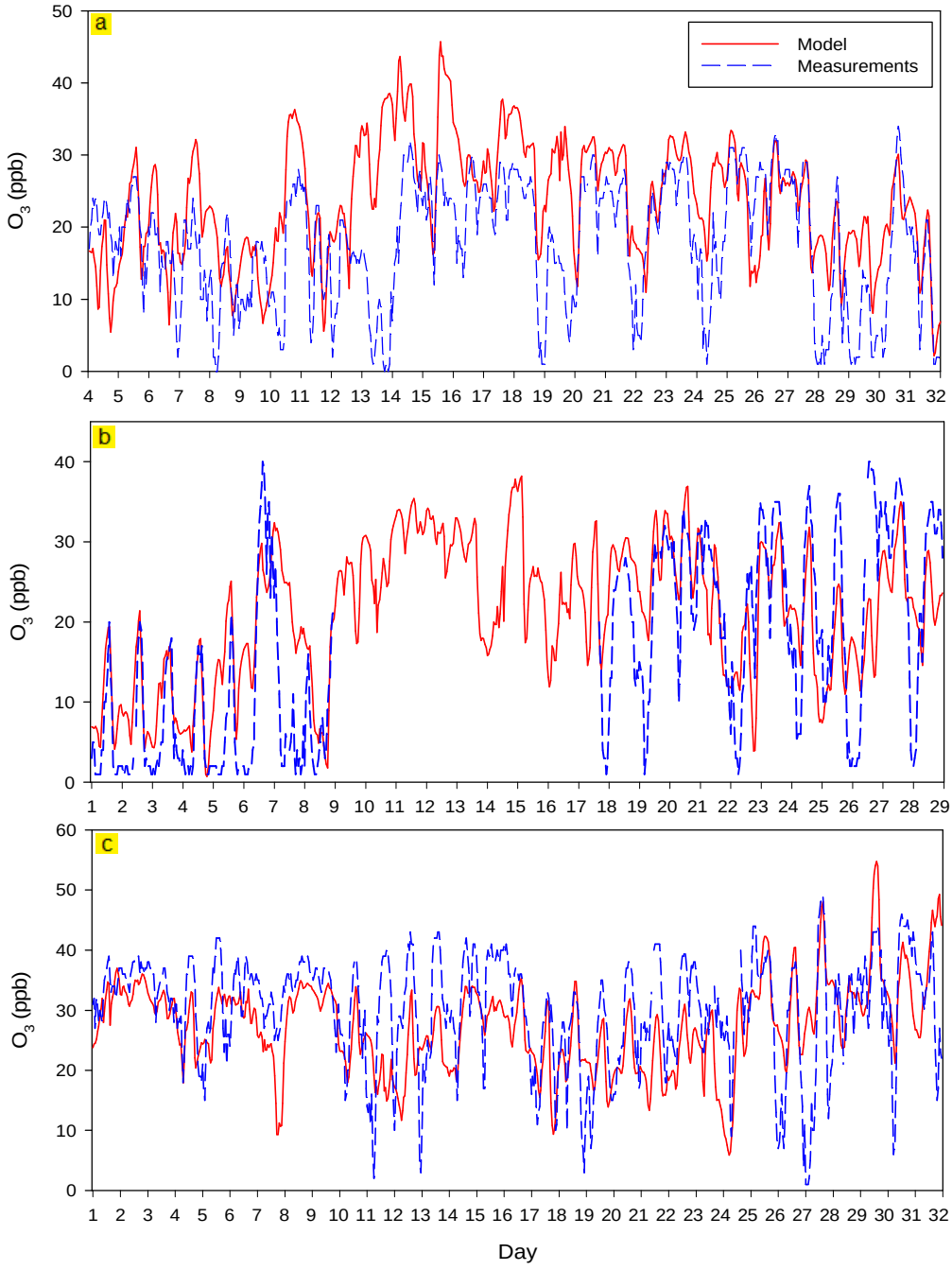

Figure 16. Comparisons of modelled and measured 1-h averaged surface ozone (O_3) mixing ratios for Ottawa during 2005 (a) January (b) February and (c) March 2005.

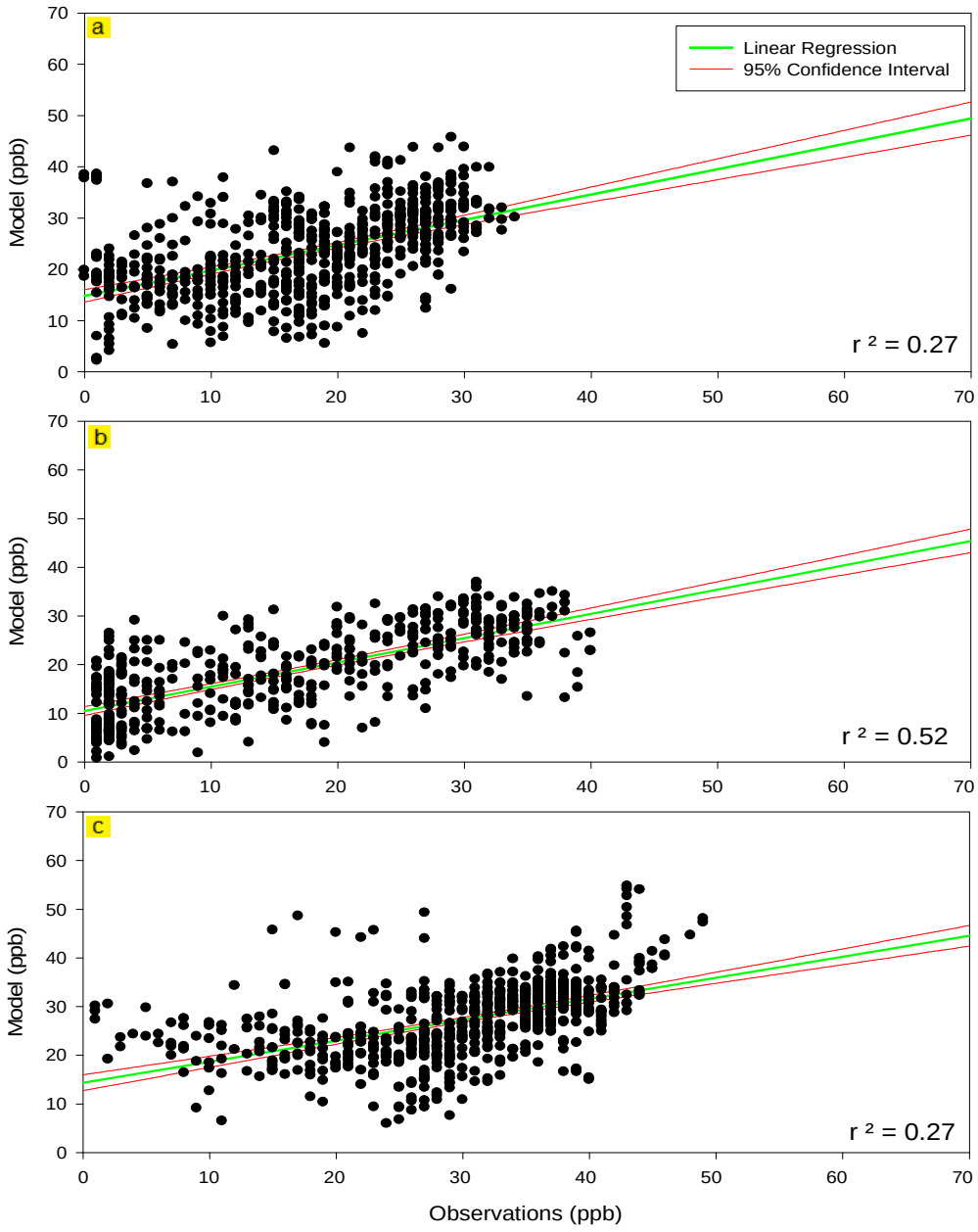

Figure 17. The 1-h averaged ozone (O_3) scatter plots of model result plotted against measurements taken from provincial monitoring stations for Ottawa during (d) January, (e) February and (f) March 2005.

Eight hour averages and maximum O_3 values were also graphed for Ottawa and their statistics were recorded in Table 12 and Table 13. Figure 18 shows that the peak ozone levels were exceeded by CMAQ during the first part of winter and underestimated during the latter half of the season. Figure 18 exhibits a small negative bias in model results during early to mid-March when the 8-h maximum of the measurements rose above 40 ppb and the model results were about 5-10 ppb below that. CMAQ over-predicted ozone throughout much of January for both the 8-h maximum and 8-h average plots, but was able to mimic a decline in O_3 concentrations at the end of January and beginning of February similar to the measurements. The statistics show a decreasing trend with an overall negative bias in the 8-h maximum results. The 8-h O_3 average also decreases from one month to the next, but retains its overall positive value. The UPA values for each table are positive overall which indicates that CMAQ over-predicted the maximum peak values.

The NO_2 1-h average time series and scatter plots were evaluated next to establish how well CMAQ can replicate the species. Unlike the NO_2 plots for North Bay, the model did not display vast under-prediction throughout the entire winter for Ottawa, though there is an overall negative bias of MB= -4.37 ppb. The model showed difficulty in simulating concentrations above approximately 30 ppb in January and February, and was not able to reproduce NO_2 mixing ratios above 13 ppb in March, though compared to North Bay, the NO_2 scatter plots for Ottawa (Figure 19) show better agreement between the model and the measurements. While the correlation coefficients for January and March are only 0.32 and 0.29, respectively, the R^2 value for February is 0.60 which shows good agreement between the two datasets. The time series for both O_3 and NO_2 reveal the interconnected relationship of the two species. As O_3 levels rise, NO_2 concentrations decline. This is the same pattern that is described by the North Bay results and detailed by the spatial resolution of the modelling domain in Section 5.3.1. Overall, the results indicate that CMAQ is working well and that the emissions dataset does not have any major errors.

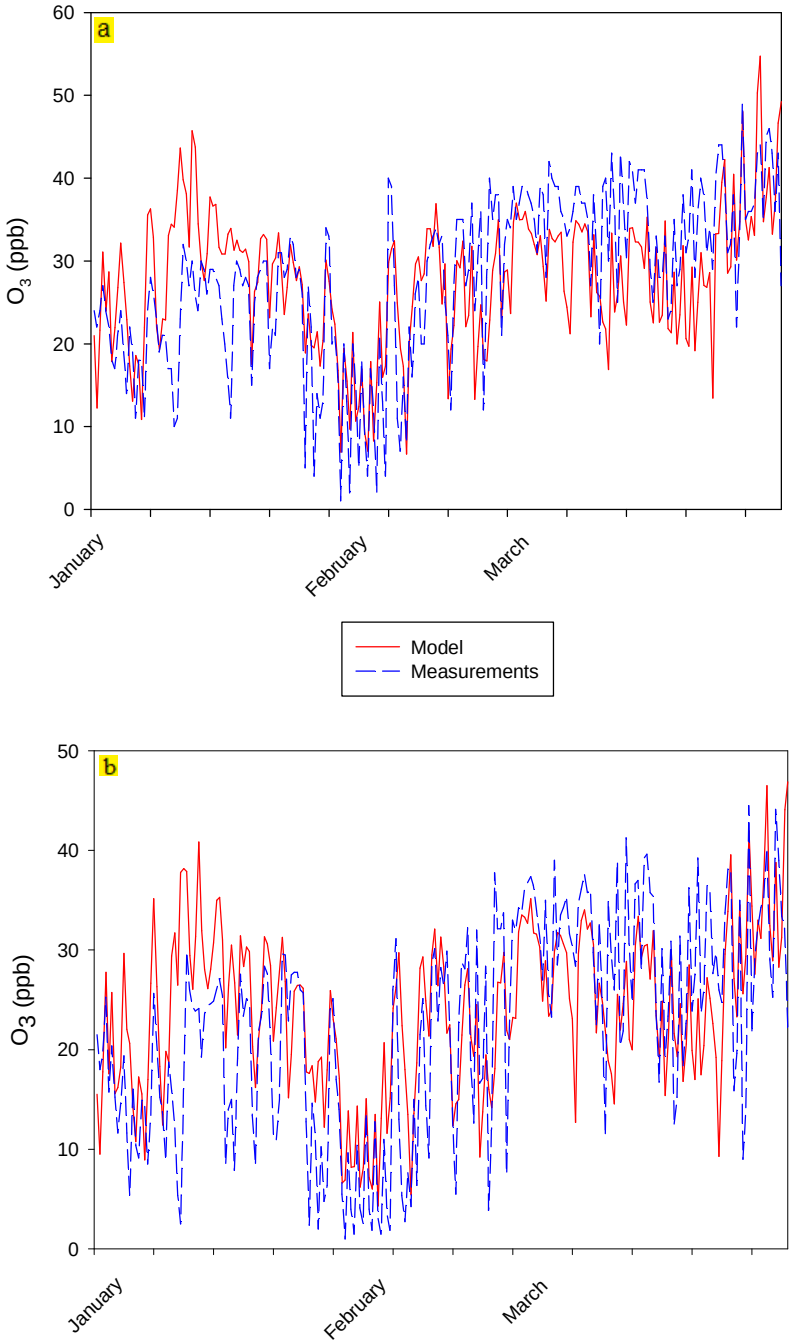

Figure 18. Comparisons of modelled (—) and measured (--) ozone (O_3) (a) 8-h maximum and (b) 8-h average mixing ratios for Ottawa during winter 2005.

Table 12. Model evaluation statistics for 8-hour maximum ozone (O_3) mixing ratios for January to March 2005.

Month	MB (ppb)	MNBE (%)	MNGE (%)	UPA (%)
January	5.0	16	24	34
February	-0.50	-1.0	29	-8
March	-4.71	-19	23	12
Winter Total	-0.14	-2	25	10

Table 13. Model evaluation statistics for 8-hour average ozone (O_3) mixing ratios for January to March 2005.

Month	MB (ppb)	MNBE (%)	MNGE (%)	UPA (%)
January	6.02	86	91	37
February	2.04	87	102	-15
March	-2.63	-3	23	5
Winter Total	1.68	51	67	5

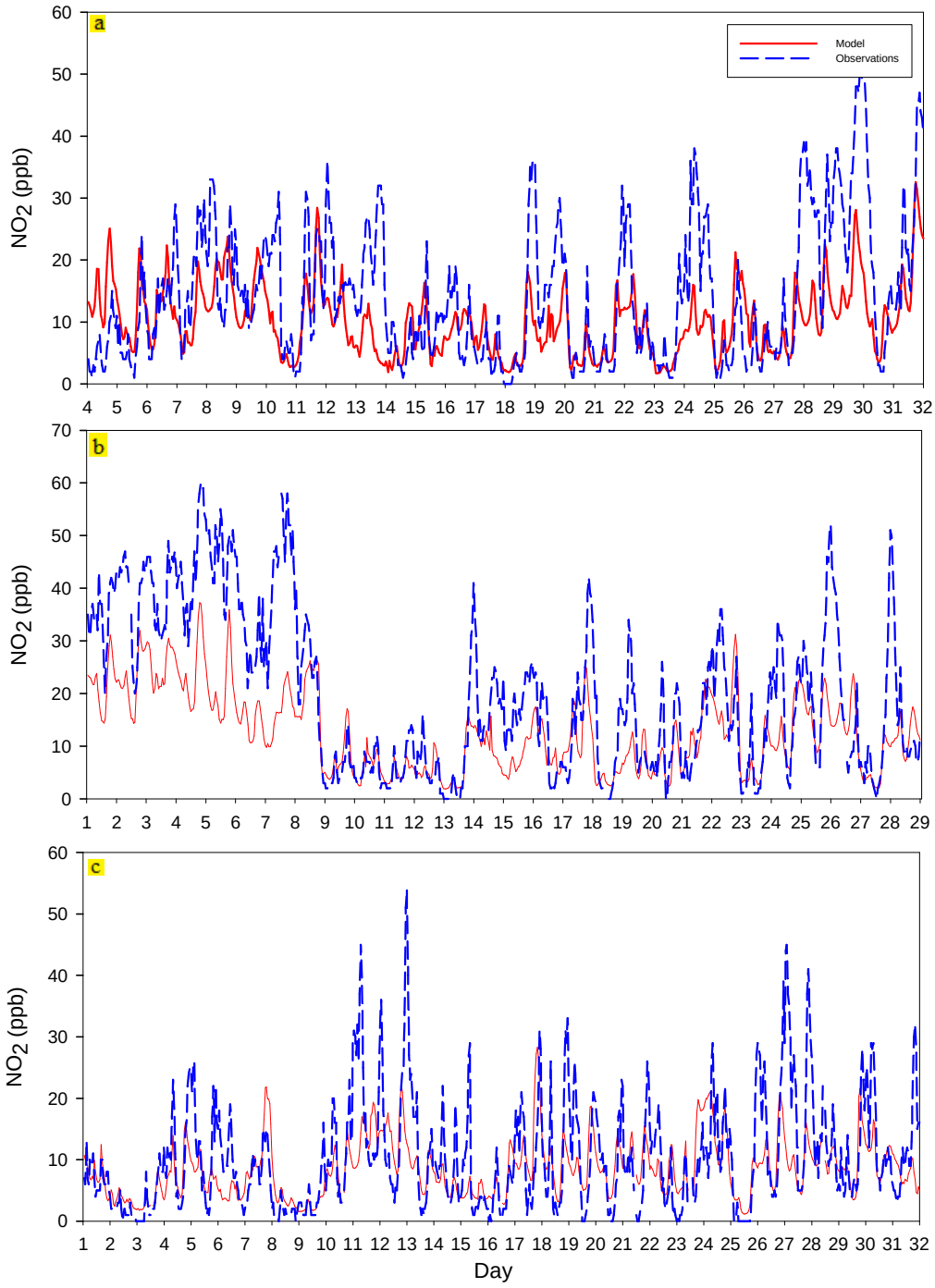

Figure 19. Comparisons of modelled (—) and measured (--) 1-h averaged surface nitrogen dioxide (NO_2) mixing ratios for Ottawa during 2005 (a) January (b) February and (c) March 2005.

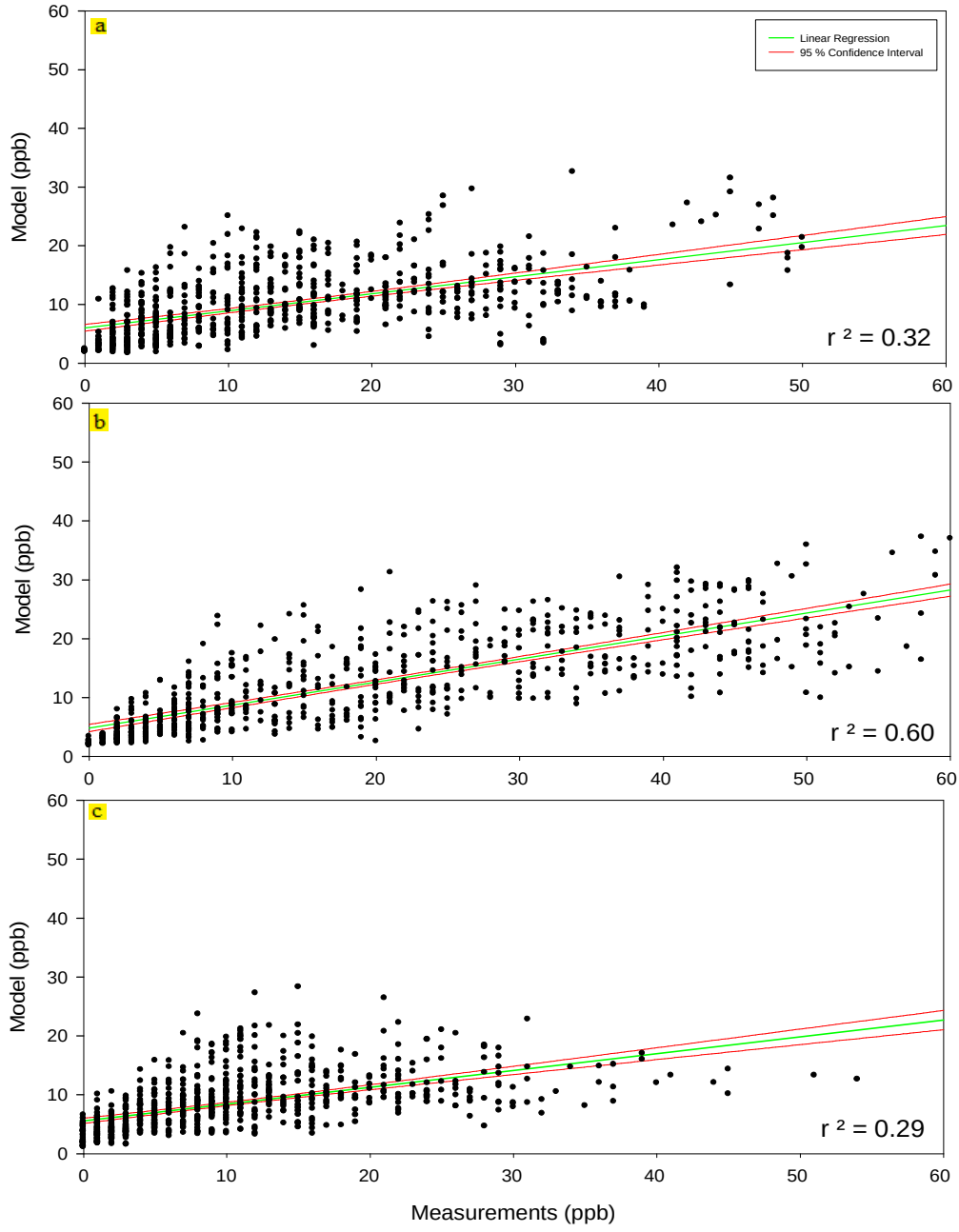

Figure 20. The nitrogen dioxide (NO_2) 1-h averaged scatter plots of model results plotted against measurements taken from the provincial monitoring station for downtown Ottawa during (d) January, (e) February and (f) March 2005.

A plot for NOx was also created to get a better sense of the contribution of NO_2 to overall NOx concentration within an urban location. The NOx plot shows a large increase of NOx at the end of January into early February. A smog episode which occurred from February 4-9 may be a contributing factor to this feature of the curve. The modelling results appear to follow the same trend as the measurements, however the model is unable to match peak NOx concentrations which means that the NOx emissions are much lower overall than the measurements.

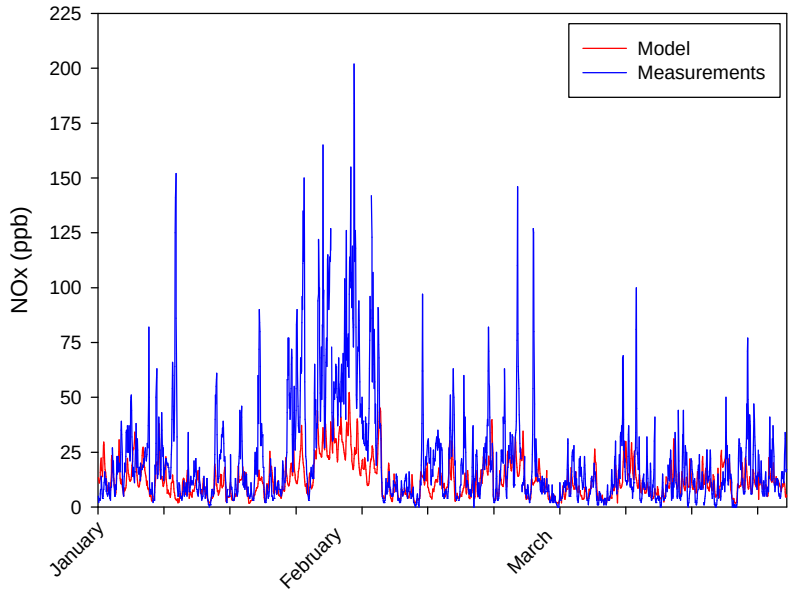

Figure 21. A comparison between modelled (—) and measured (--) 1-h averaged NOx mixing ratios for (a) Januray, (b) February and (c) March for Ottawa 2005.

The diurnal cycles were the next to be analyzed for the urban region. One can observe from Figure 22 that the timing of the ozone peaks in the two curves for January and March are measured to be at the same hour, while the datasets are only divergent by one hour in February. The smaller, secondary peak which normally occurs overnight is shifted to the early morning hours. The simulated diurnal cycles for Ottawa are much more prominent than those for North Bay. A possible reason for this may be because CMAQ often under-predicts O_3 at rural sites while overestimating it at urban sites (Eder & Yu, 2006; Yu et al.,

2008) because of the levels of NO_2 that exist in emissions datasets for urban and rural areas. These curves compare well to the NO_2 diurnal cycles (Figure 22) which show the characteristic double peaks at approximately 9 am and 6 pm for each month. The drop in NO_2 levels between noon and 2 pm for each cycle coincides with the spike in O_3 concentrations in O_3 diurnal cycle. The PBL cycle for Ottawa is similar to that for North Bay except for a slight phase shift in January and is seen to go as low as 160 m. This is not unexpected since the PBL height for Ottawa – as well as North Bay – is known to drop very low during the winter nights (Harris, 2010). These results show that although CMAQ was not able to properly reproduce the hourly temporal distribution of O_3 or NO_2 very well, the model is running correctly given the accurate reproduction of the diurnal cycles.

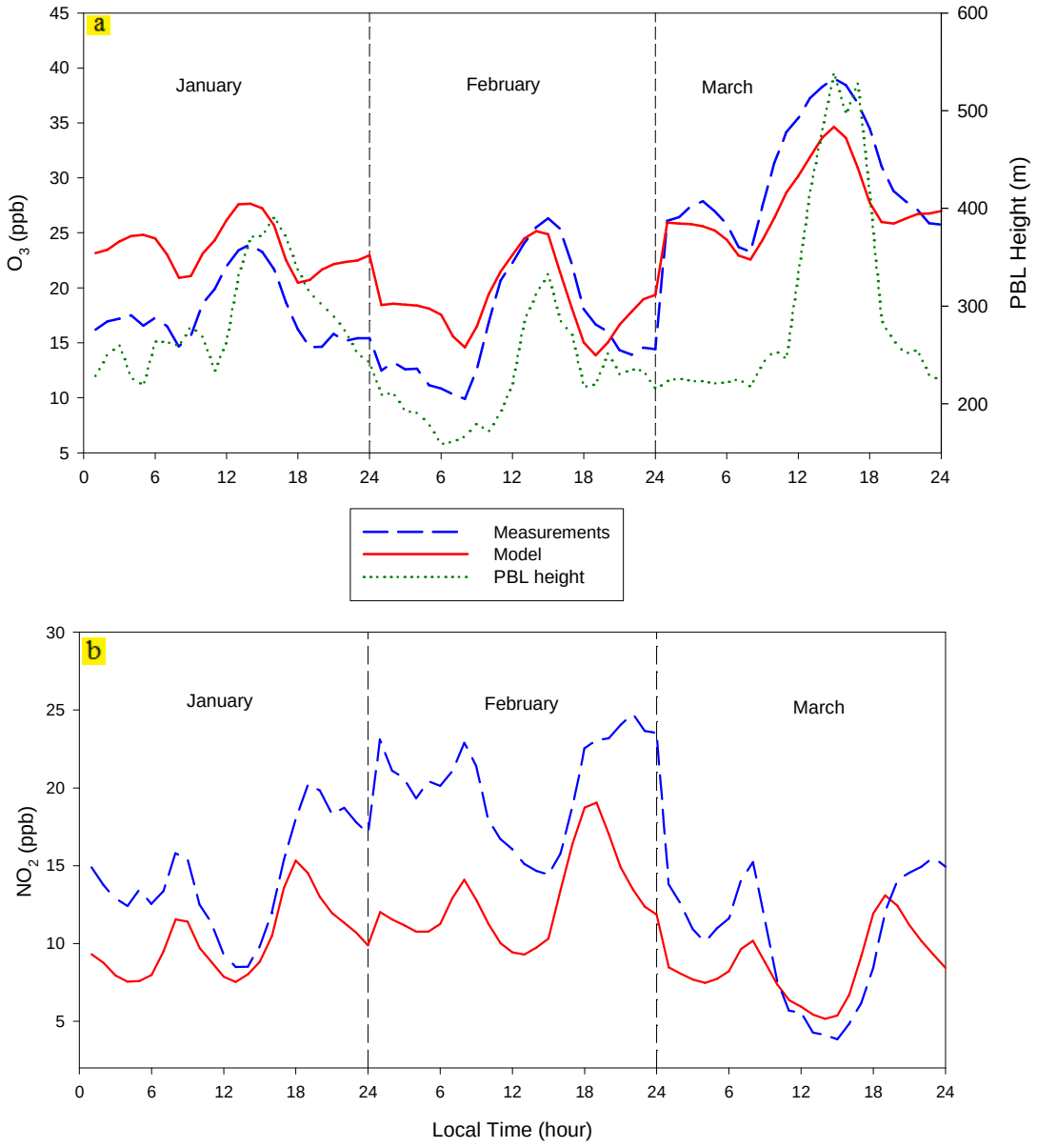

Figure 22. The 2005 wintertime diurnal cycles of (a) ozone (O_3), the planetary boundary layer (PBL) height and (b) NO_2 for Ottawa. Model (—), measurements (--), simulated PBL height (···).

Once validated, the simulation results can then be used to assess the emissions inventory by evaluating how the levels of oxidant (Ox) vary. Previous studies by Clapp et al. (2000) have concluded that the relationship between NOx and Ox is linear such that Ox at a given location contains a NOx-dependent and a NOx-independent contribution. The former is produced by local sources and depends on the level of primary pollution, whereas the latter, being a regional contribution, represents the regional background concentrations of O_3 (Clapp & Jenkin, 2001; Mazzeo et al., 2005). While this study does not address the sources of pollution, Ox concentrations are used to study the air quality because it encompasses the total O_3 and NO_2 in a given location. Evaluating either species alone is often difficult in urban setting because O_3 is normally very low while NO_2 is very high. The Ox comparisons indicate that the emissions inventories for urban cities do not have major uncertainties. The modelled and measured results generally rise and fall with the same temporal pattern, though the amplitudes of the curves show some bias. The scatter plots also indicate this since they are all below the standard R^2 value of 0.5.

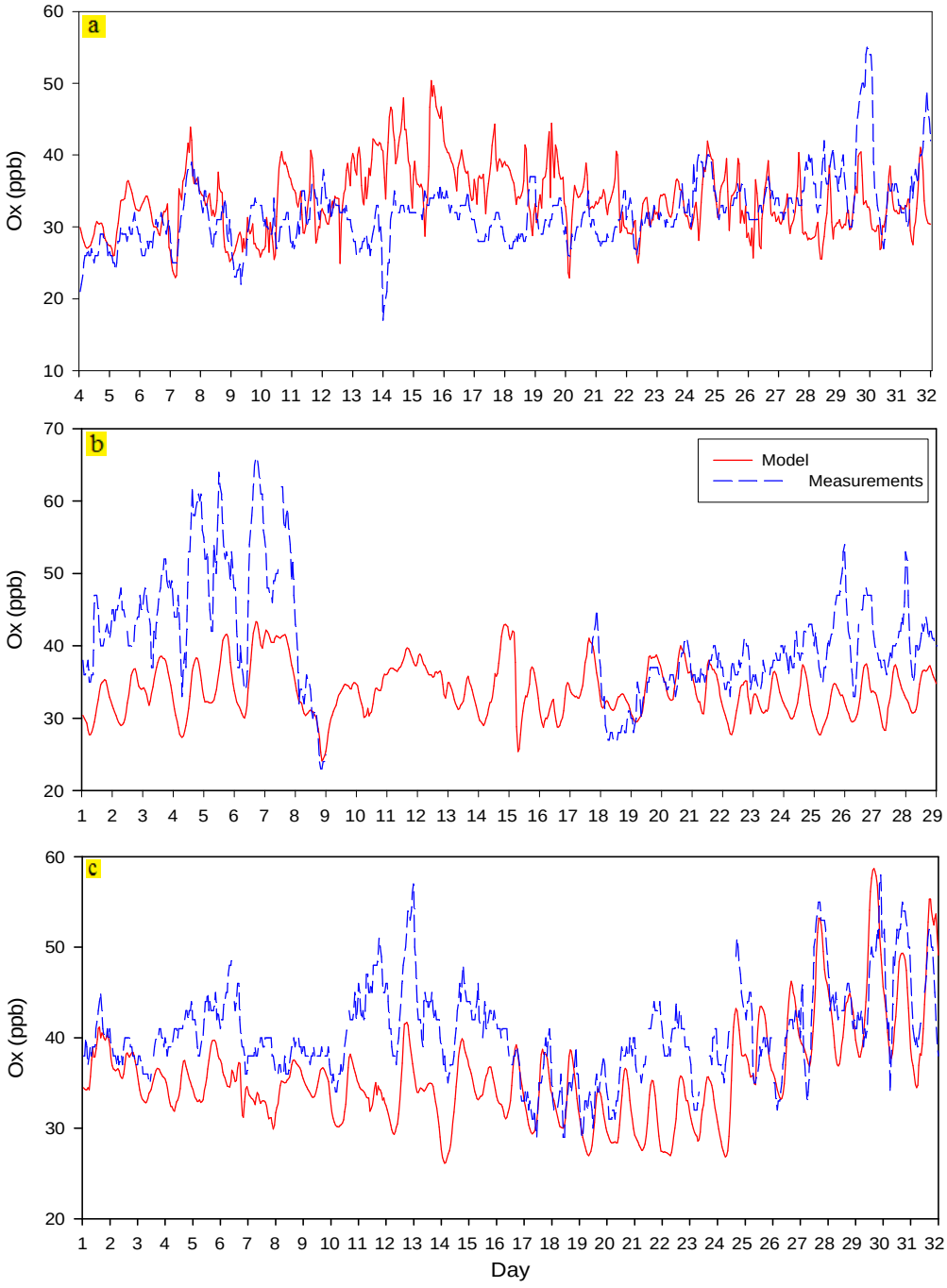

Figure 23. Comparisons of modelled (—) and measured (--) 1-h averaged oxidant (Ox) mixing ratios for (a) January, (b) February and (c) March 2005 for Ottawa.

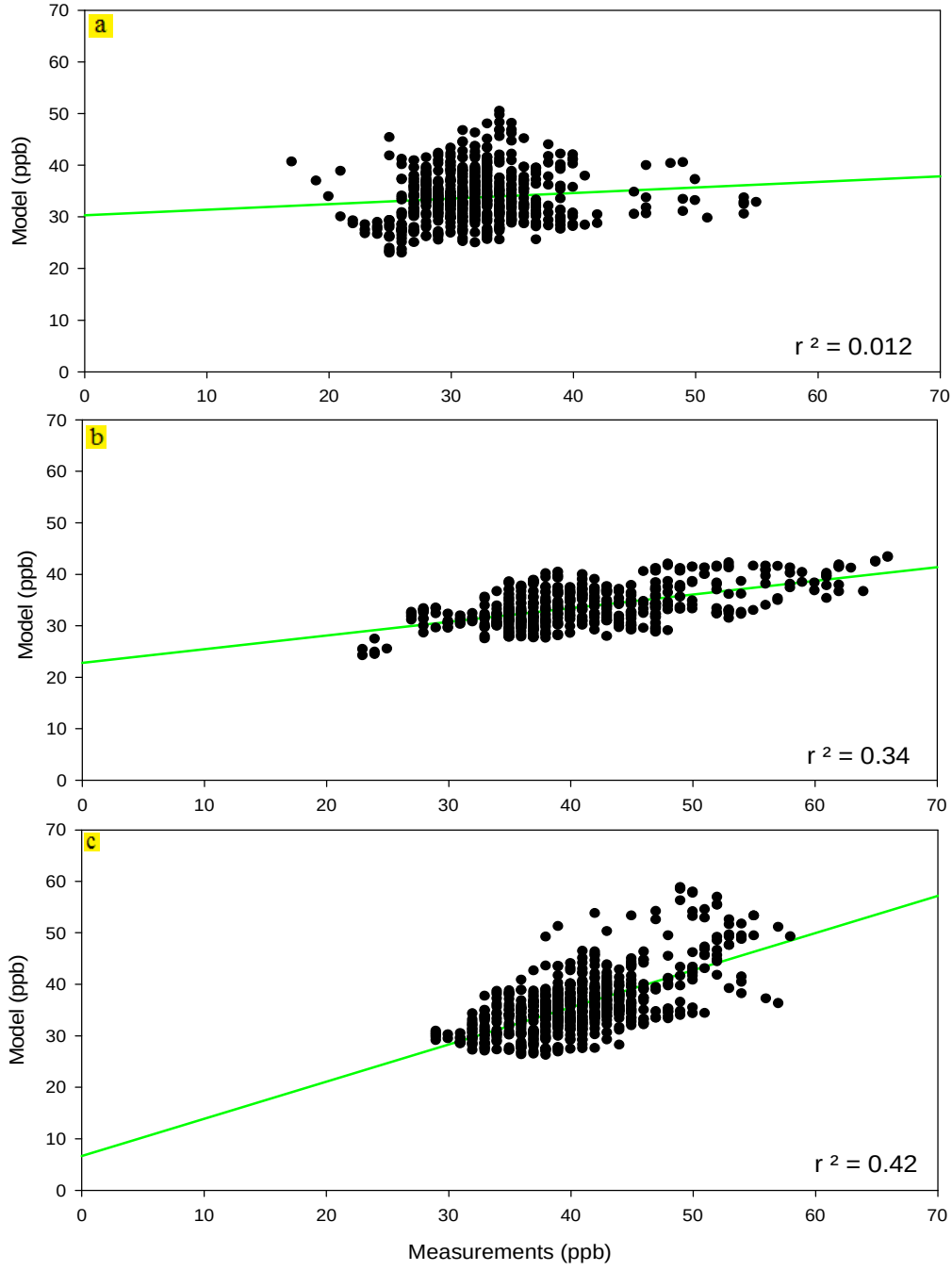

Figure 24. The oxidant (Ox) 1-h averaged scatter plots for Ottawa for (a) January, (b) February and (c) March 2005.

5.4 Summary and Conclusion

Using a coarse resolution, this study simulates the observed hourly and diurnal patterns of surface ozone and nitrogen dioxide over two cities in Ontario during the winter of 2005. The first city is North Bay which represents a rural region, and the second city is Ottawa which is urban. The model's spatial representation of both species over each city is as expected, though the temporal results showed a continuous under-prediction of NO_2, especially in Ottawa. This effect is particularly clear over the nighttime hours where the hourly NO_2 measurements are drastically higher than the model results. During the evening and overnight, measured NO_2 mixing ratios are observed to reach over 50 ppb at many points throughout the modelling period. In response to these values, ozone mixing ratios correspondingly decrease to zero or almost zero ppb. These results are not surprising given that the monitoring stations for both sites are located near sources of NOx which suggests that the emissions inventory under-represents local NOx emissions at both monitoring sites. Though North Bay is not an urban centre, as previously mentioned its monitoring station is located in the more populated part of the region, and is about 10 minutes northeast of the local airport causing elevated levels of NOx to be recorded. In Ottawa, the monitoring station is within the downtown core and is subject to high levels of NOx from motor vehicles especially during the rush hour which is typical of urban areas. Both stations are also located close to major road ways. This may be why the MB for Ottawa is smaller compared to North Bay for both O_3 and NO_2.

The main reason why CMAQ over-predicted O_3 and under-predicted NO_2 was because the grid resolution used in this study was 36 km x 36 km. Many authors have found that the grid resolution can also influence the model-measurement correlation (Sokhi et al., 2006; M. Zhang et al., 2006) because O_3 and NO_2 production are sensitive to the size of the grid cell. Not only do coarser resolutions (i.e. large cell size) average out small-scale variations in emissions and chemistry, they result in an increase in ozone production efficiency due to higher NOx dilution across larger grid cells (Shrestha, Kondo, Kaga, & Inoue, 2009). This

generates greater average ozone concentrations, and consequently, local maxima are not adequately resolved (Carey Jang, Jeffries, & Tonnesen, 1995). Thus local or small scale features such as diurnal cycles or O_3 variability in Ottawa or North Bay generated by from point measurements will not be represented in the grid-averaged concentrations resulting in a poor comparison between the two datasets.

To observe the behaviour of pollutants on a local scale, the best practice would be to use nested domains with very low resolution of a few kilometres (Yu et al., 2008; Y. Zhang, Liu, Pun, & Seigneur et al., 2006b). Some studies have even used 1 km x 1 km resolution with success (Sokhi et al., 2006), and have found that finer resolution grids provide better spatial variability for low ozone episodes (Shrestha et al., 2009) such as those often found in urban environments. There are however, other factors which may influence model performance in addition to location and grid resolution. Model performance may also vary with season due to the changes in solar radiation, temperature and emission rates of various pollutants. Thus, in order to gain a comprehensive assessment of CMAQs ability to simulate O_3 and NO_2, the same study must be completed for the summer months at a time when ozone production is observed to be at a maximum rate.

Chapter 6

Summer Study

In Ontario, the summer season is a significant time of the year for pollution especially O_3 and NO_2. It is during this time that humans and vegetation experience the most exposure to the hazards of surface-ozone and nitrogen oxides. With conditions favourable to O_3 formation and accumulation, the summer of 2005 saw the cities of Ottawa and North Bay go through a combined total of 30 smog days. This is not surprising since the peak ozone season occurs during the months of May to September (Geddes et al., 2009) after which O_3 levels decline as the weather cools in the fall and then raise in the spring as the amount of daily solar radiation increases. To evaluate CMAQs performance in simulating this seasonal cycle, ozone and its precursor species, NO_2, were modelled over the summer months of June to August. Increased solar radiation and temperatures during the summer provide ideal conditions for ozone production making ozone episodes a common occurrence in Ontario.

The seasonality of O_3 is the reason why most CMAQ investigations for ozone and NOx are conducted for time periods during the summer months. Sokhi et al. (2005) compared CMAQ O_3 predictions generated over London, England during ozone episodes in July and August 2002 with observations taken from local urban monitoring stations. It was found that CMAQ was able to capture the temporal patterns of O_3 but could not replicate the peak magnitudes very well, and over-predicted nighttime O_3 levels. The study performed by Tong et al. (2006) also simulated O_3 concentrations across the United States and determined that the accuracy of the simulation depended on O_3 concentrations and location. The model underestimated O_3 at rural sites while over-predicting it at urban sites. Appel et al. (2007) conducted a CMAQ performance evaluation for O_3 from June through August 2001 for the Eastern Unites States under various meteorological conditions. Sensitivity studies were also conducted to determine the effects of the choice of chemical mechanisms, CMAQ model

version, and boundary conditions. They found that CMAQ (over-) under-predicted at (low) high maximum 8-hour average O_3 mixing ratios although the diurnal cycles were represented sufficiently. The influences of meteorological parameters such as vertical layer collapsing and synoptic conditions were also investigated. CMAQ successfully simulated O_3 under typical summertime synoptic conditions, and still showed that meteorological conditions played a role in the summertime cycling of O_3 and NO_2.

The interaction between wind direction, wind speed, local weather and topography all contribute to ideal ozone or NOx conditions. During the summer in particular, the long range transport of ozone and NO_2 from heavily polluted areas in the United States mid-west have been found to cause approximately 95 percent of the O_3 episodes experienced in Ontario (H. Wang et al., 2009). Polluted air masses originating south and southwest of the Great Lakes in the Ohio River Valley (ORV) where large electrical generating units exist, typically contribute 50-60 percent of Ontario's total summertime ozone levels (Yap et al., 1988).

6.1 Method

The air quality model used in this study is CMAQ version 4.6. The model performance was evaluated for both urban and rural regions from June 1 to August 31, 2005 with a two-day spin up period at the end of May. Similar to the winter evaluation, ozone and nitrogen dioxide levels in the cities of Ottawa and North Bay were simulated and compared with measurements taken from the MOEs air quality network. A detailed description of the method can be found in Section 5.2, and readers can refer to Chapter 5 for details on all parameters and procedures including the modelling domain and statistical analysis.

6.2 Results and Discussion

6.2.1 **Spatial Variability of Model Performance**

Figure 25Figure 25 and Figure 16 describe the spatial distribution patters of O_3 and NO_2 during the day of July 25, 2005. This date was chosen at random to provide a visual representation of the relationship between the O_3 and NO_2 cycles. The surface-ozone concentrations at 7 am local time (12 UTC) (Figure 25a) are seen to be much lower than those simulated for 6 pm local time (18 UTC). The average O_3 mixing ratio during the morning rush hour varies between 27 to 60 ppb over south and central Ontario. The higher levels that occur along the mid-Atlantic coast – caused in part by the difference in time zones – are typical of summer high ozone summers (Godowitch, Gilliland, Draxler, & Rao, 2008) . Figure 25b displays ozone levels at 1 pm local time which is the peak ozone production period of the day. Concentrations as high as 95 ppb were simulated in various parts of the domain, though the majority of Ontario is seen to be green which corresponds to ozone levels between 40 to 60 ppb. It must be noted that O_3 values represented by the red areas in the figure may be higher than 95 ppb however this was the limit of the mixing ratio scale. The patterns seen in this figure are to be expected since it is known that ozone falls to a minimum during the morning traffic and reaches a maximum value between 1-3 pm when solar radiation is high. This spatial distribution agrees with that of Figure 26 which shows the nitrogen cycle during the morning and evening high traffic hours. The grey colour over most of the domain represents NO_2 levels as low as 1 ppb while the areas of colour represent a surge in NO_2 emissions due to motor vehicle traffic. Highly populated cities such as Detroit, Windsor, Toronto, Boston and Montreal are seen to experience NO_2 mixing ratios as high as 21 ppb, while some other cities like New York show even larger values. The pattern of NO_2 distribution is fairly discontinuous compared to that simulated for the winter episode.

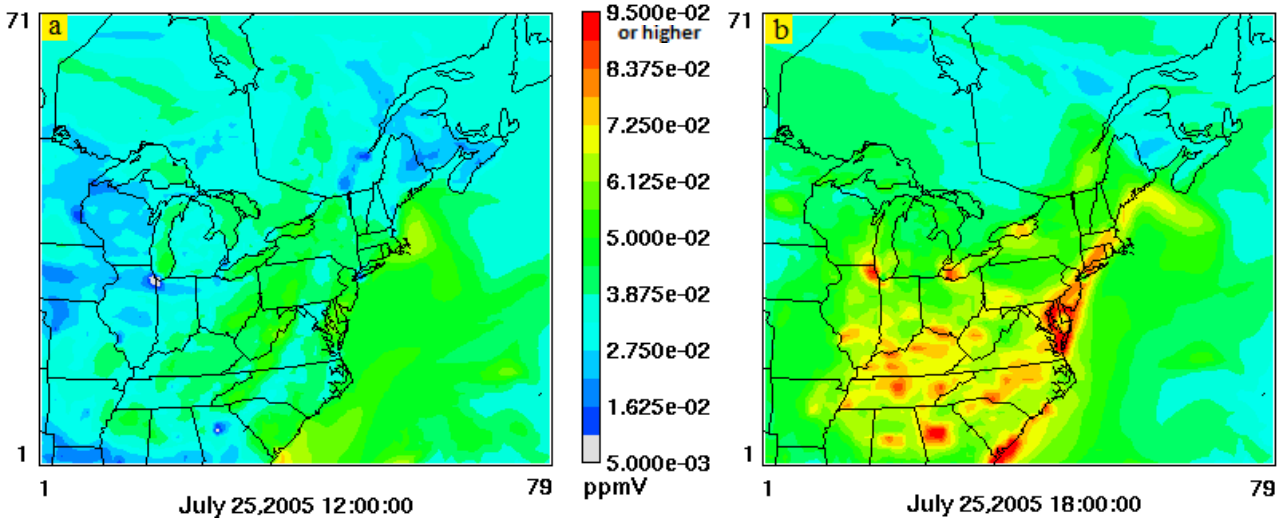

Figure 25. Surface mixing ratios of ozone (O3) over Ontario and the north eastern U.S. for July 25 2005 during (a) the morning rush traffic hour at 7 am local time (12 UTC) and (b) the expected daytime high at 1 pm local time (18 UTC).

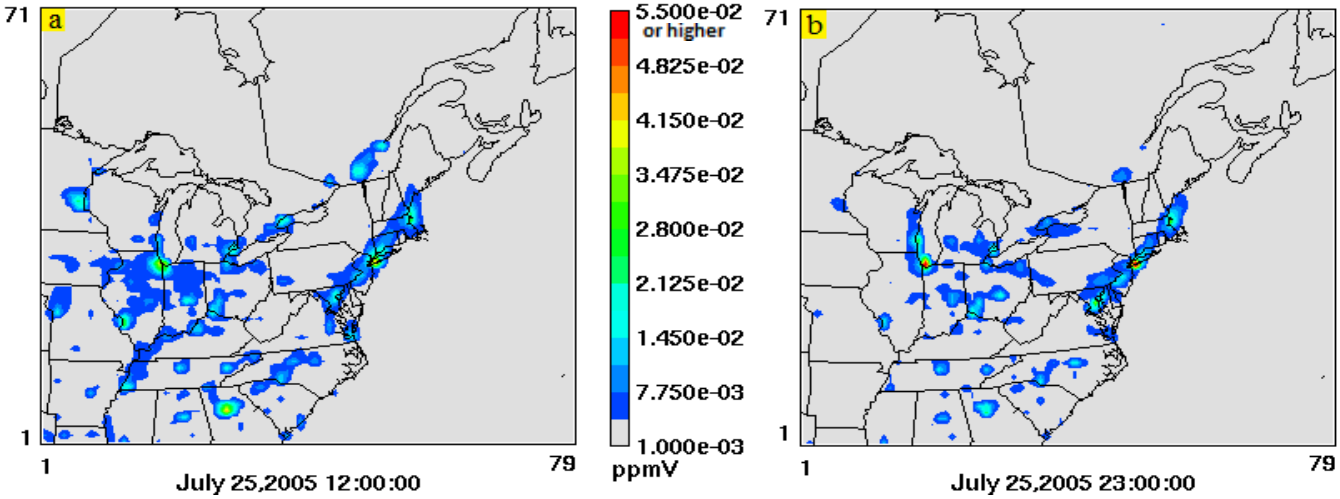

Figure 26. Nitrogen dioxide (NO_2) spatial variation over southern Ontario and the north eastern U.S. for July 25 2005 during (a) the 7 am morning rush traffic hour (12 UTC) and (b) the 6 pm evening rush traffic hour (23 UTC).

The ozone levels simulated over the St. Lawrence River are comparable to those simulated during the winter, though the Great Lakes are seen to have much higher ozone levels during the summer. Wind patterns are a key factor in the circulation of ozone because meteorology can provide the ideal conditions for an ozone episode by altering the chemical and physical dynamics of the troposphere; thus making O_3 a regional concern (Brankov et al., 2003; C. Hogrefe et al., 2006). Stationary or slowly migrating anticyclone (high pressure) systems can cause dispersion, diffusion and deposition. It is these processes which are conducive to summertime ozone episodes. For example, during the winter, from November to May, prevailing winds around the Ottawa area are from the northwest. Conversely, from June to October the prevailing winds originate in the south western United States (Air & Energy Initiatives Environmental Management Division, 2004), and carry polluted air masses from cities like Detroit, Cleveland and Chicago by advection into Southern Ontario and then through the Ottawa region. Because summertime south westerly winds are often slow-moving or stagnant, pollutants have enough time to collect, mix together and react. Physical processes like wind speed and wind direction however, do not have an appreciable effect on NO_2, itself, because it is a short lived species with a lifetime in the PBL that varies from a few hours to a few days (R. Atkinson, 2000), thus causing it to remain close to its sources (Laj et al., 2009). The wind direction and corresponding ozone distribution are shown in Figure 27.

In the first two frames, the wind direction along the east coast is around 150-200 degrees which corresponds to south-southeast and south-southwest directions, thus directing polluted air masses away from the St. Lawrence River as illustrated in the related ozone patterns which show low O_3 mixing ratios in that location. Later in the day at 20 UTC (3 pm local time) the wind direction in these areas turns northward bringing ozone toward the St. Lawrence River. Conversely, the wind direction over the heavily industrialized American Midwest ranges from west to north over all three frames bringing O_3 and NO_2 to the Great Lakes. Many authors (Brankov et al., 2003; Galvez, 2007; Godowitch et al., 2008) have

reported that long range transport (LRT) increases the probability of summertime O_3 episodes in (southern) Ontario when air flow is from the south and south west. While the results reported above show that CMAQ is able to reproduce the spatial variability of O_3 and NO_2, the statistical metrics outlined in Section 5.2.3 must also be examined as part of a comprehensive assessment of the model's performance.

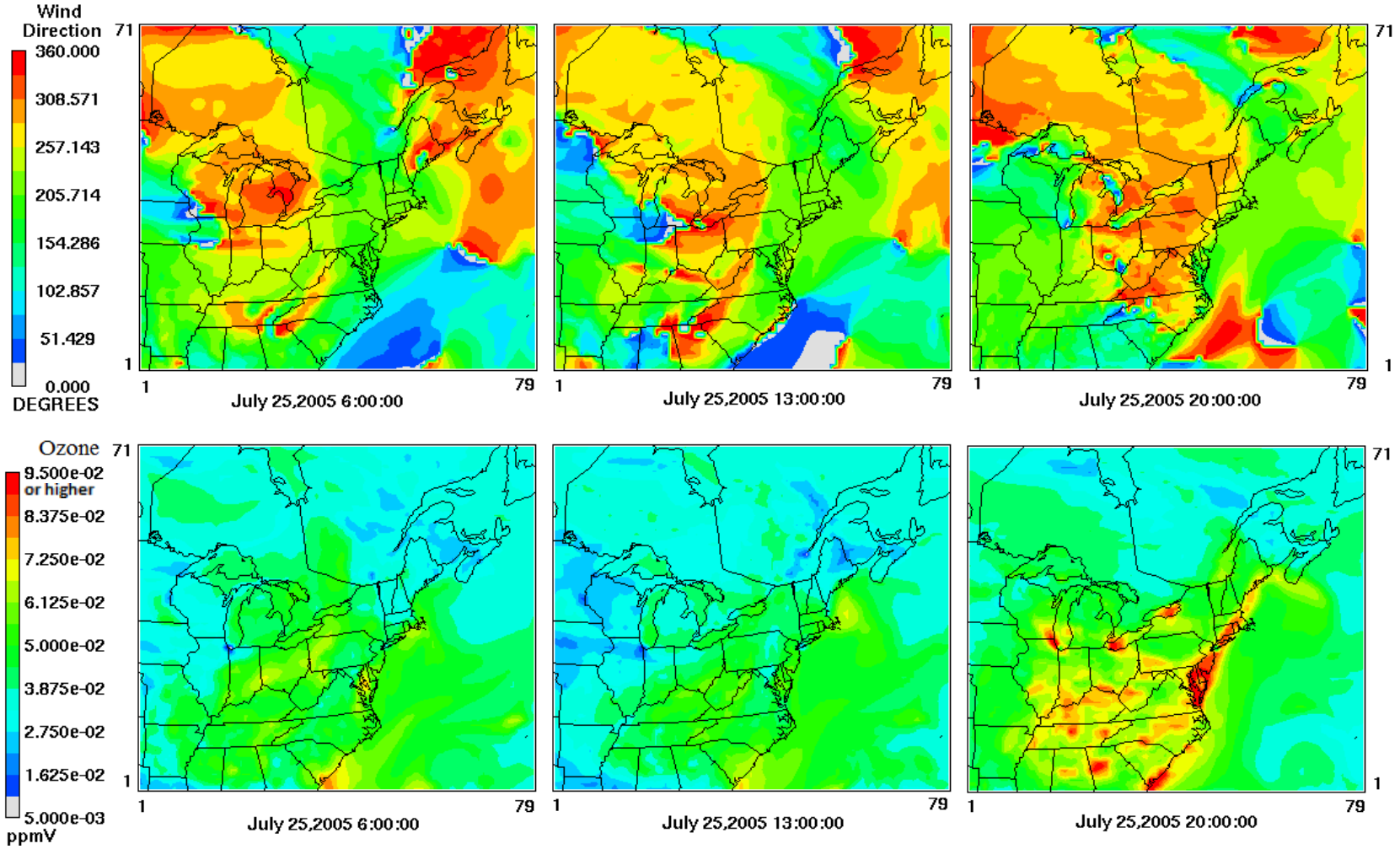

Figure 27. The wind direction over a representative fourteen hour period during the summer of 2005 (top panel), and the corresponding ozone (O_3) changes over the same period (bottom panel). North (348.75-11.25), east (78.75-101.25), south (168.75-191.25), west (258.75-281.25).

6.2.1.1 *Quantitative Analysis: Base Case*

Table 14, Table 15 and the accompanying visualization (Figure 28) provide a quantitative look at the spatial variation of O_3 and NO_2 at individual monitoring stations. They report the biases and errors of the model predictions for both species with respect to the measurements obtained from the MOEs monitoring stations in North Bay and Ottawa. No cut-off value was applied to the base case in order to provide a stringent analysis of the model's performance. Figure 28 reveals an overestimation of simulated O_3 for North Bay (0 ppb < MB < 5 ppb) as well as Ottawa (MB > 10 ppb). The large bias of Ottawa suggests that O_3 production and accumulation is overly robust in the CCTM. This is supported by the MNBE and MNGE for both sites which are well over their acceptable ranges outlined by the EPA. The UPA value for Ottawa was the only statistic for O_3 which did fit within the EPAs limits ($\pm$15-20%), while the UPA for North Bay fell just below this range at -13%. In contrast to O_3, the calculated metrics for the modelled NO_2 mixing ratios displayed an overall negative bias. The monthly values from June to August become progressively less negative for North Bay, but more negative for Ottawa. Both sites had mean biases in the range of -5 ppb to 0 ppb which shows good agreement with the measurements. Unlike the winter statistics, the NO_2 biases are smaller relative to those for O_3. The above results indicate that CMAQ performs acceptably in reproducing the spatial variation of O_3 and NO_2. This is substantiated by the over-prediction of the former and the under-prediction of the latter which is to be expected since the concentrations of each species rise and fall in opposition to each other.

Table 14. Model evaluation statistics for hourly ozone concentrations for June-August 2005.

City	Month	MB (ppb)	MNBE (%)	MNGE (%)	UPA (%)
North Bay	June	5.64	104	114	-13
	July	3.21	66	80	-7
	August	5.18	111	122	-11
	Summer Total	4.66	93	105	-13
Ottawa	June	10.41	106	109	23
	July	8.58	60	65	32
	August	11.14	81	85	16
	Summer Total	10.05	81	86	16

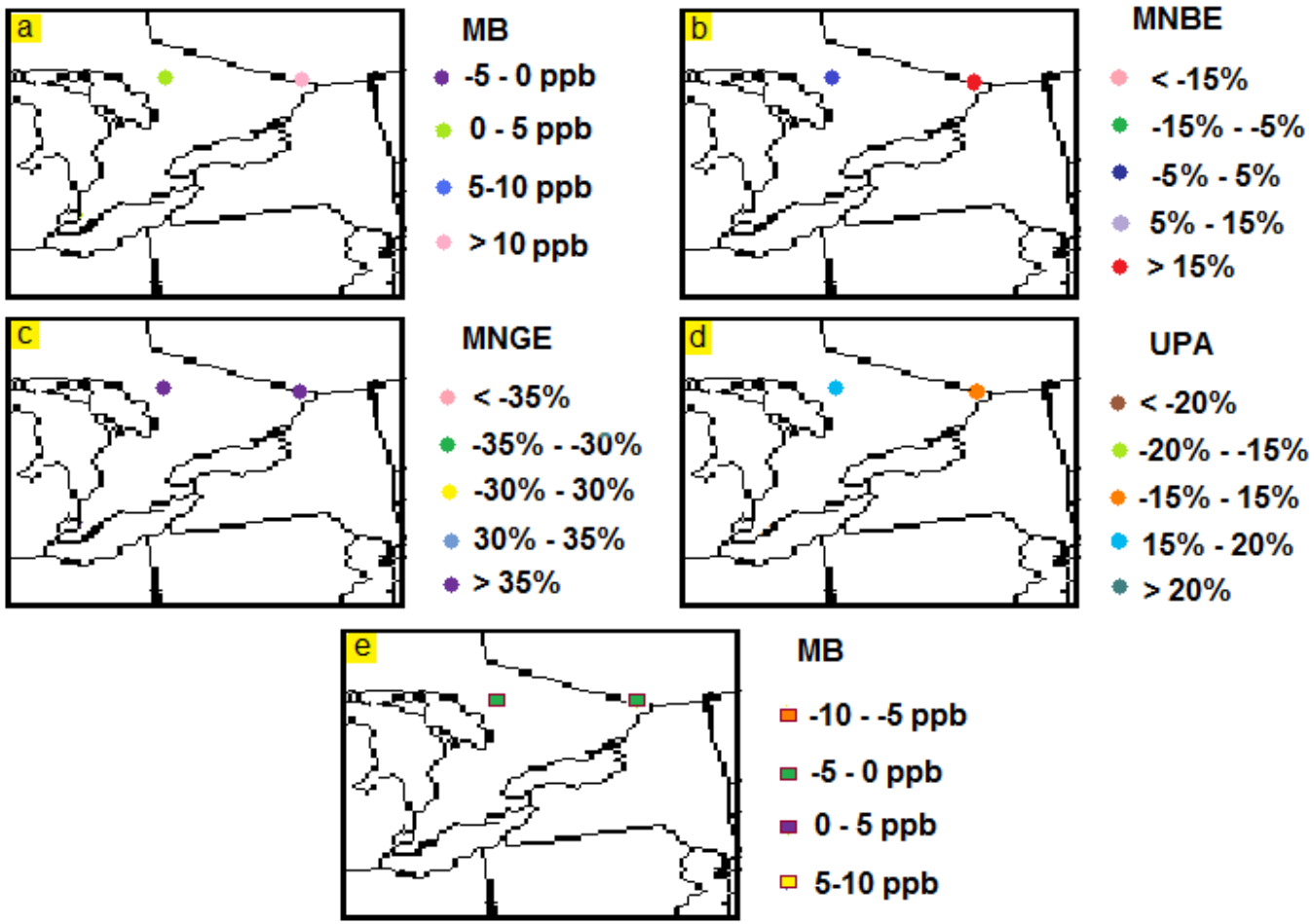

Figure 28. A statistical comparison of (a) mean bias, (b) mean normalized bias error, (c) mean normalized gross error and (d) the unpaired peak prediction accuracy for the 1-h average surface ozone (O3) mixing ratios between CMAQ output and the individual monitoring stations at North Bay and Ottawa. Mean bias for (e) nitrogen dioxide (NO_2) 1-h average mixing ratios are also reported. Model predictions that did not have a corresponding measurement value were not included in the analysis.

Table 15. Mean Bias for hourly nitrogen dioxide (NO_2) concentrations for June-August 2005.

	June (ppb)	July (ppb)	August (ppb)	Summer Total
North Bay	-2.49	-2.40	-1.75	-2.21
Ottawa	0.769	1.95	-10.05	-2.53

6.2.1.2 *Quantitative Analysis: Cases 2 and 3*

Continuing with the model evaluation, the statistical measures detailed in Section 5.2.3 were reapplied to the simulations and measurements using cut-off values of 40 ppb and 60 ppb for Case 2 and Case 3, respectively. The purpose of this was to monitor how CMAQ ozone predictions vary with concentration. Summertime O_3 background levels are on average 40 ppb in Ontario. This value was chosen as the first limit (Case 2) in the quantitative analysis. The next limiting value used was 60 ppb which was also selected by Tong et al. (2006) as the second cut-off value because they found that CMAQ best simulated O_3 mixing ratios between 40-60 ppb during the summer. Thus by eliminating the measurements below 40 ppb, the overall MB was reduced. The results of this analysis are reported in Table 16 and Table 17.

Table 16. Model evaluation statistics for hourly ozone (O_3) concentrations for June-August 2005 using a measurement cut-off value of 40 ppb.

City	MB (ppb)	MNBE (%)	MNGE (%)	UPA (%)
North Bay	-6.60	-11	18	-13
Ottawa	5.37	11	19	11

Table 17. Model evaluation statistics for hourly ozone (O_3) concentrations for June-August 2005 using a measurement cut-off value of 60 ppb.

City	MB (ppb)	MNBE (%)	MNGE (%)	UPA (%)
North Bay	-14.02	-20	22	-13
Ottawa	4.49	7	12	11

Examining the statistics at multiple locations provides a useful measure of spatial distribution in the simulation which could not be obtained if the concentrations were averaged over the entire domain. After applying the cut-offs, the MB for both Ottawa and North Bay became progressively smaller. With no cut-off, the MB for North Bay was positive, but turned negative once the limits were imposed. The MB for Ottawa remained positive with all three cases, but was reduced to less than 5 ppb for Case 3. The negative bias for North Bay is greater when 60 ppb is used rather than 40 ppb, whereas for Ottawa, the bias becomes smaller (i.e. the values move closer to zero) as larger cut-off standards are employed. A reduction in MB was expected because each imposed cut-off eliminated a great amount of data pairs in which over-prediction occurred since most hourly measurements were below 40 ppb and 60 ppb. The trend toward negative biases, which was also reported by Tong et al. (2006), is representative of CMAQs inability to replicate low concentrations of O_3. Using the EPAs criteria for model evaluation, it is seen in Table 16 and Table 17 that the results for the MB were matched by the MNBE which changed from a large positive integer at no cut-off, to being within the EPAs suggested range of accuracy ($\pm$5-15%) with a 40 ppb and 60 ppb cut-off. Only the MNBE for North Bay with a 60 ppb cut-off value was outside of this range. None of the calculated values for the MNGE fell within the EPAs recommended range of $\pm$30-35%, though all the values were smaller compared to when no cut-off was used. Similarly, none of the calculated UPA statistics met the EPAs standards as well. This means that CMAQ was not able to match the peak maxima. Similar to the winter episode, the overall performance of CMAQ has shown that it has the capability to sufficiently

simulate the spatial distribution of O_3 and NO_2. Thus the biases and errors reported in this section are likely a consequence of the emissions inventory having a greater concentration of one or both species relative to ambient conditions at both North Bay and Ottawa. A full evaluation of the model requires an examination of the temporal variability of CMAQs performance.

6.2.2 **Temporal Variability of Model Performance**

6.2.2.1 *North Bay*

In this section, the ability of CMAQ to reproduce the temporal features of O_3 and NO_2 measurements is evaluated for North Bay. Figure 29 exhibits the comparison of the hourly surface-O_3 mixing ratios for each month of the modelling period. The corresponding monthly scatter plots are shown in Figure 30. By observing both sets of graphs it can be seen that CMAQ is able to simulate the timing of the daily O_3 cycle, as the peaks and troughs of the modelled results are generally in phase with those of the measurements. However, CMAQ is not able to match the lower mixing ratios of the measurements which indicate weak titration of O_3 by the CCTM. The ozone measurements decline to zero, or close to zero, periodically over the duration of the modelling period. This pattern, which was not reproduced by the simulation, occurs from the late evening into the early morning hours. The over-prediction shown by the hourly time series matches with the overall positive bias reported in Table 14 for the summer period. The summer MB for North Bay was calculated to be 4.66 ppb, while the individual months varied between 3-6 ppb. The evaluation by Yu et al. (2008) which used CMAQ to estimate O_3 and its precursors in London, England, also found that CMAQ was inclined to over-predict minimum O_3 mixing rations during the night and early morning hours at times when the measured O_3 levels were low. A negative bias toward the maximum peak values is also revealed. This is corroborated by the UPA for the summer that was calculated to be -13% which lies just outside of the acceptable range of $\pm$15-20%. Despite the model's inability to simulate low concentrations of O_3, the

corresponding scatter plots (Figure 30) reveal a fairly good correlation between the model-measurement data pairs. The scatter plot for June shows little scatter away from the perfect correlation line, and has an R^2 value of 0.59 which is above the acceptable minimum of R^2= 0.50. The R^2 values for July and August are slightly below the standard at 0.44 and 0.49, respectively. They exhibit some scatter toward the higher end of O_3 mixing ratios, but appear to underestimate O_3 when its levels are between 20-40 ppb. Overall, CMAQ under-predicts O_3 at high concentrations, and over-predicts it at low concentrations. These findings are in agreement with those by Hogrefe et al. (2004) who examined an annual simulation of O_3, PM2.5 and the related meteorology over the continental United States. They are also in agreement with the winter results which indicated that the comparisons between modelled and measured values will not produce high correlation given the nature of datasets (i.e. point measurements versus grid-averaged concentrations).

In addition to the hourly dataset, it is necessary to consider 8-h maximum and average values. Analyzing CMAQs capability to estimate daily maximum and average 8-h O_3 concentrations is an important step in this model evaluation because even though Environment Canada and the US EPA have both set their own standards for acceptable O_3 exposure, many authors have found that no clear threshold value exists below which O_3 exposure is deemed safe (Mudway & Kelly, 2000). Thus it is necessary to consider 8-h maximum and averages in addition to the hourly dataset for a complete performance evaluation of CMAQ.

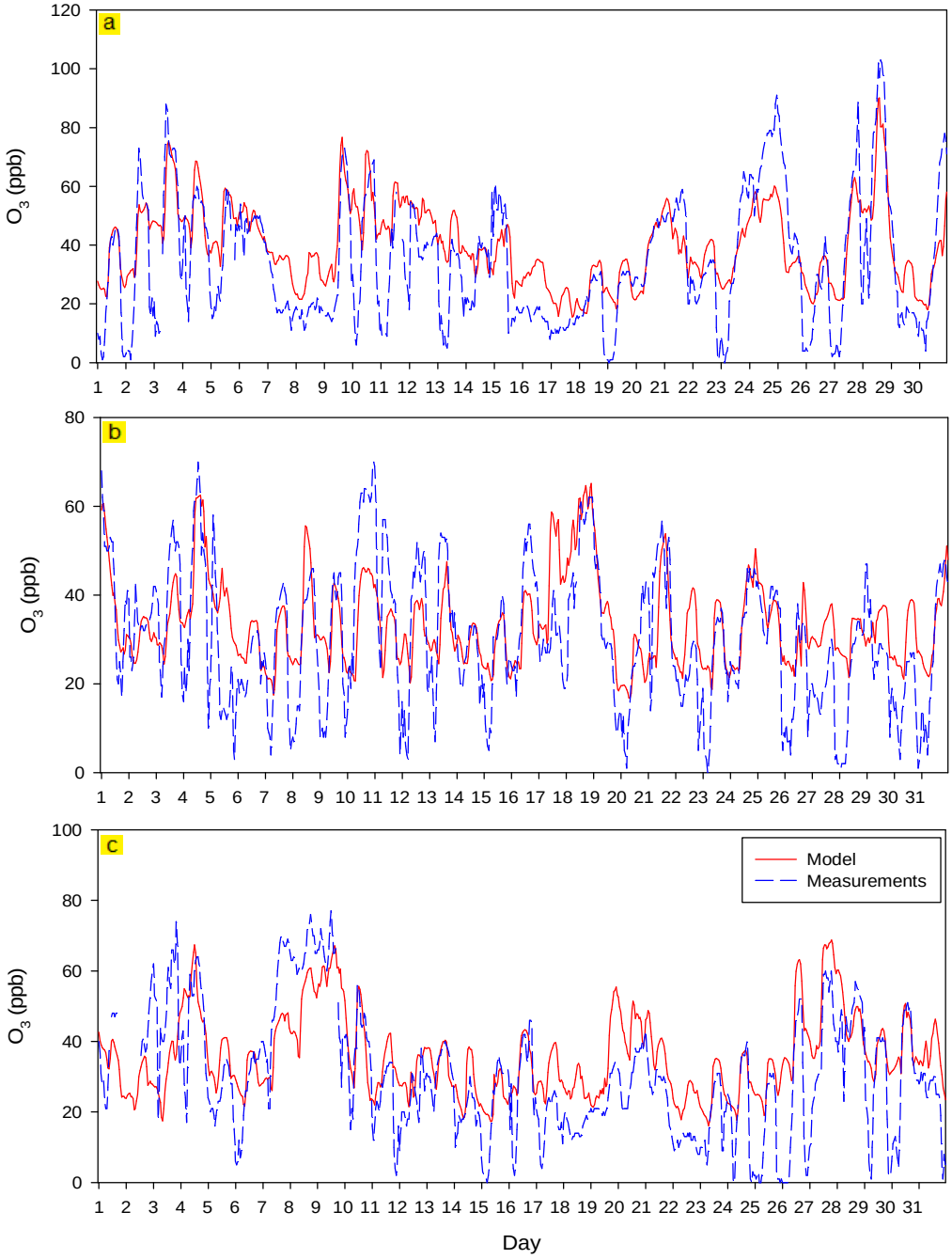

Figure 29. Comparisons of modelled (—) and measured (--) 1-h averaged surface ozone (O_3) mixing ratios for North Bay during 2005 (a) June (b) July and (c) August 2005.

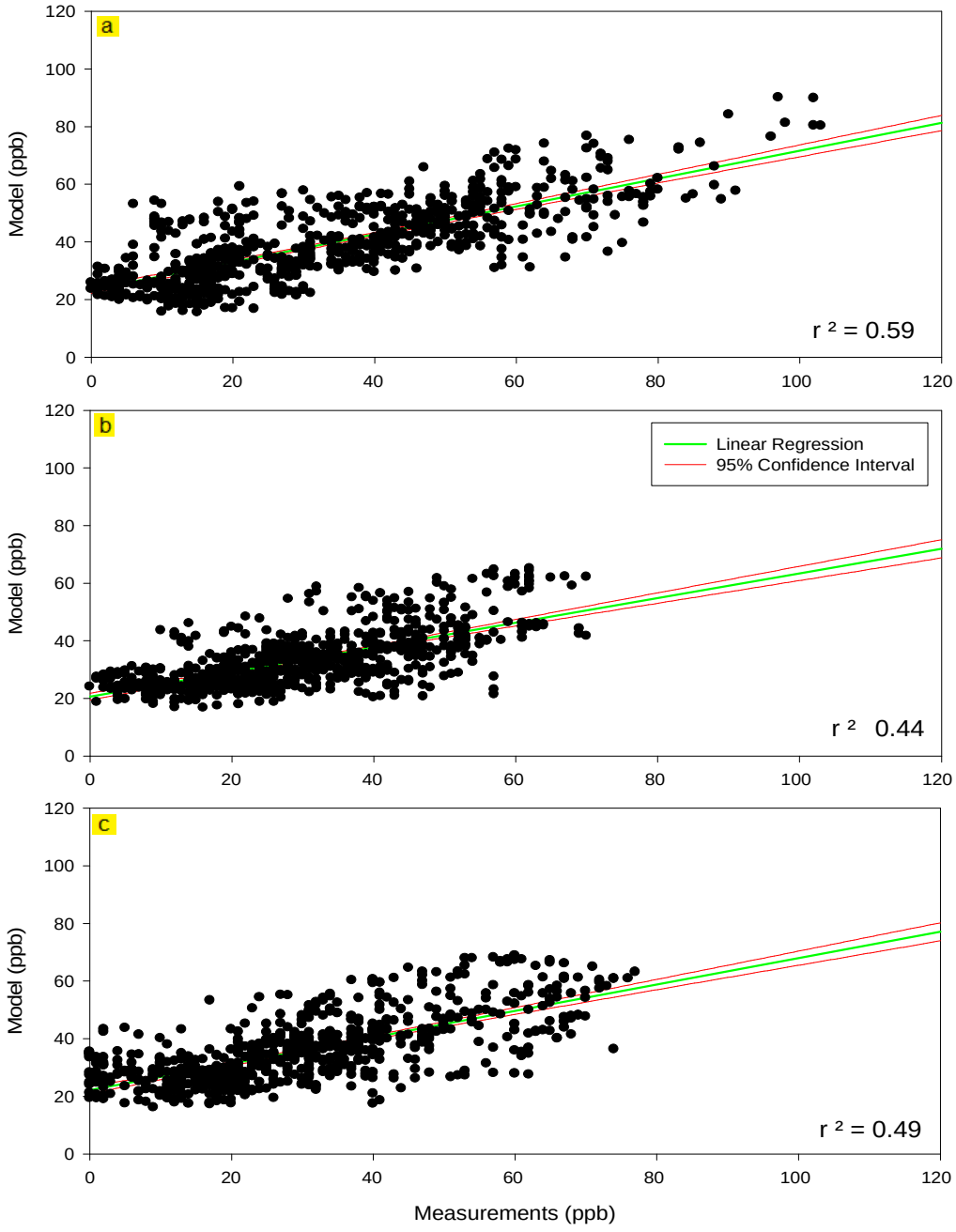

Figure 30. The O_3 1-h averaged scatter plots of model result plotted against measurements taken from the provincial monitoring station for North Bay during (d) June, (e) July and (f) August 2005.

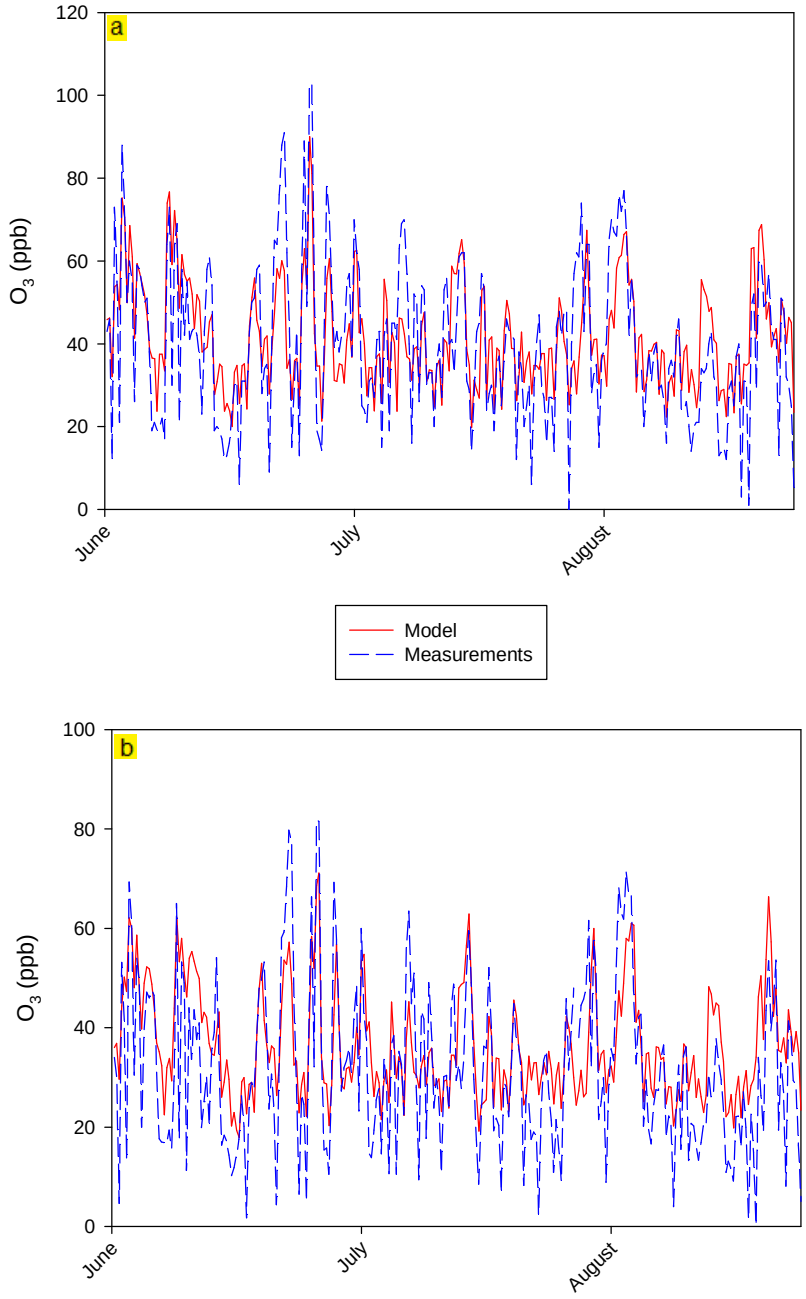

Figure 31. Comparisons of modelled (—) and measured (--) ozone (O_3) 8-h maximum and 8-average mixing ratios for North Bay during (a) June (b) July and (c) August 2005.

Table 18. Model evaluation statistics for 8-hour maximum ozone (O_3) mixing ratios for June-August 2005.

Month	MB (ppb)	MNBE (%)	MNGE (%)	UPA (%)
June	2.21	31	39	3
July	-1.84	15	32	-9
August	-5.70	6	39	-15
Summer Total	-1.90	17	37	-15

Table 19. Model evaluation statistics for 8-hour average ozone (O_3) mixing ratios for June-August 2005.

Month	MB (ppb)	MNBE (%)	MNGE (%)	UPA (%)
June	7.45	77	80	4
July	3.25	96	103	-5
August	0.29	59	82	-15
Summer Total	3.46	71	83	-15

Figure 31 presents the maximum and average 8-h time series comparisons for O_3 at the North Bay site. The accompanying summary statistics are shown in Table 18 and Table 19. Both the Canada Wide Standard and the US EPAs 8-h daily maximum limits were surpassed multiple times in contrast to the winter results (Figure 10). The 8-h maximum shows a gradual underestimation by CMAQ as the MB changes from positive to a negative value from June to August, cumulating in a summer total of -1.90 ppb. Though the summer total MB for the 8-h average O_3 values showed a positive bias at 3.46 ppb, the monthly values followed a similar trend to the 8-h maximum where the MB decreased from 7.45 ppb in June to 0.29 in August. Model evaluations by Appel et al. (2007) found similar results when modelling a summertime episode in 2001 over the eastern U.S.A. They reported that the 8-h average O_3 mixing ratio was over-predicted in both the winter and the summer.

In Figure 32, a comparison of the 1-hour NO_2 mixing ratios for June to August 2005 are displayed for North Bay. The model reproduced the temporal variation of the measurements adequately, as the peaks and troughs of the curves are in phase with each other. However, similar to the winter prediction for North Bay, the model showed a great amount of under-prediction throughout the summer period as it was not able to replicate mixing ratios of NO_2 above 5 ppb. These conclusions are corroborated by Shi et al. (2008) who reported that, while the agreement was good, NO_2 was systematically underestimated by CMAQ when compared to satellite column measurements for southern Ontario and the north eastern U.S.A. The summary statistics for NO_2 (Table 15) verify these results. The MB for June to August was quantified as -2.49 ppb, -2.40 ppb and -1.75 ppb, respectively, while the overall MB had a value of -2.21 ppb. The poor correlation between the simulation and measurements was also detailed by the NO_2 scatter plots whose monthly R^2 values were all well below 0.50. What is seen in the scatter plots is that although the measurements have a tendency to drop to zero ppb, the model still produces a mixing ratio value for the same hour. The hourly time series also shows this, and at low measured values, the plots reveal good correlations between the data pairs. Conversely, the amount of scatter in the plots increases as the measured concentrations increase. These results do coincide well with the ozone hourly time series such that when NO_2 increases, O_3 levels decrease. To develop a better understanding of how the two species interact, and to provide a more in depth test of CMAQs performance in modelling the temporal variation of O_3 and NO_2, the diurnal cycles of both species were analyzed.

Graphical analysis of the diurnal cycles of O_3 and NO_2 (Figure 34a and b) show that CMAQ can accurately simulate temporal features of each species. Both modelled and measured curves follow the same general pattern though the minimum O_3 concentrations due to titration by NOx during the morning rush hour appear to occur a few hours later in the model results compared to the measurements. The steepness of the incline is likely due to strong ozone formation and accumulation chemistry in the CCTM. Despite that difference, the

timing of the maximum peak height is the same for both curves except for the peak in June which has a slight phase shift of a few hours. The timings of the peaks vary according to the month. Normally the daily maximum ozone concentration occurs from 1-3 pm when solar radiation is greatest. However June and August both experience maximum observed values around 5 pm which then rapidly decline implying strong titration by NOx during the evening rush hour. The modelled results show a more gradual decrease which may be generated by slower titration with NOx.

In comparison to the winter O_3 cycle, the model results for the summer have a broader range between the daily maximum and minimum simulated values. Various factors contribute to the intraday fluctuations of O_3 such as increased daylight hours during the summer which prolong ozone formation and accumulation. The height of the PBL is important as well. During the winter in North Bay, the greatest PBL height simulated was just over 500 m in March, whereas the summer heights for all three months are between 1500-1700 m. The higher the PBL, the more O_3 is transported down toward the surface allowing for the accumulation of polluted air and thus an increase in O_3 concentration. The lowering of the PBL at night is accompanied by a decline in O_3 at the surface. Because mixing is limited, O_3 cannot replenish itself until the morning traffic generates an influx of precursors into the troposphere.

The height of the PBL also has an effect on the amount of NO_2 at the surface. The NO_2 cycle, observed in Figure 34b, is connected to the daily temporal pattern of O_3 and the PBL. During the morning and evening rush traffic hours when NO_2 reaches a maximum concentration, minimum O_3 levels are reached. This is the same cycle that is described by Figure 25 and Figure 26. The ability of CMAQ to accurately replicate this cycle for the summer episode leads to the conclusion that the model chemistry and transport processes are acceptable. Though the measurement curve is more pronounced than the simulation – which means that the NO_2 emissions may be deficient in the emissions inventory – the results do

agree with each other. This suggestion is also supported by the hourly NO_2 time series (Figure 32) which displayed a significant under-prediction of the simulated NO_2 mixing ratios relative to measurements. Overall, the model was able to reproduce the expected temporal pattern of both O_3 and NO_2 which indicates that it is working correctly. Next the level of Ox was examined because it incorporates both O_3 and NO_2, and thus is a measure of the accuracy of the emissions inventory. If the modelled and measured values significantly diverge, then one could conclude that the inventory inputs are erroneous. As noted by Lin et al. (2005), the emissions inventories – along with the meteorology – are the leading causes of errors in air quality simulations.

Figure 35 exhibits a good comparison of the modelled and measured Ox mixing ratios for the summer period, given that the simulation follows the same temporal pattern as the measurements. No large discrepancies exist between the two curves, though the model does appear to be unable to replicate the lower concentrations of Ox similar to the predictions made for the hourly surface-O_3 comparisons from Figure 29. The Ox scatter plots (Figure 36) also show good agreement between the two datasets. Very little scatter can be seen in the plot for June, while the opposite holds true for July. The August plot shows good correlation at the lower end of O_3 mixing ratios but starts to diverge away from the perfect correlation line as O_3 increases. These observations are supported by the R^2 values which are a respectable 0.65 and 0.54, respectively, for June and August, and 0.42 for July. Due to the conformity between the model-measurement pairs, the emissions inventory likely does not contain any large sources of error which would cause a deviation in the comparisons. It can be concluded then, that the comparison between two different datasets – the 36km averaged modelling results and the point measurements from the AQ station – was the main cause of inaccuracy in the hourly and diurnal comparisons.

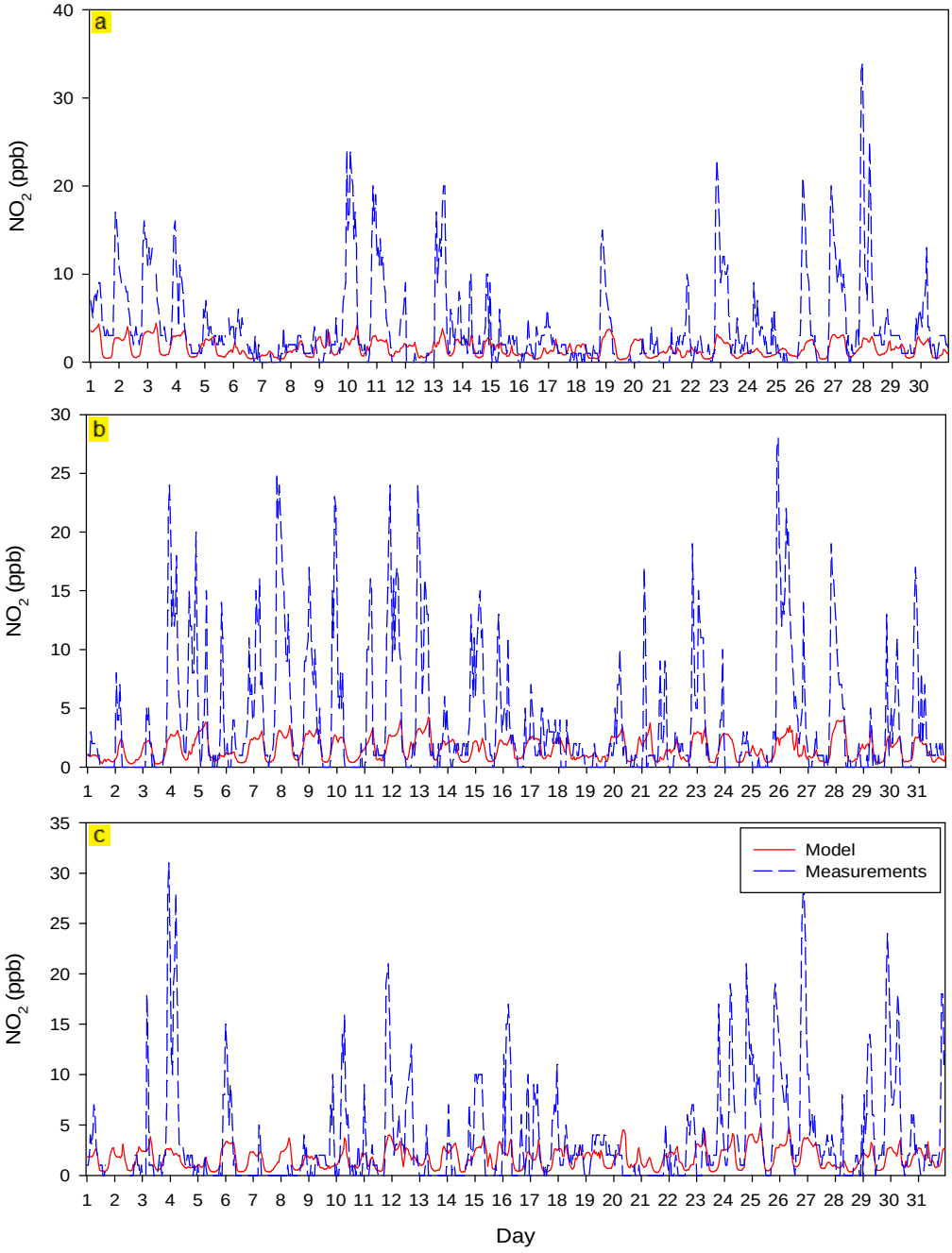

Figure 32. Comparisons of modelled (—) and measured (--) 1-h averaged surface nitrogen dioxide (NO_2) mixing ratios for North Bay during (a) June (b) July and (c) August 2005.

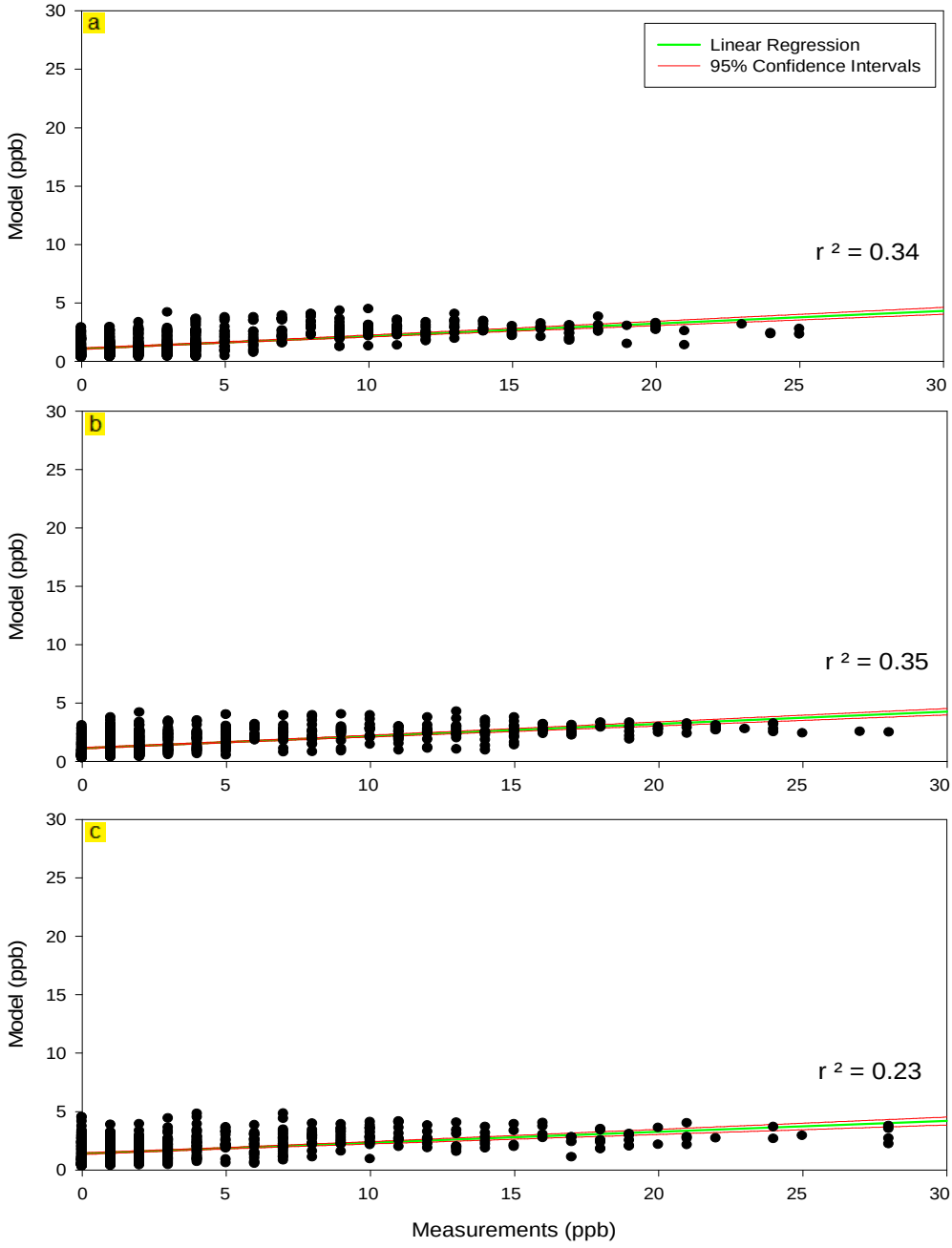

Figure 33. The nitrogen dioxide (NO_2) 1-h averaged scatter plots of model results plotted against measurements taken from provincial monitoring stations for North Bay during (d) June, (e) July and (f) August 2005.

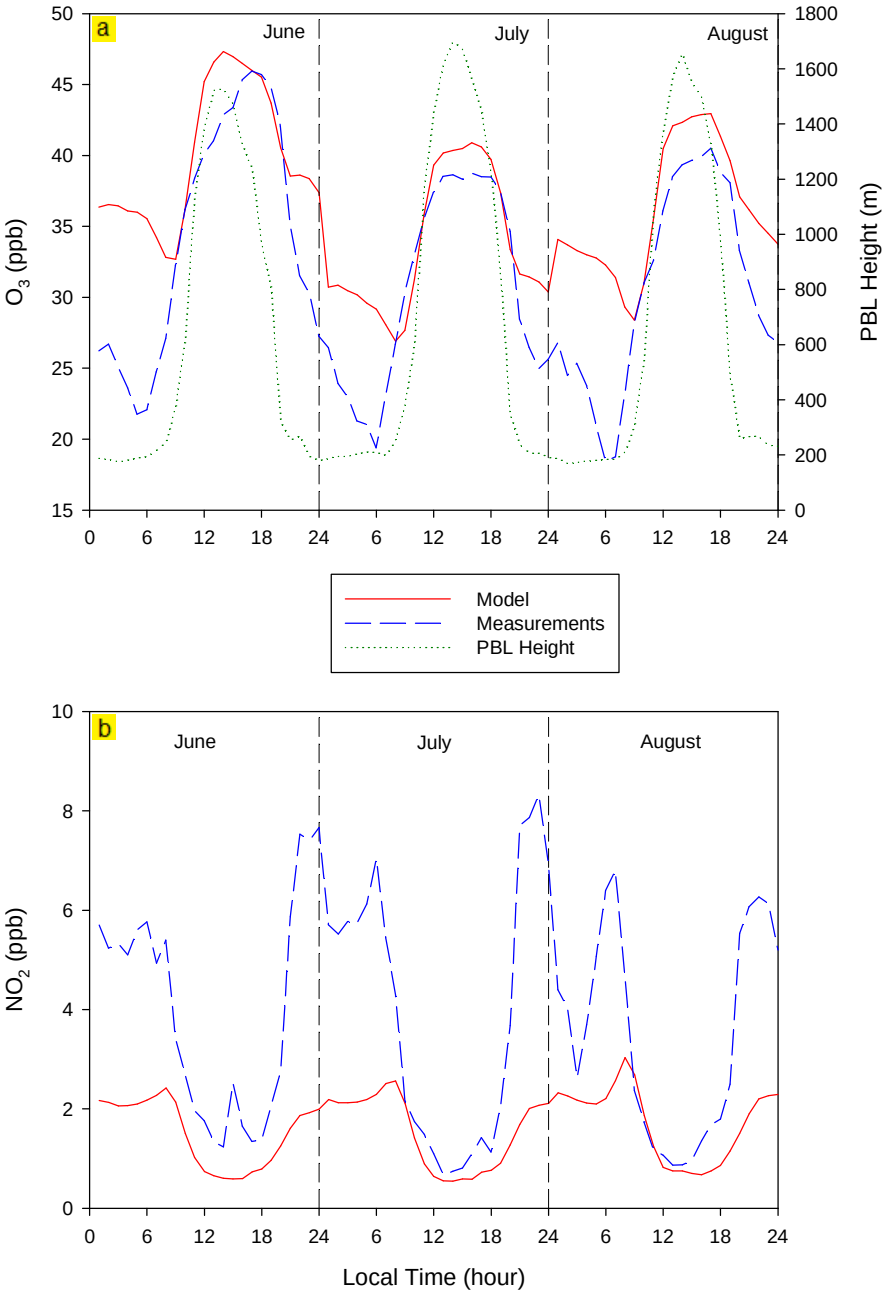

Figure 34. The 2005 summertime diurnal cycles of (a) ozone (O_3) and the planetary boundary layer (PBL) height and (b) nitrogen dioxide (NO_2) for North Bay. Model (—), measurements (--), simulated PBL height (···).

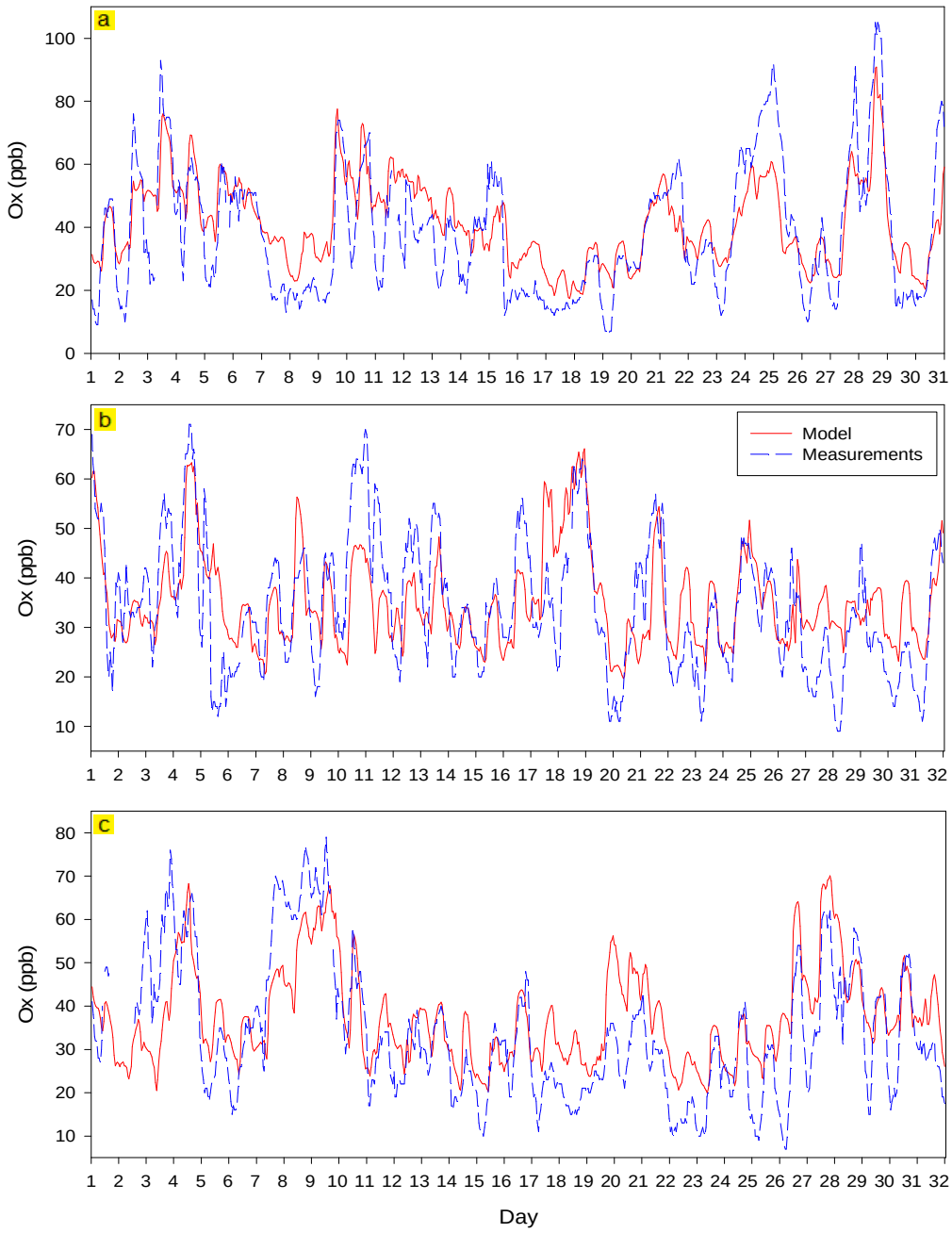

Figure 35. Comparisons of modelled (—) and measured (--) 1-h averaged oxidant (Ox) mixing ratios for North Bay during (a) June (b) July and (c) August 2005.

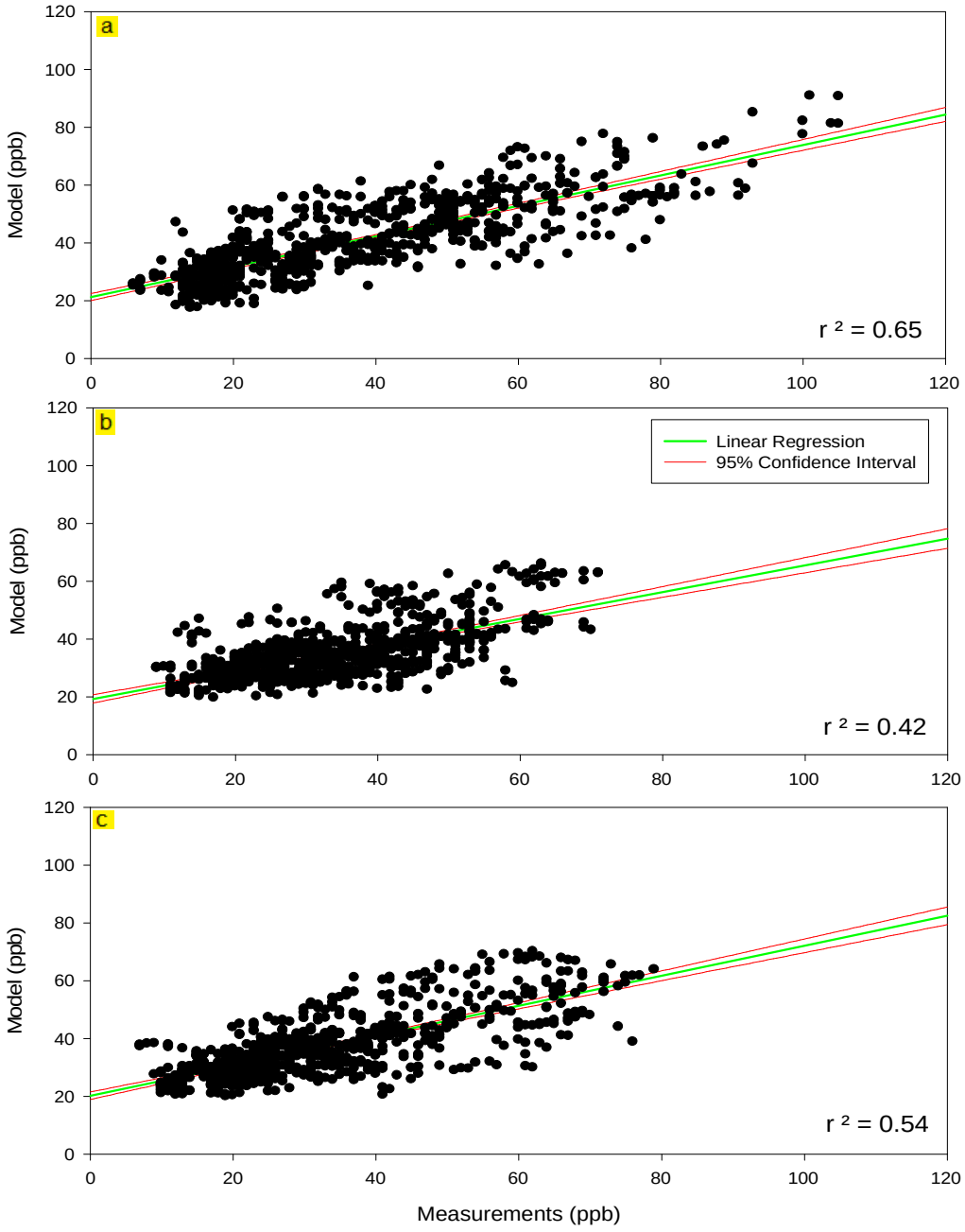

Figure 36. The hourly averaged oxidant (Ox) scatter plots of model results plotted against measurements taken from provincial monitoring stations for North Bay during (d) June, (e) July and (f) August 2005.

6.2.2.2 *Ottawa*

The CMAQ summer simulations for the rural site of North Bay showed a strong correlation between the model simulations and the measurements. In this section, I investigate the model's performance in an urban environment. The 1-h ozone time series and scatter plots for Ottawa are shown in Figure 37 and Figure 38. The time series show a strong correlation between the timing of the model results and the measurements with a consistent overestimation of O_3 at both high and low concentrations. A likely source of this overestimation may be that O_3 production chemistry in the CCTM is too robust, possibly due to too little cloud formation. The statistical summary from Table 14 verifies this graphical analysis given that the MB for June (MB= 10.41 ppb), July (MB= 8.58 ppb) and August (MB= 11.14 ppb) all show a positive bias. The overall MB for the summer is seen to be 10.05 ppb. In June, there is high correlation between the model results and measurements as confirmed by the scatter plot for the month (Figure 38a) which gave an R^2 value of 0.68 with very little scatter. The plots for July and August also reveal good agreement between the data sets with correlation coefficients of R^2= 0.56 for July and R^2=0.58 for August. The summer total MNBE (93%) and MNGE (81%) are both well over their designated ranges, as are the monthly values. The UPA, a measure of peak prediction accuracy, all show an over-prediction by CMAQ though only the value for August (16%) – which is the same as the summer total value – falls within the EPAs acceptable range of $\pm$15-20%. These calculations are similar to those generated for Ottawa during the winter episode although the much larger summer biases can be attributed to the increase in ozone production efficiency from the extended daylight hour and warmer temperatures.

It should be noted that the majority of the measurements are in the range of 20-40 ppb even though, as previously mentioned, the established summertime background O_3 levels for southern Ontario are considered to be 40 ppb. Thus one would expect higher O_3 mixing ratio to be measured in lieu of long range transport contributions. However because Ottawa is a major urban centre O_3 levels are lowered by the titration effect due to excess NOx emissions.

In rural regions, the ratio of precursors is more balanced such that the titration effect is less significant (Moussiopoulos et al., 2009). The titration effect also helps explain the CMAQ over-prediction in the hourly time series, as it makes evident the over-active ozone production in the CCTM which gets averaged out across the entire grid cell without accounting for concentration gradients.

A plot of the 8-h maximum and average O_3 mixing ratios was created to supplement the preceding analysis. The statistical analyses for these graphs are presented in Table 20 and Table 21. The graphs show that CMAQ was not able to replicate the minimum values of O_3, but over-predicted the maximum values which is supported by the MB for the 8-h maximum (MB= 10.84 ppb) and the 8-h average (MB= 9.95 ppb). The MNBE, MNGE and UPA statistics also have a positive bias. By generating the 8-h average and 8-h maximum graphs, one can see whether the US EPAs or the CWS was breached during the summer period. The results show that both are repeatedly surpassed by the simulation and measurements. This shows that the 8-h maximum and average graphs are a useful tool in prevention and monitoring.

Table 20. Model evaluation statistics for 8-hour maximum ozone (O_3) mixing ratios for June to August 2005.

Month	**MB (ppb)**	**MNBE (%)**	**MNGE (%)**	**UPA (%)**
Summer Total	10.84	45	47	11

Table 21. Model evaluation statistics for 8-hour average ozone (O_3) mixing ratios for June to August 2005.

Month	**MB (ppb)**	**MNBE (%)**	**MNGE (%)**	**UPA (%)**
Summer Total	9.95	62	64	5

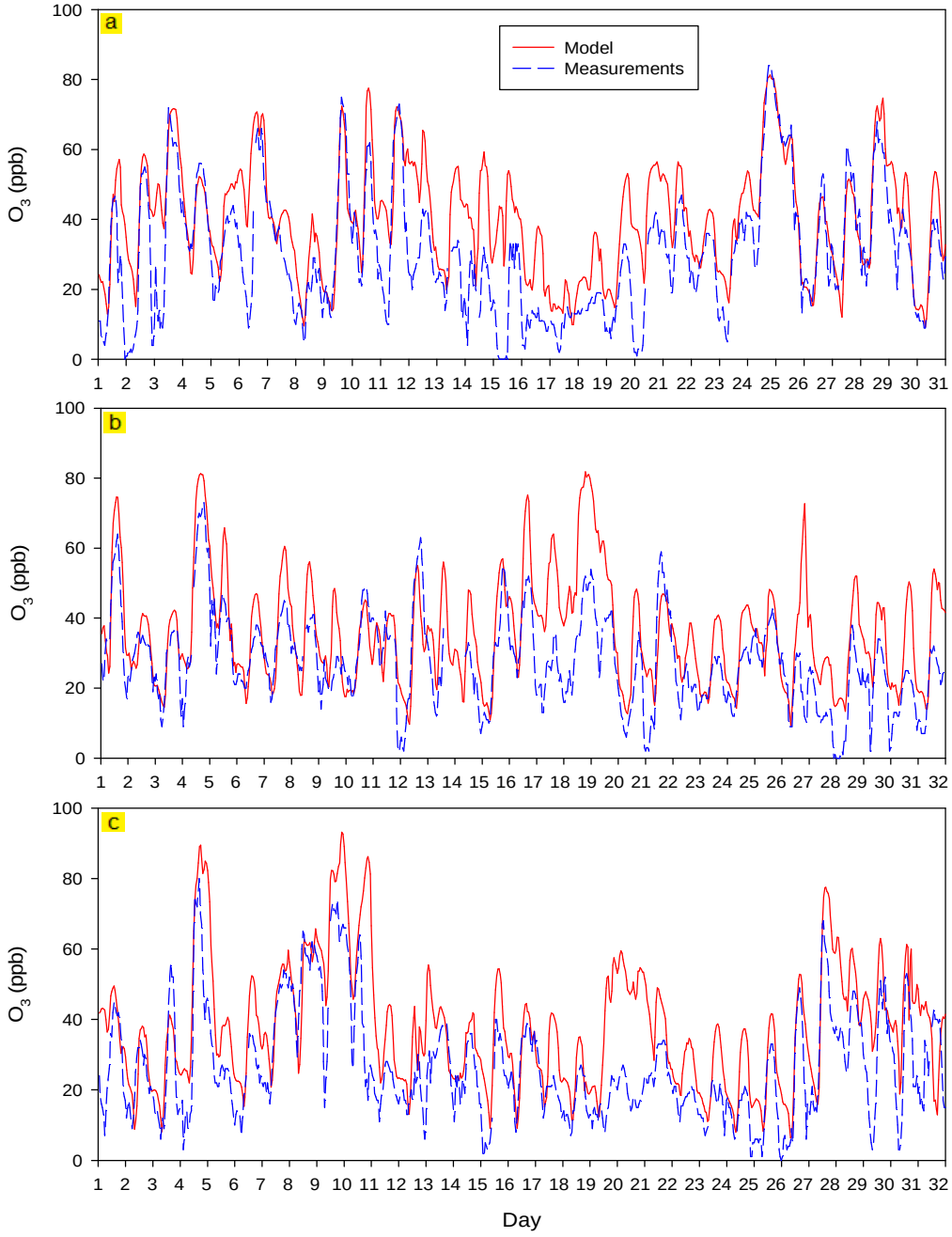

Figure 37. Comparisons of modelled (—) and measured (--) 1-h averaged surface ozone (O_3) mixing ratios for Ottawa during (a) June (b) July and (c) August 2005

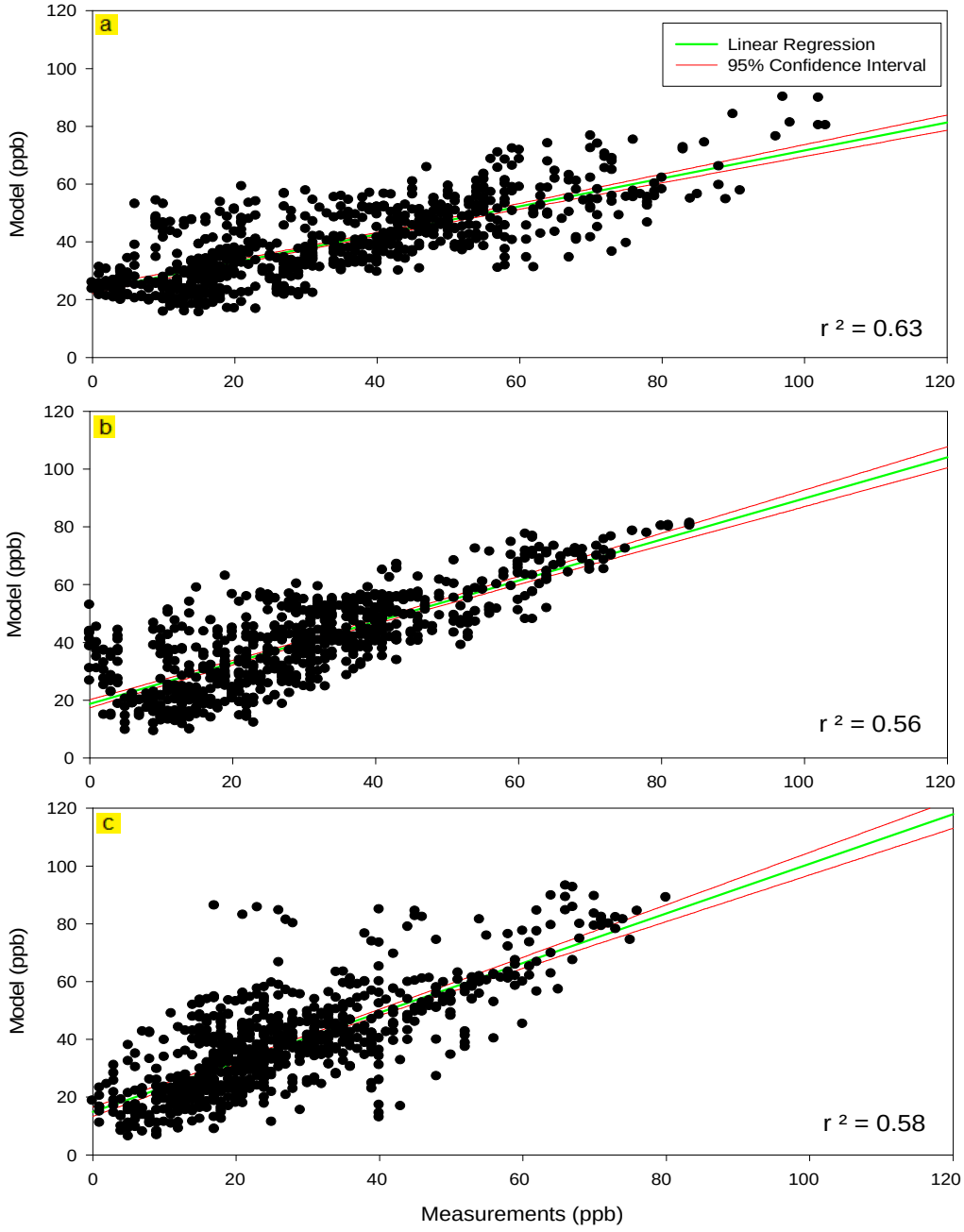

Figure 38. The hourly averaged ozone (O_3) scatter plots of model result plotted against measurements taken from the provincial monitoring station for downtown Ottawa during (d) June, (e) July and (f) August 2005.

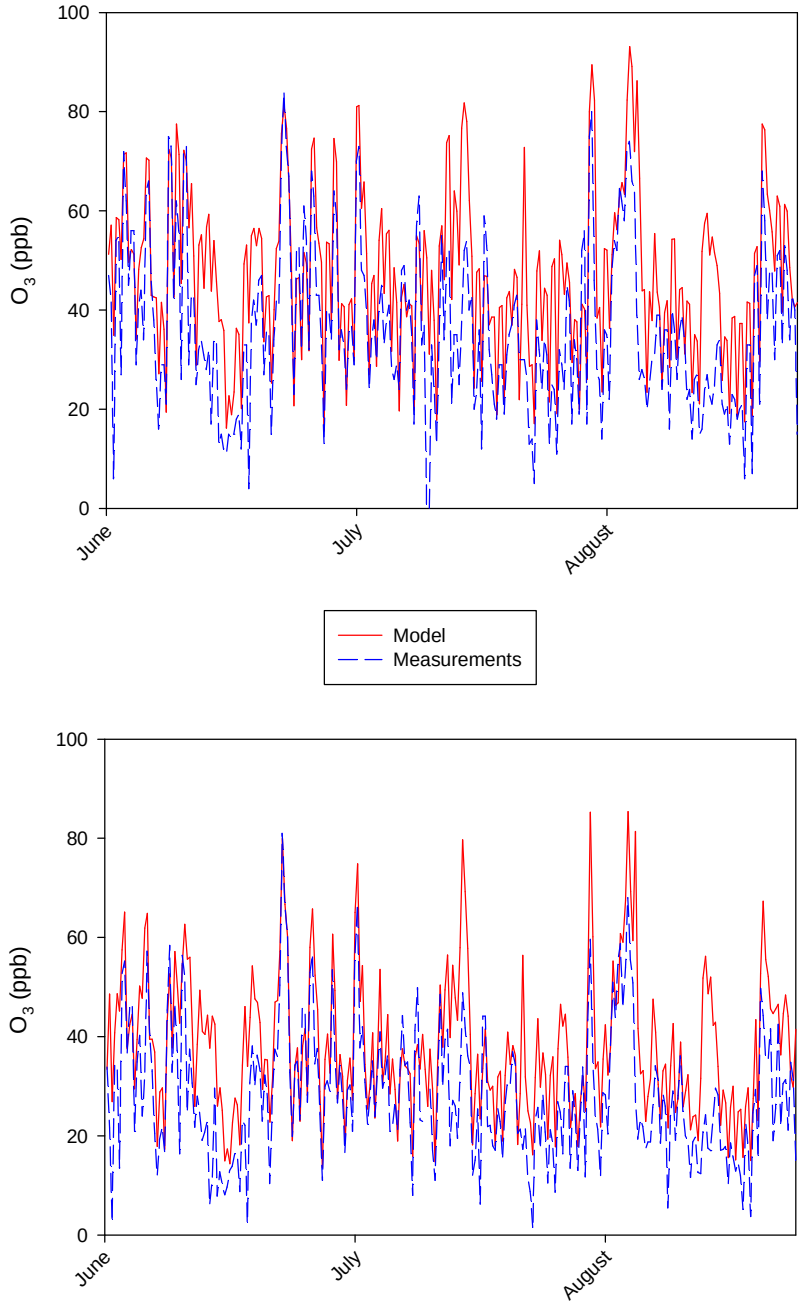

Figure 39. Comparisons of modelled (—) and measured (--) ozone (O_3) 8-h maximum and 8-average mixing ratios for Ottawa during (a) June (b) July and (c) August 2005.

Because the amount of O_3 in urban regions is highly influenced by NOx emissions, the 1-h NO_2 time series was created to compare against the O_3 results. Figure 40 describes the accuracy of the CMAQ output with respect to NO_2. The monthly graphs show that the there is a general temporal agreement between the model and measurements, although the model moderately under-predicted the overall NO_2 given the MB which equals -2.53 ppb. This trend is supported in the scientific review by Laj et al. (2009). A clear difference between Figure 40 and the North Bay NO_2 time series from Figure 32 is that major urban areas like Ottawa have larger NO_2 mixing ratios which are accounted for by the model. CMAQ over-estimated NO_2 for June (MB= 0.77 ppb) and July (MB= 1.95 ppb) but generated a MB of -10.05 ppb for August. These calculations should be looked at critically because most data from the month of August were not available. Had more measurements been incorporated into the statistics, the MB for the month may possibly have followed a positive trend. This would have also resulted in the overall MB being a positive value. The NO_2 mixing ratios extended from around 2-20 ppb for Ottawa which implies that the emissions inventories contain more NO_2 and NOx emissions for urban environments than for rural areas. Additionally, the scatter plots in Figure 41 do not illustrate good correlation between the two datasets as all the R^2 values are below 0.3. Again, the result for August must be scrutinized due to a lack of data points available for the comparison.

A plot of hourly NOx mixing ratios is analyzed next to observe the behaviour of NO_2 relative to NOx emissions as a whole. Comparing the simulated and measured NOx concentrations is a valuable method to determine if the NO_2 emissions described in the emissions inventories are correct since the majority of NO_2 is created through conversion from NO. Due to the relationship between the two species, NO_2 is expected to follow the same pattern as NO (R. Atkinson, 2000). The comparison of modelled and measured NOx shows that the model does not match the high or low mixing ratios of the measurements. The measurements exceed 30 ppb on many days, but the model mostly simulates NO_2 between 5-15 ppb. The

differences may be due to the chemical mechanism of choice. As mentioned in Section 3.3.6, SAPRC-99 has upgraded radical recycling which allows more oxidized nitrogen species like HNO_3 to go back into the nitrogen cycle rather than acting as termination species (Luecken et al., 2008).

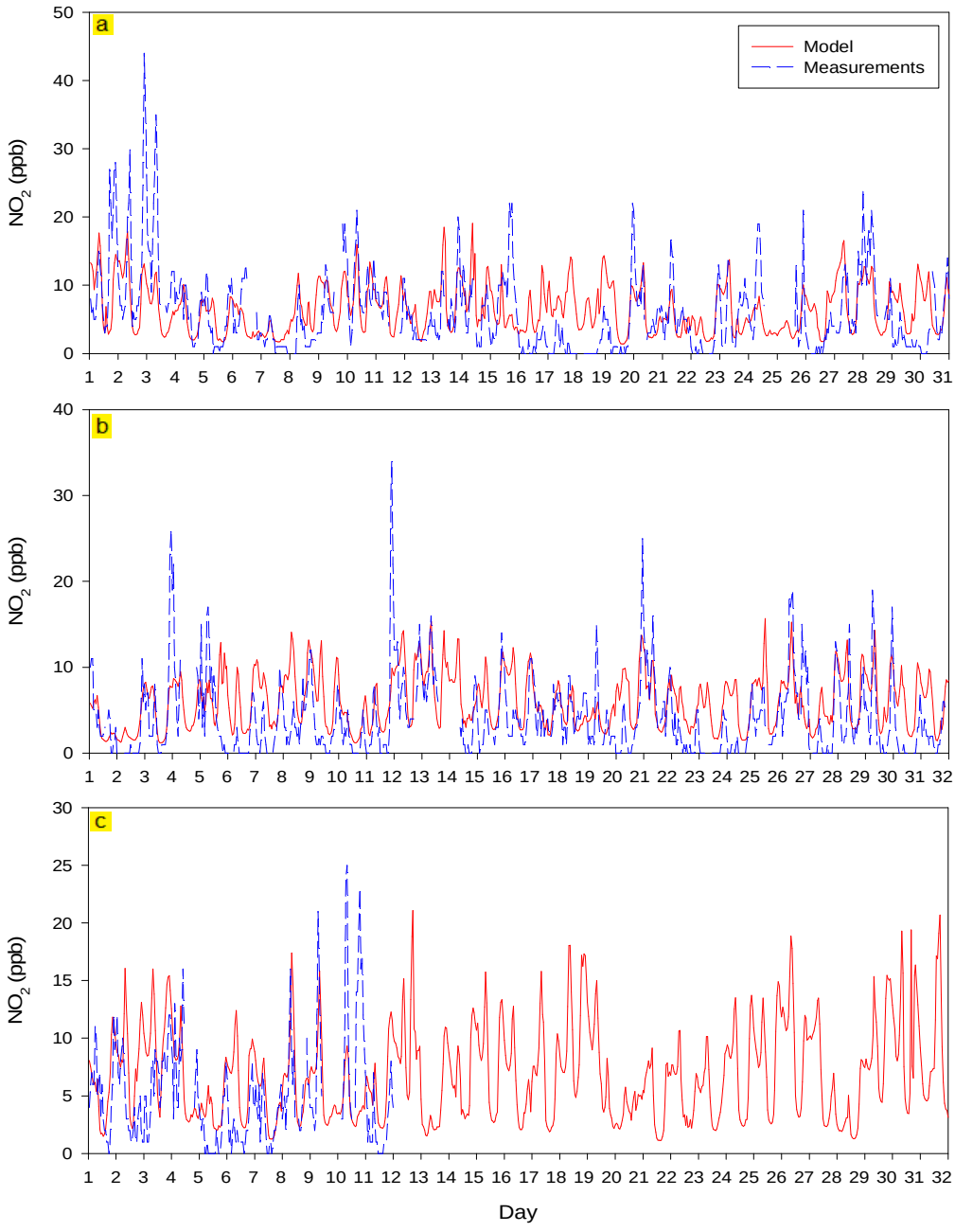

Figure 40. A comparison of the modelled (—) and measured (--) 1-hour averaged surface nitrogen dioxide (NO_2) mixing ratios for Ottawa during (a) June, (b) July and (c) August 2005.

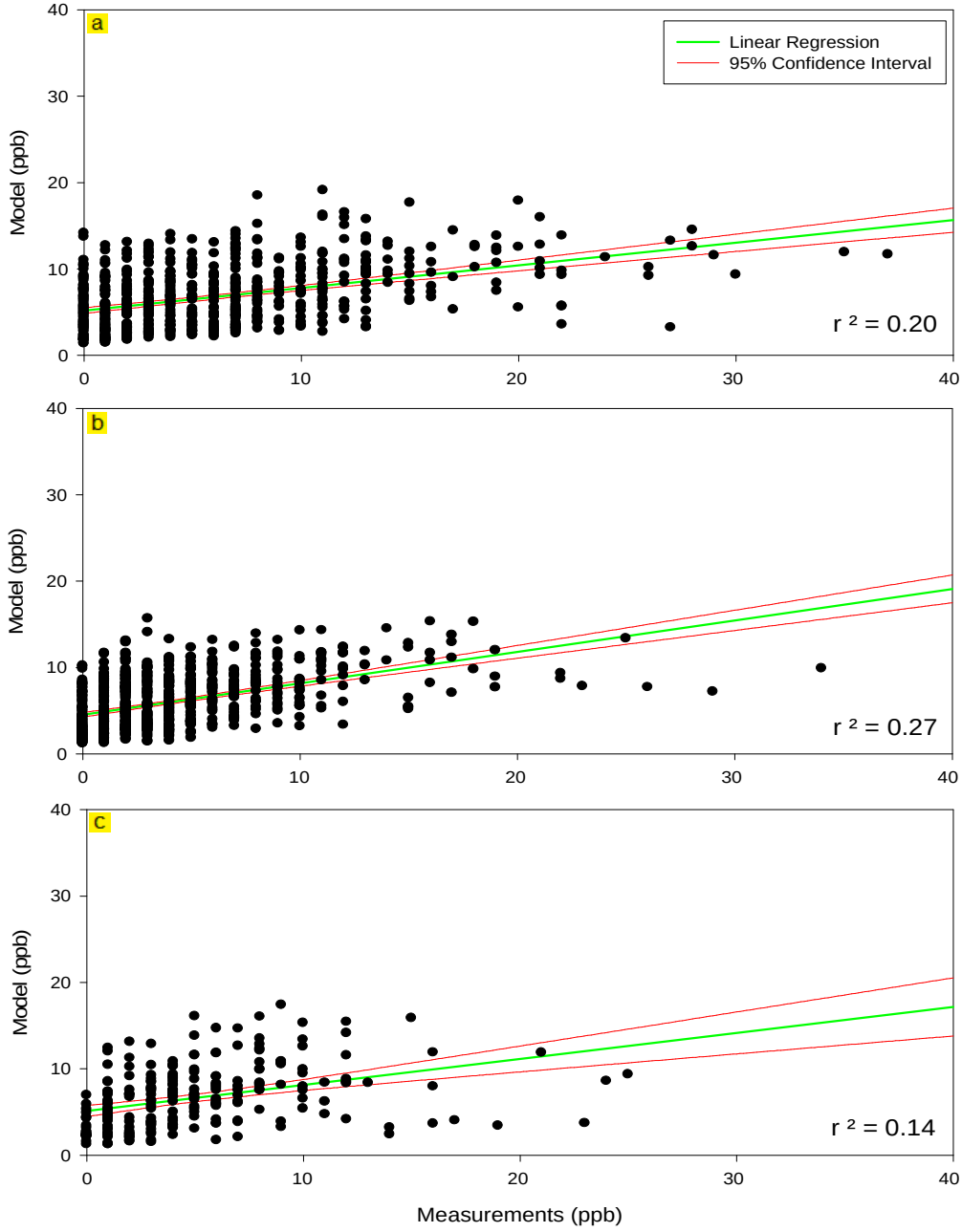

Figure 41. The 1-h averaged nitrogen dioxide (NO_2) scatter plots of model results plotted against measurements taken from provincial monitoring stations for Ottawa during (a) June, (b) July and (c) August 2005.

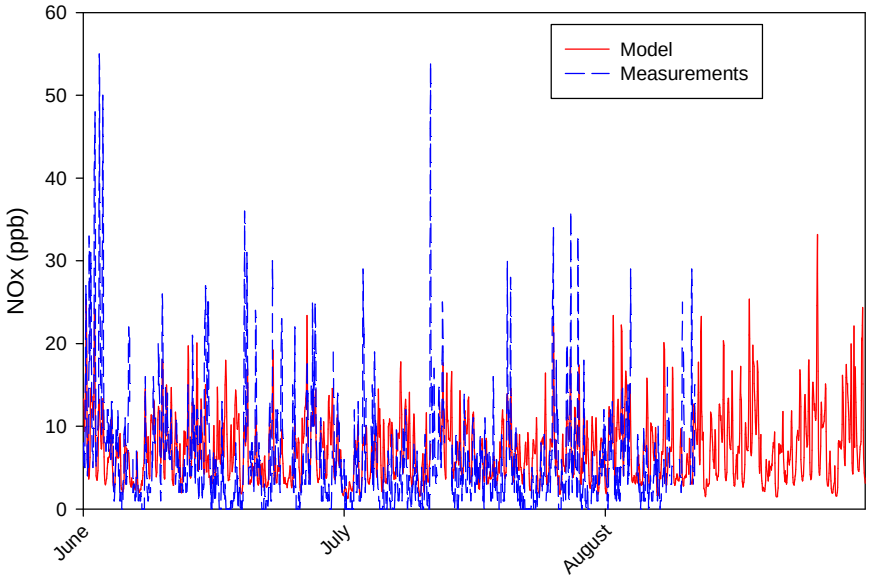

Figure 42. Comparison between modelled (—) and measured (--) 1-h averaged NOx mixing ratios for Ottawa from June to August 2005. A significant portion of the month of August was not available for the comparisons.

The diurnal cycles of O_3 and NO_2 are shown in Figure 43. CMAQ shows the ability to accurately reproduce the temporal cycle of each species with fairly good accuracy. By observing the O_3 cycle, it can be seen that the timing of the measured and simulated peaks for June and August occur between 1-3 pm in occurrence with the literature, while the modelled O_3 in August reaches its maximum value at 4 pm. These maxima coincide exactly with the minimum values of the NO_2 cycle. In the morning around 7 am, NO_2 begins to rise from fossil fuel emissions and O_3 reaches its daily minimum. As the volume of traffic slows, NO_2 starts its daily decline while O_3 reaches its peak value in the afternoon. During the early evening (6-9 pm) O_3 starts to decline as NO_2 accumulates from rush hour traffic. This is in agreement with the spatial distribution results from Section 6.2.1. Previous studies have reported that the rate of ozone destruction at this time depends on the altitude, with the highest rate occurring near the surface due to NOx titration and dry deposition (J. Lin et al., 2008). Although the evening O_3 levels do deteriorate as the NO_2 concentrations increase,

there is no distinct minimum value seen during the evening rush traffic hour as was the case for the winter analysis. A possible explanation for the elevated levels of nighttime O_3 may be because when winds approach from the south or southwest, they are transporting polluted air masses from the ORV into Ontario (Yu et al., 2008). The ORV is heavily polluted from large point source emissions which, when transported by physical processes, raise O_3 levels downwind (Brankov et al., 2003; Sillman, 1993).

The levels of O_3 and NO_2 in the troposphere also largely depend on the height of the PBL. During the day, the concentration of ozone increases rapidly with the influx of solar radiation as it speeds up the rate of photolytic reactions. This also warms the earth's surface heating the air above it causing an elevated, unstable PBL where ozone at higher altitudes can be transported to the surface by vertical mixing (J. Lin et al., 2008). During the nighttime, the earth's surface cools allowing for a stable, shallow (nocturnal) boundary layer where O_3 can start to accumulate due to limited mixing. The PBL appears to be much higher during the summer compared to the winter, though ozone levels are higher in the summer given the more favourable O_3-producing conditions. The simulations generate maximum monthly heights from 1400-1600 m and monthly minima at approximately 200 m. In general, the YSU scheme that I used has been found to generate higher O_3 mixing ratios and lower NOx levels than other PBL parameterizations. The YSU scheme, developed by YonSei University, is a vertical diffusion package with nonlocal turbulent mixing in the PBL. This is a key contributing factor to the large PBL height produced by the model. Overall, CMAQ was able to successfully reproduce the temporal features of O_3 and NO_2 diurnal cycles.

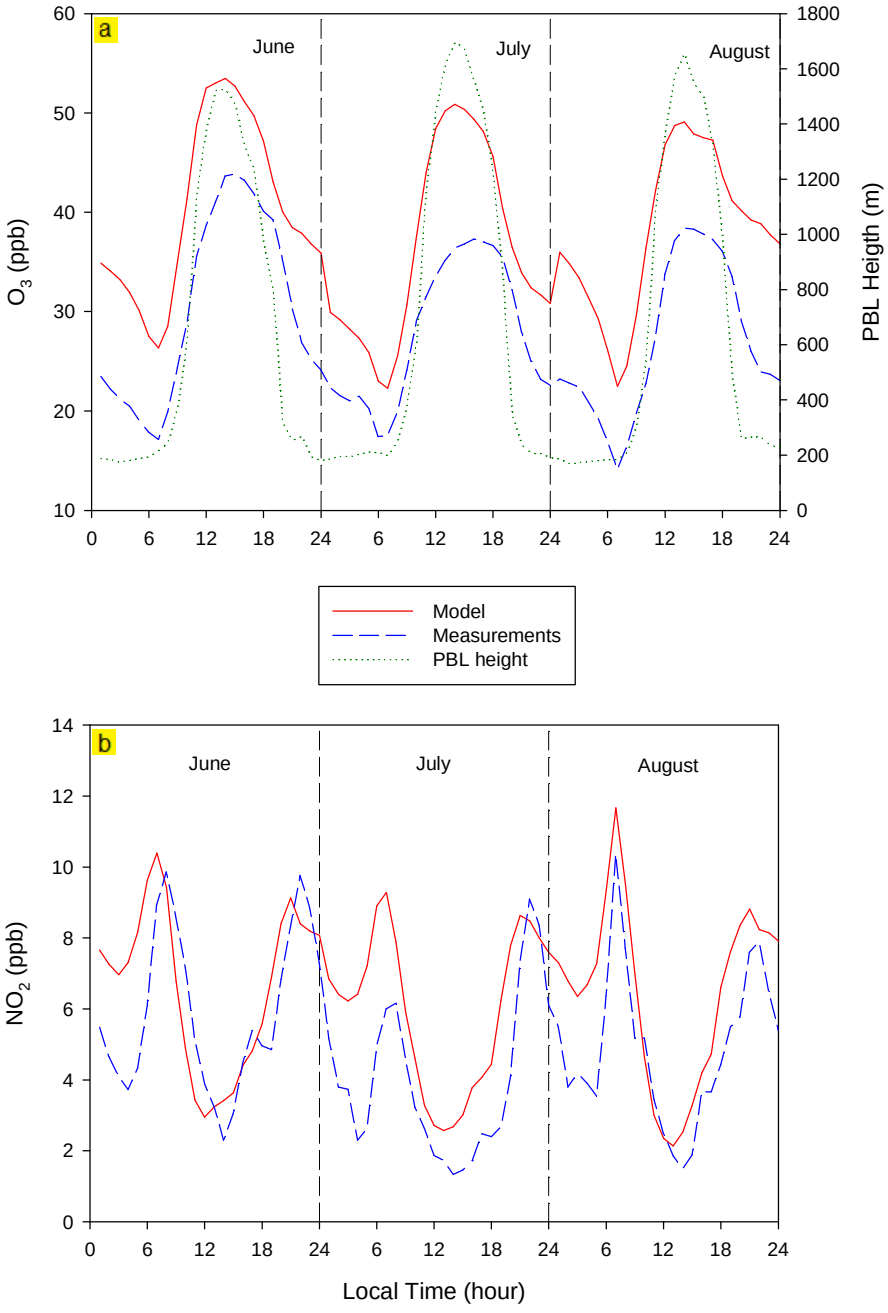

Figure 43. The 2005 summertime diurnal cycles of (a) ozone (O_3), the planetary boundary layer (PBL) height and (b) NO_2 for Ottawa. Model (—), measurements (--), simulated PBL height (···).

The last analysis to be completed was that for Ox. Figure 44 and Figure 45 illustrate the capability of the CMAQ system in simulating the hourly mixing ratios of O_3 and NO_2 during the summer in an urban centre. The comparison between the model output and measurements shows very good agreement as established by the correlation coefficients from the scatter plots which were all between 0.52-0.54. As with O_3, Ox tends to simulate levels above the measurements, causing the maxima and minima to be over-predicted. The accuracy in the graphs indicates that absences of major errors in the emissions inventories. Because Ox is normally a species used to describe urban settings due to their high levels of NOx, any large errors in the emissions input to the model would be seen in these graphs. In general, the model does a good job in reproducing the levels of Ox when compared to the measurements.

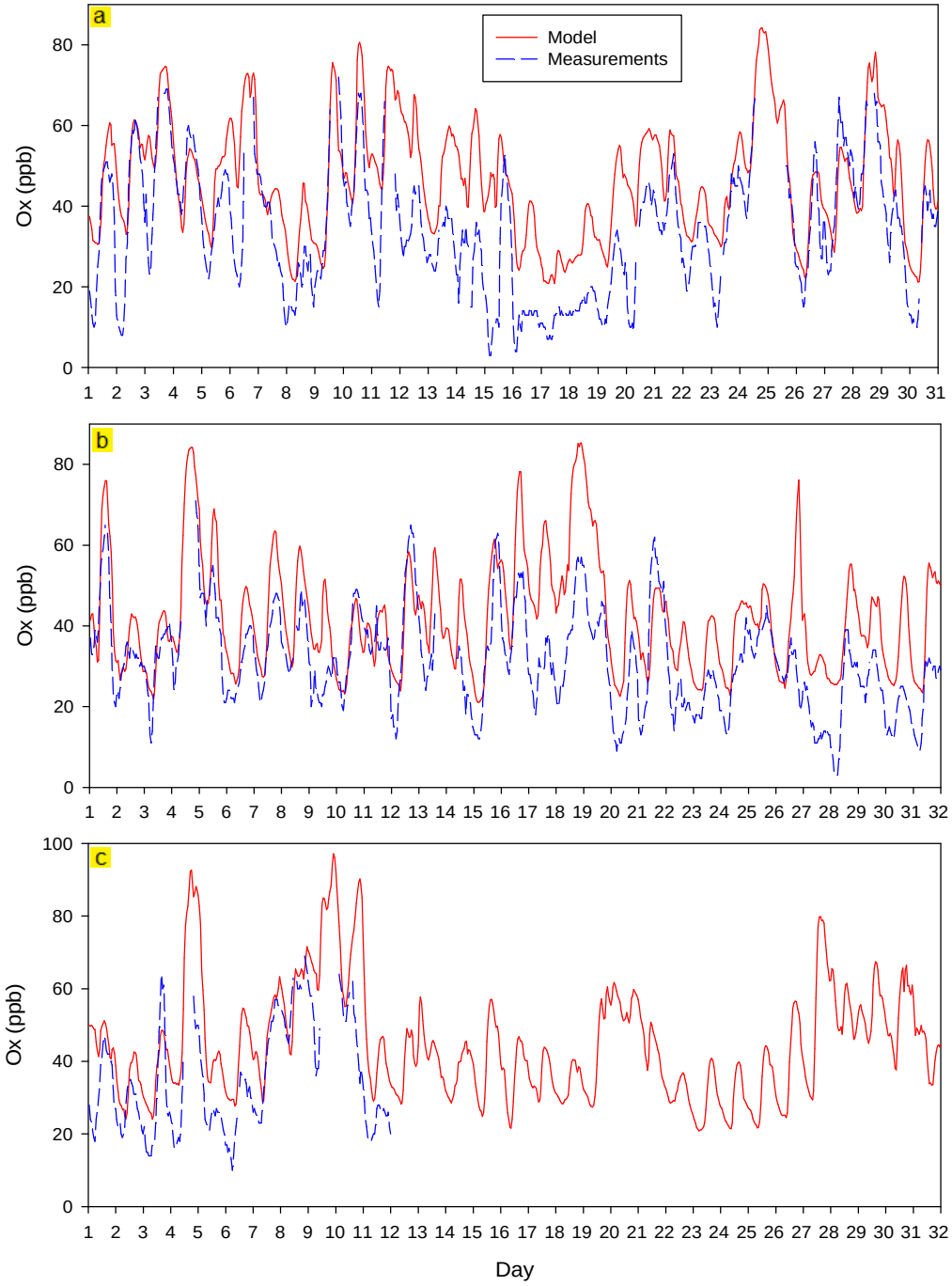

Figure 44. A comparison of modelled (—) and measured (--) 1-h averaged oxidant (Ox) mixing ratios for (a) June, (b) July and (c) August 2005 for Ottawa.

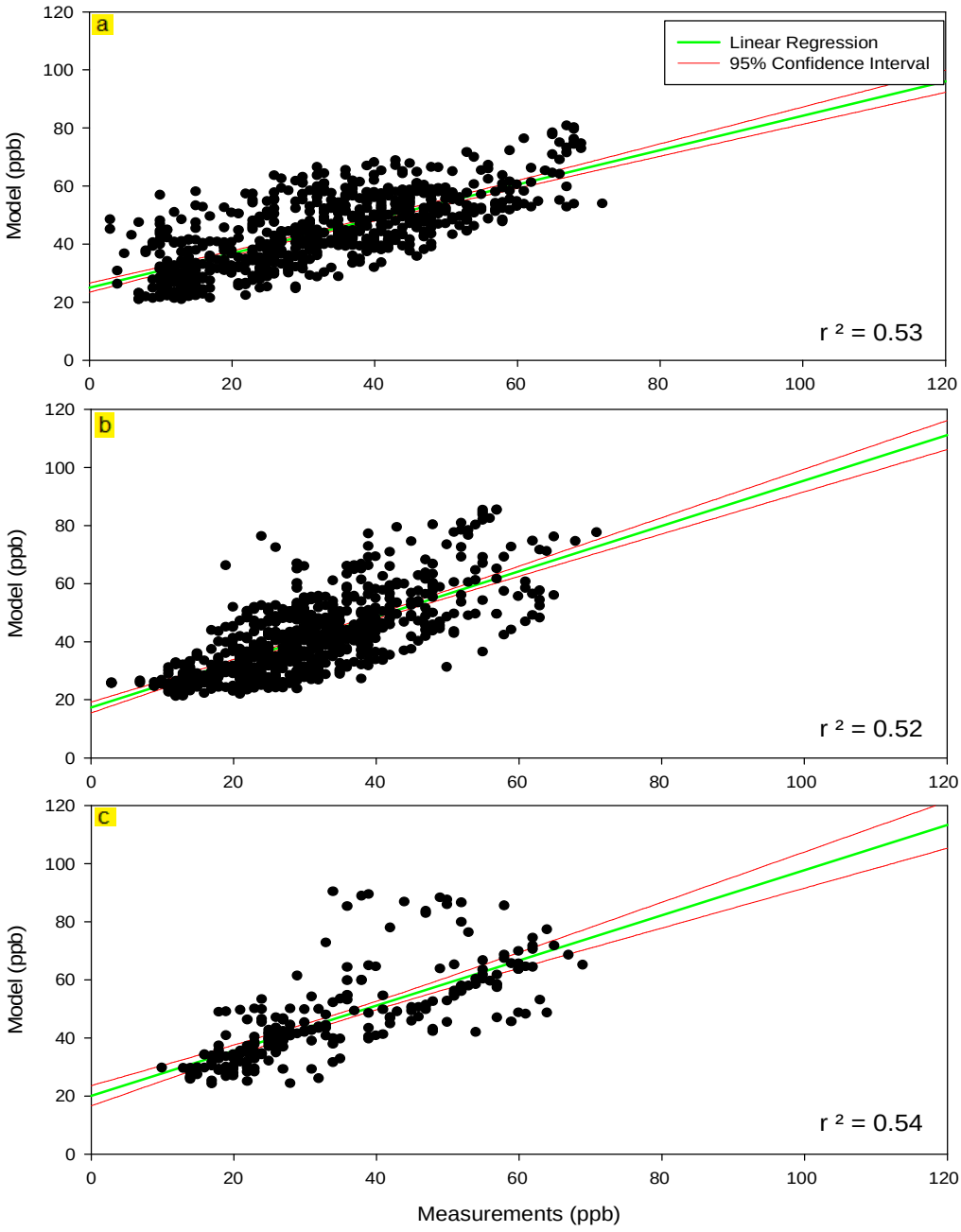

Figure 45. The oxidant (Ox) 1-h averaged scatter plots of model results plotted against measurements taken from the provincial monitoring station for Ottawa during (a) June, (b) July and (c) August 2005.

6.3 Summary and Conclusion

The summer study of O_3 and NO_2 was conducted for the regions of North Bay and Ottawa to examine how each species behaves in the summer under different settings. The simulations for North Bay and Ottawa show better correlation with the measurements than during the winter investigation. The hourly temporal variations for both species at both sites were adequately represented, but CMAQ was still incapable of reproducing the lower values of O_3 and the higher values of NO_2 for North Bay. The main reasons for these results are similar to those outlined in Section 5.4. With the resolution of the grid and given the fact that 36 km-averaged concentrations were being compared to point measurements, it was not surprising that most of the EPA's criteria did not fit within their defined ranges of acceptability. Furthermore, any ambiguities in the model-measurement comparisons were not surprising. Grid resolution along with the location of the North Bay monitoring site, also favour lower NO_2 mixing ratios. Ozone production rates rise with coarser resolutions because NOx is diluted more readily across each cell (Shrestha et al., 2009) and the monitoring station in North Bay is in a high NOx environment which the emissions inventory does not account for. Additionally, the increased solar radiation and temperatures during the summer all favour O_3 production which explains why ozone levels during the summer were higher than during the winter months.

Chapter 7

Conclusions and Future Work

7.1 Conclusions

The results presented in this work provide valuable insight into the seasonal air quality in Ontario. The Community Multiscale Air Quality modelling (CMAQ) system was employed to examine the behaviour of O_3 and NO_2 during the 2005 summer and winter seasons under both rural and urban settings. The cities of North Bay and Ottawa were chosen to represent these conditions, respectively. The output was then compared against ground measurements from the MOEs monitoring network taken at both sites to determine how well the model could reproduce the ambient conditions. The results presented in this study are the first reported comparisons of hourly modelled results and surface measurements for these two municipalities using the MOEs monitoring network and CMAQ output.

For both the winter and summer episodes, CMAQ was able to skilfully represent the spatial variability of O_3 and NO_2 model output as seen by the visual images and statistical measurements. The temporal time series however, revealed that the performance of CMAQ varies by season and by region. The hourly comparisons for North Bay showed similar results in both the summer and winter episodes. CMAQ had a difficult time simulating the low values of O_3 as well as the higher mixing ratios of NO_2. The Ottawa results showed a better agreement between modelled and measured results than those for North Bay. Ozone and NO_2 in Ottawa were both simulated with a fair amount of accuracy for winter and summer, with the summer results being slightly more precise. The results of this study are consistent with the literature which reports that CMAQ has a tendency to over-predict O_3 at urban sites and under-predict it at rural sites. At both monitoring sites, O_3 reached near–zero levels less frequently in the summer than the winter. This is related to the PBL diurnal cycle whose minimum values were lower during the winter than in the summer causing less

mixing. Lower mixing generates reduced accumulation of O_3 at the surface and higher NO_2 concentrations.

Overall, the model was running well as determined by its ability to replicate the diurnal cycles for all sites and seasons. Because the CMAQ modelling parameters remained the same for both investigations, I conclude that the difference in NO_2 and O_3 mixing ratios during both seasons was due mainly to the input data that was used by CMAQ. The exclusion of excess NO_2 in the emissions inventory and the difference in meteorological parameters generated varying results for both seasons at each site. Low input NOx emissions at the North Bay site resulted decreased NO_2 output which affected the O_3 levels. The Ottawa results did not show this pattern. This suggests that the levels of NOx in urban centres are accurately accounted for in the emissions while a deficiency exists for rural regions. Additionally, the meteorology played a significant role in the modelling results. The lower concentrations of O_3 in the summer output relative to the winter results can be attributed to factors like increased summertime solar radiation, elevated temperatures and relative humidity, all of which speed up photolysis rates – such as the photolysis of NO_2 to form O_3 – and elevate the amount of ground-level O_3 produced.

7.2 Future Work

Because the concentration of O_3 in a given location depends on the NOx/VOC ratio in that area as well as regional meteorological processes, all of these factors must be taken into account when conducting a complete modelling investigation of ground-level O_3 pollution. This study considered only the relationship between O_3 and NO_2, as it was a base case investigation into the performance of CMAQ. Now that successful model performance has been established, upcoming projects should contain a broader focus on the future air quality of rural and urban municipalities in Ontario. Creating future year emissions inventories by updating the current inventories with 2010 data would allow one to project what affect

current control and emissions programs in Ontario and the United States will have on the province's air quality. Including VOCs in the analysis is also a necessity as it would provide a sound assessment of local O_3 production because depending on the location, O_3 can be either NOx-sensitive or VOC-sensitive. Ozone formation in rural environments is NOx-sensitive as these areas are rich in VOCs from biogenic sources and deficient in NOx since fossil fuel combustion from vehicles is minimal. Urban area can exhibit the dependency on either precursor depending on their concentrations (Byun et al., 2007; Duncan et al., 2009; Kleinman et al., 1997) although recent studies have shown that O_3 formation in the eastern United States is becoming more NOx-sensitive in response to the more than 10% decrease in NOx emissions between 2005 and 2007 due to the EPAs NOx SIP Call and NOx Budget Trading Program (Duncan et al., 2009). Thus controlling the emissions of a given precursor can have diverse effects in different areas which makes the choice of monitoring stations important. This study roughly touched upon such differences, though a larger number of sites across the province would provide more compelling results.

Future work should also consider a complete analysis of synoptic-scale meteorology to properly predict future O_3 levels in the province because O_3 is a regional phenomenon. For example, areas of high pressure over the North Atlantic Ocean have been found to be conducive to warm, dry conditions in eastern North America (Appel et al., 2007) which enhances the production of biogenic VOCs like isoprene. This in turn generates additional VOC radicals that contribute to the net increase in O_3 concentrations (Sofiev et al., 2009). This study did briefly examine some meteorological parameters such as wind speed and wind direction, but other factors like temperature, cloud formation or solar radiation which must be intensely investigated and analyzed against O_3 because they all hold critical roles in photochemical processes. However, because a significant portion of Ontario experiences cold weather for most of the year, particular attention should be paid to wintertime NOx and VOC emissions and O_3 formation. Furthermore, if an all-encompassing evaluation of air quality in Ontario is to be carried out, regions in northern Ontario must be investigated since

they are lacking in the literature as most authors focus on major cities adjacent to the Canada-U.S.A. border. Undertaking such a project would be beneficial to the residents of Ontario because it would allow policy makers to determine the best methods for reducing O_3 and its precursors throughout the province and the region.

References

Adelman, Z., Vukovich, J., & Carter, W. (2005). *Final report: Integration of the SAPRC chemical mechanism in the SMOKE emissions processor for the CMAQ/Models-3 airshed model*. Riverside, North Carolina: University of North Carolina at Riverside.

Air & Energy Initiatives Environmental Management Division. (2004). *Air quality and climate change management plan.* Ottawa: Air & Energy Initiatives Planning and Growth Management Division.

Altshuller, A. P. (1986). The role of nitrogen oxides in nonurban ozone formation in the planetary boundary layer over N America, W Europe and adjacent areas of ocean. *Atmospheric Environment, 20*(2), 245-268. doi:10.1016/0004-6981(86)90029-6

Appel, K. W., Bhave, P. V., Gilliland, A. B., Sarwar, G., & Roselle, S. J. (2008a). Evaluation of the community multiscale air quality (CMAQ) model version 4.5: Sensitivities impacting model performance part II-particulate matter. *Atmospheric Environment, 42*(24), 6057-6066. doi:10.1016/j.atmosenv.2008.03.036

Appel, K. W., Bhave, P. V., Gilliland, A. B., Sarwar, G., & Roselle, S. J. (2008b). Evaluation of the community multiscale air quality (CMAQ) model version 4.5: Sensitivities impacting model performance; part II—particulate matter. *Atmospheric Environment, 42*(24), 6057-6066. doi:10.1016/j.atmosenv.2008.03.036

Appel, K. W., Gilliland, A. B., Sarwar, G., & Gilliam, R. C. (2007). Evaluation of the community multiscale air quality (CMAQ) model version 4.5: Sensitivities impacting model performance part I-ozone. *Atmospheric Environment, 41*(40), 9603-9615. doi:10.1016/j.atmosenv.2007.08.044

Appel, K. W., Roselle, S. J., Gilliam, R. C., & Pleim, J. E. (2009). Sensitivity of the community multiscale air quality (CMAQ) model v4.7 results for the eastern United States to MM5 and WRF meteorological drivers. *Geoscientific Model Development Discussions, 2*, 1081-1114. doi:10.5194/gmd-3-169-2010

Arnold, J. R., & Dennis, R. L. (2006). Testing CMAQ chemistry sensitivities in base case and emissions control runs at SEARCH and SOS99 surface sites in the south eastern US. *Atmospheric Environment, 40*(26), 5027-5040. doi:10.1016/j.atmosenv.2005.05.055

Atkinson, R. (2007). Gas-phase tropospheric chemistry of organic compounds: A review. *Atmospheric Environment, 41*, 200-240. doi:10.1016/j.atmosenv.2007.10.068

Atkinson, R. (2000). Atmospheric chemistry of VOCs and NOx. *Atmospheric Environment, 34*(12-14), 2063-2101. doi:10.1016/S1352-2310(99)00460-4

Atkinson, R., Kwok, E. S. C., Arey, J., & Aschmann, S. M. (1995). Reactions of alkoxyl radicals in the atmosphere. *Faraday Discussions, 100*, 23-37. doi:10.1039/FD9950000023

Baldasano, J. M., Valera, E., & Jiménez, P. (2003). Air quality data from large cities. *The Science of the Total Environment, 307*(1-3), 141-165. doi:10.1016/S0048-9697(02)00537-5

Bao, H., Shrestha, K. L., Kondo, A., Kaga, A., & Inoue, Y. (2010). Modeling the influence of biogenic volatile organic compound emissions on ozone concentration during summer season in the Kinki region of Japan. *Atmospheric Environment, 44*(3), 421-431. doi:10.1016/j.atmosenv.2009.10.021

Beaney, G., & Gough, W. A. (2002). The influence of tropospheric ozone on the air temperature of the city of Toronto, Ontario, Canada. *Atmospheric Environment, 36*(14), 2319-2325. doi:10.1016/S1352-2310(02)00184-X

Beckerman, B., Jerrett, M., Brook, J. R., Verma, D. K., Arain, M. A., & Finkelstein, M. M. (2008). Correlation of nitrogen dioxide with other traffic pollutants near a major expressway. *Atmospheric Environment, 42*(2), 275-290. doi:10.1016/j.atmosenv.2007.09.042

Bell, M. L., Goldberg, R., Hogrefe, C., Kinney, P. L., Knowlton, K., Lynn, B., Rosenthal, J., Rosenzweig, C., & Patz, J. A. (2007). Climate change, ambient ozone, and health in 50 US cities. *Climatic Change, 82*(1-2), 61-76. doi:10.1007/s10584-006-9166-7

Binkowski, F. S. (1999). Aerosols in models-3 CMAQ. In D. W. Byun, & J. K. S. Ching (Eds.), *Science algorithms of the EPA models-3 community multiscale air quality (CMAQ) modeling system* (). Research Triangle Park, North Carolina: National Exposure Research Laboratory, U.S. EPA.

Brankov, E., Henry, R. F., Civerolo, K. L., Hao, W., Rao, S. T., Misra, P. K., Bloxam, R., & Reid, N. (2003). Assessing the effects of transboundary ozone pollution between Ontario, Canada and New York, USA. *Environmental Pollution, 123*(3), 403-411. doi:10.1016/S0269-7491(03)00017-4

Brulfert, G., Galvez, O., Yang, F., & Sloan, J. J. (2007). A regional modelling study of the high ozone episode of June 2001 in southern Ontario. *Atmospheric Environment, 41*(18), 3777-3788. doi:10.1016/j.atmosenv.2007.01.030

Buchdahl, R., Willems, C. D., Vander, M., & Babiker, A. (2000). Associations between ambient ozone, hydrocarbons, and childhood wheezy episodes: A prospective observational study in south east London. *Occupational and Environmental Medicine, 57*, 86-93. doi:10.1136/oem.57.2.86

Byun, D. (2002). A study of photochemical processes of the Houston-Galveston metropolitan airshed with EPA CMAQ. *2002 Model-3 User's Workshop,* Research Triangle Park, North Carolina.

Byun, D., & Dennis, R. (1995). Design artifacts in eulerian air quality models: Evaluation of the effects of layer thickness and vertical profile correction on surface ozone concentrations. *Atmospheric Environment, 29*(1), 105-126. doi:10.1016/1352-2310(94)00225-A

Byun, D., Kim, S. T., & Kim, S. B. (2007). Evaluation of air quality models for the simulation of a high ozone episode in the Houston metropolitan area. *Atmospheric Environment, 41*(4), 837-853. doi:10.1016/j.atmosenv.2006.08.038

Byun, D., Pleim, J., Tang, R., & Bourgeois, A. (1999). Meteorology-chemistry interface processor (MCIP) for models-3 community multiscale air quality (CMAQ) modeling system. In D. Byun, & J. Ching (Eds.), *Science algorithms of the EPA model-3 community multiscale air quality (CMAQ) modelling system* (). Washington, D.C.: Environmental Protection Agency.

Byun, D., & Schere, K. (2006). Review of the governing equations, computational algorithms, and other components of the models-3 community multiscale air quality (CMAQ) modeling system. *Applied Mechanics Reviews, 59*(2), 51-138. doi:10.1115/1.2128636

Cape, J. N. (2008). Surface ozone concentrations and ecosystem health: Past trends and a guide to future projections. *Science of the Total Environment, 400*(1-3), 257-269. doi:10.1016/j.scitotenv.2008.06.025

Carey Jang, J., Jeffries, H. E., & Tonnesen, S. (1995). Sensitivity of ozone to model grid resolution -- II. detailed process analysis for ozone chemistry. *Atmospheric Environment, 29*(21), 3101-3114. doi:10.1016/1352-2310(95)00119-J

Carolina Environmental Program. (2003). *Sparse matrix operator kernel emissions (SMOKE) modeling system*. Chapel Hill, NC: University of Carolina, Carolina Environmental Programs.

Carslaw, D. C. (2005). Evidence of an increasing NO2/NOX emissions ratio from road traffic emissions. *Atmospheric Environment, 39*(26), 4793-4802. doi:10.1016/j.atmosenv.2005.06.023

Carslaw, D. C., & Beevers, S. D. (2005). Estimations of road vehicle primary NO2 exhaust emission fractions using monitoring data in London. *Atmospheric Environment, 39*(1), 167-177. doi:10.1016/j.atmosenv.2004.08.053

Carslaw, D. C., Beevers, S. D., & Bell, M. C. (2007). Risks of exceeding the hourly EU limit value for nitrogen dioxide resulting from increased road transport emissions of primary nitrogen dioxide. *Atmospheric Environment, 41*(10), 2073-2082. doi:10.1016/j.atmosenv.2006.10.074

Carter, W. (1994). Development of ozone reactivity scales for volatile organic compounds. *Journal of the Air and Waste Management Association, 44*(7), 881-899.

Carter, W. (2000a). *Additions and corrections to the SAPRC-99 maximum incremental reactivity (MIR) scale: Report to the California air resources board.* Riverside, California: California Air Resources Board.

Carter, W. (2000b). *Implementation of the SAPRC-99 chemical mechanism into the models-3 framework.*Unitetd States Environmental Protection Agency.

Carter, W. (2008). *Documentation of the SAPRC-99 chemical mechanism for VOC reactivity assessment: Final report to the California air resources board, 00-AP-RT4P-001-FR.* No. 00-AP-RT4P-001-FR). Riverside, California: California Air Resources Board.

Challa, V. S., Indracanti, J., Rabarison, M. K., Young, J., Patrick, C., Baham, J. M., Hughes, R., & Yerramilli, A. (2007). Numerical experiments on the sensitivity of WRF-CMAQ simulations of air quality in the mississippi gulf coastal region to PBL and land surface models. Paper presented at the *Annual CMAS Conference,* Chapel Hill, North Carolina. 1-4.

Chemel, C., Sokhi, R. S., Yu, Y., Hayman, G. D., Vincent, K. J., Dore, A. J., Tang, Y. S., Prain, H. D., & Fisher, B. E. A. (2010). Evaluation of a CMAQ simulation at high resolution over the UK for the calendar year 2003. *Atmospheric Environment, 44*(24), 2927-2939. doi:10.1016/j.atmosenv.2010.03.029

Chen, L., Stein, M., Zubrow, A., & Kotamarthi, V. (2006). *Statistical comparison of observed and multi-resolution CMAQ modeled hourly ozone concentrations.* (Technical No. 40).

Ching, J., Herwehe, J., & Swall, J. (2006). On joint deterministic grid modeling and sub-grid variability conceptual framework for model evaluation. *Atmospheric Environment, 40*(26), 4935-4945. doi:10.1016/j.atmosenv.2006.01.021

Chtcherbakov, A., Pagowski, M., Sloan, J., Soldatenko, S., Lin, X., Bloxam, R., Wong, S., & Misra, P. K. (2002). Models-3/CMAQ evaluation during high particulate episodes over eastern North America in summer 1995 and winter 1998. *8th International Conference on Harmonisation within Atmospheric Dispersion Modelling for Regulatory Purposes,* Sofia, Bulgaria.

Clapp, L. J., & Jenkin, M. E. (2001). Analysis of the relationship between ambient levels of O_3, NO_2 and NO as a function of NOx in the UK. *Atmospheric Environment, 35*(36), 6391-6405. doi:10.1016/S1352-2310(01)00378-8

Czader, B. H., Byun, D. W., Kim, S. T., & Carter, W. P. L. (2008). A study of VOC reactivity in the houston-galveston air mixture utilizing an extended version of SAPRC-99 chemical mechanism. *Atmospheric Environment, 42*(23), 5733-5742. doi:10.1016/j.atmosenv.2008.01.039

Dennis, R., Byun, D., Novak, J., Galluppi, K., Coats, C., & Vouk, M. (1996). The next generation of integrated air quality modeling: EPA's models-3. *Atmospheric Environment, 30*(12), 1925-1938.

Dodge, M. (2000). Chemical oxidant mechanisms for air quality modeling: Critical review. *Atmospheric Environment, 32*(12-14), 2103-2130. doi:10.1016/S1352-2310(99)00461-6

Duncan, B., Yoshida, Y., Sillman, S., Retscher, C., Pickering, K., Martin, R., & Celarier, E. (2009). The sensitivity of U.S. surface ozone formation to NOx and VOCs as viewed from space. *8th Annual CMAS Conference,* Chapel Hill, North Carolina.

Ebi, K., & McGregor, G. (2008). Climate change, tropospheric ozone and particulate matter, and health impacts. *Environmental Health Perspectives, 116*(11), 1449-1455. doi:10.1590/S1413-81232009000600037

Eder, B., Kang, D., Mathur, R., Yu, S., & Schere, K. (2006). An operational evaluation of the eta-CMAQ air quality forecast model. *Atmospheric Environment, 40*(26), 4894-4905. doi:10.1016/j.atmosenv.2005.12.062

Eder, B., & Yu, S. (2006). A performance evaluation of the 2004 release of models-3 CMAQ. *Atmospheric Environment, 40*(26), 4811-4824. doi:10.1016/j.atmosenv.2005.08.045

Environmental Monitoring and Reporting Branch of the Ontario Ministry of the Environment. (2008). *Border air quality study - an ambient air quality overview for southwestern Ontario (summer 2007).* Toronto, Ontario: Queen's Printer for Ontario. doi:AQI Publication

Environmental Monitoring and Reporting Branch of the Ontario Ministry of the Environment. (2009). *Air quality in ontario:2008 report.* (AQI Publication Toronto, Ontario: Queen's Printer for Ontario.

Escobedo, F. J., & Nowak, D. J. (2009). Spatial heterogeneity and air pollution removal by an urban forest. *Landscape and Urban Planning, 90*(3-4), 102-110. doi:10.1016/j.landurbplan.2008.10.021

Eyth, A., & Ran, L. (2009). *Emissions modeling framework surrogate tool: User's guide.* Chapel Hill, North Carolina: University of North Carolina.

Faraji, M., Kimura, Y., McDonald-Buller, E., & Allen, D. (2008). Comparison of the carbon bond and SAPRC photochemical mechanisms under conditions relevant to southeast Texas. *Atmospheric Environment, 42*(23), 5821-5836. doi:10.1016/j.atmosenv.2007.07.048

Fast, J. D., & Heilman, W. E. (2005). Simulated sensitivity of seasonal ozone exposure in the great lakes region to changes in anthropogenic emissions in the presence of interannual variability. *Atmospheric Environment, 39*(29), 5291-5306. doi:10.1016/j.atmosenv.2005.05.032

Finlayson-Pitts, B. J., & Pitts, J. N. (2000). *Chemistry of the upper and lower atmosphere: Theory, experiments and applications*. San Diago, California: Academic Press.

Foley, K. M., Roselle, S. J., Appel, K. W., Bhave, P. V., Pleim, J. E., Otte, T. L., Mathur, R., Sawar, G., Young, J. O., Gilliam, R., Nolte, C. G., Kelly, J. T., Gilliland, A., & Bash, J. O. (2010). Incremental testing of the community multiscale air quality (CMAQ) modeling system version 4.7. *Geoscientific Model Development, 3*(1), 205-226. doi:10.5194/gmd-3-205-2010

Fowler, D., Pilegaard, K., Sutton, M. A., Ambus, P., Raivonen, M., Duyzer, J., Simpson, D., Fagerli, H., Fuzzi, S., Schjoerring, J. K., Granier, C., Neftel, A., Isaksen, I. S. A., Laj, P., Maione, M., Monks, P. S., Burkhardt, J., Daemmgen, U., Neirynck, J., Personne, E., Wichink-Kruit, R., Butterbach-Bahl, K., Flechard, C., Tuovinen, J. P., Coyle, M., Gerosa, G., Loubet, B., Altimir, N., Gruenhage, L., Ammann, C., Cieslik, S., Paoletti, E., Mikkelsen, T. N., Ro-Poulsen, H., Cellier, P., Cape, J. N., Horváth, L., Loreto, F., Niinemets, Ü., Palmer, P. I., Rinne, J., Misztal, P., Nemitz, E., Nilsson, D., Pryor, S.,

Gallagher, M. W., Vesala, T., Skiba, U., Brüggemann, N., Zechmeister-Boltenstern, S., Williams, J., O'Dowd, C., Facchini, M. C., de Leeuw, G., Flossman, A., Chaumerliac, N., & Erisman, J. W. (2009). Atmospheric composition change: Ecosystems–Atmosphere interactions. *Atmospheric Environment, 43*(33), 5193-5267. doi:10.1016/j.atmosenv.2009.07.068

Fraser, D. (2010). *O_3 measurements-winter 2005*

Galvez, O. (2007). Synoptic-scale transport of ozone into southern Ontario. *Atmospheric Environment, 41*(38), 8579-8595. doi:10.1016/j.atmosenv.2007.07.019

Geddes, J. A., Murphy, J. G., & Wang, D. K. (2009). Long term changes in nitrogen oxides and volatile organic compounds in toronto and the challenges facing local ozone control. *Atmospheric Environment, 43*(21), 3407-3415. doi:10.1016/j.atmosenv.2009.03.053

Gego, E., Steven Porter, P., Hogrefe, C., & Irwin, J. S. (2006). An objective comparison of CMAQ and REMSAD performances. *Atmospheric Environment, 40*(26), 4920-4934. doi:10.1016/j.atmosenv.2005.12.045

Gery, M. W., Whitten, G. Z., Killus, J. P., & Dodge, M. (1989). A photochemical mechanism for urban and regional-scale computer modeling. *Journal of Geophysical Research, 94*, 12925-12956.

Gilliland, A. B., Hogrefe, C., Pinder, R. W., Godowitch, J. M., Foley, K. L., & Rao, S. T. (2008). Dynamic evaluation of regional air quality models: Assessing changes in O_3 stemming from changes in emissions and meteorology. *Atmospheric Environment, 42*(20), 5110-5123. doi:10.1016/j.atmosenv.2008.02.018

Godowitch, J. M., Gilliland, A. B., Draxler, R. R., & Rao, S. T. (2008). Modeling assessment of point source NOx emission reductions on ozone air quality in the eastern United States. *Atmospheric Environment, 42*(1), 87-100. doi:10.1016/j.atmosenv.2007.09.032

Government of Ontario. (2010). *North bay.* Retrieved May 14, 2010, from http://www.ontario.ca/en/about_ontario/004661.html

Harris, G. (2010). In Rebello Z. (Ed.), *PBL heights*

Hastie, D. R., Narayan, J., Schiller, C., Niki, H., Shepson, P. B., Sills, D. M. L., Taylor, P. A., Moroz, W. J., Drummond, J. W., Reid, N., Taylor, R., Roussel, P. B., & Melo, O. T. (1999). Observational evidence for the impact of the lake breeze circulation on ozone concentrations in southern ontario. *Atmospheric Environment, 33*(2), 323-335.

Hertel, O., Berkowicz, R., Christensen, J., & Hov, O. (1993). Test of two numerical schemes for use in atmospheric transport-chemistry models. *Atmos.Environ., 27A*(16), 2591-2611. doi:10.1016/0960-1686(93)90032-T

Hidy, G. M. (2000). Ozone process insights from field experiments – part I: Overview. *Atmospheric Environment, 34*(12-14), 2001-2022. doi:10.1016/S1352-2310(99)00456-2

Hogrefe, C., Porter, P. S., Gego, E., Gilliland, A., Gilliam, R., Swall, J., Irwin, J., & Rao, S. T. (2006). Temporal features in observed and simulated meteorology and air quality over the eastern United States. *Atmospheric Environment, 40*(26), 5041-5055. doi:10.1016/j.atmosenv.2005.12.056

Hogrefe, C., Lynn, B., Goldberg, R., Rosenzweig, C., Zalewsky, E., Hao, W., Doraiswamy, P., Civerolo, K., Ku, J., Sistla, G., & Kinney, P. L. (2009). A combined model–observation approach to estimate historic gridded fields of PM2.5 mass and species concentrations. *Atmospheric Environment, 43*(16), 2561-2570. doi:10.1016/j.atmosenv.2009.02.031

Hogrefe, C., Rao, S. T., Kasibhatla, P., Hao, W., Sistla, G., Mathur, R., & McHenry, J. (2001). Evaluating the performance of regional-scale photochemical modeling systems: Part II—ozone predictions. *Atmospheric Environment, 35*(24), 4175-4188. doi:10.1016/S1352-2310(01)00183-2

Hogrefe, C., Rao, S. T., Kasibhatla, P., Kallos, G., Tremback, C. J., Hao, W., Olerud, D., Xiu, A., McHenry, J., & Alapaty, K. (2001). Evaluating the performance of regional-scale photochemical modeling systems: Part I—meteorological predictions. *Atmospheric Environment, 35*(24), 4159-4174. doi:10.1016/S1352-2310(01)00182-0

Hong, S. Y., & Kim, S. W. (2008). Stable boundary layer mixing in a vertical diffusion scheme. *18th Symposium on Boundary Layers and Turbulence,* Stockholm, Sweeden.

Huie, R. (1994). The reaction kinetics of NO_2. *Toxicology, 89*(3), 193-216. doi:10.1016/0300-483X(94)90098-1

Jacob, D. J. (1999). *Introduction to atmospheric chemistry*. Princeton, New Jersey: Princeton University Press.

Jenkin, M. E. (2004a). Analysis of sources and partitioning of oxidant in the UK-part 1: The NOx-dependence of annual mean concentrations of nitrogen dioxide and ozone. *Atmospheric Environment, 38*(30), 5117-5129. doi:10.1016/j.atmosenv.2004.05.056

Jenkin, M. E. (2004b). Analysis of sources and partitioning of oxidant in the UK-part 2: Contributions of nitrogen dioxide emissions and background ozone at a kerbside location in London. *Atmospheric Environment, 38*(30), 5131-5138. doi:10.1016/j.atmosenv.2004.05.055

Jenkin, M. E., Utembe, S. R., & Derwent, R. G. (2008). Modelling the impact of elevated primary NO_2 and HONO emissions on regional scale oxidant formation in the UK. *Atmospheric Environment, 42*(2), 323-336. doi:10.1016/j.atmosenv.2007.09.021

Jenkin, M. E., & Clemitshaw, K. C. (2000). Ozone and other secondary photochemical pollutants: Chemical processes governing their formation in the planetary boundary layer. *Atmospheric Environment, 34*(16), 2499-2527. doi:10.1016/S1352-2310(99)00478-1

Jiang, W., Smyth, S., Giroux, E., Roth, H., & Yin, D. (2006). Differences between CMAQ fine mode particle and PM2.5 concentrations and their impact on model performance evaluation in the lower Fraser Valley. *Atmospheric Environment, 40*(26), 4973-4985. doi:10.1016/j.atmosenv.2005.10.069

Jimenez, P. (2007). Initial and boundary condition for ozone modelling in very complex terrains: A case study in the northeastern Iberian Peninsula. *Environmental Modelling and Software, 22*(9), 1295-1306. doi:10.1016/j.envsoft.2006.08.004

Jimenez, P., Baldasano, J. M., & Dabdub, D. (2003). Comparison of photochemical mechanisms for air quality modeling. *Atmospheric Environment, 37*(30), 4179-4194. doi:10.1016/S1352-2310(03)00567-3

Karydis, V. A., Tsimpidi, A. P., & Pandis, S. N. (2007). Evaluation of a three-dimensional chemical transport model (PMCAMx) in the eastern United States for all four seasons. *Journal of Geophysical Research, 112*(D14), 1-23. doi:10.1029/2006JD007890

Kim, S. W., Heckel, A., McKeen, S. A., Frost, G. J., Hsie, E. Y., Trainer, M. K., Richter, A., Burrows, J. P., Peckham, S. E., & Grell, G. A. (2006). Satellite-observed US power plant NOx emission reductions and their impact on air quality. *Geophysical Research Letters, 33*, L22812.

Kleinman, L., Daum, P., Lee, J. H., Lee, Y. N., Nunnermacker, L. J., Springston, S. R., Newman, L., Weinstein-Lloyd, J., & Sillman, S. (1997). Dependence of ozone production on NO and hydrocarbons in the troposphere. *Geophysical Research Letters, 24*(18), 2299-2302. doi:0094-8534/97/97GL-02279$05.00

Kleinman, L., Daum, P., Lee, Y. N., Nunnermackeeinr, L. J., Springston, S. R., Weinstein-Lloyd, J., & Rudolph, J. (2001). Sensitivity of ozone production rate to ozone precursors. *Geophysical Research Letters, 28*(15), 2903-2906. doi:0094-8276/01/2000GL012597$05.00

Laj, P., Kllausen, J., Bilde, M., Plab-Duelmer, C., Pappalardo, G., Clervaux, C., Baltensperger, U., Hjorth, J., Simpson, D., Reimann, S., Choeur, P., Richter, A., De Maziere, M., Rudich, Y., McFiggans, G., Torseth, K., Wiedensohler, A., Morin, S., Schulz, M., Allan, J., Attie, J., Barnes, I., Birmili, W., & Cammas, J. (2009). Measuring atmsopheric composition change. *Atmospheric Environment, 43*(33), 5351-5414. doi:10.1016/j.atmosenv.2009.08.020

Lawrence, M. G., Butler, T. M., Steinkamp, J., Gurjar, B. R., & Lelieveld, J. (2007). Regional pollution potentials of megacities and other major population centers. *Atmospheric Chemistry7 and Physics, 7*(14), 3969-3987. doi:10.5194/acp-7-3969-2007

Liang, J., Martien, P. T., Soong, S., & Tanrikulu, S. (2001). A photochemical model comprarison study: CAMx and CMAQ performance in central California. *13th Conference on the Applications of Air Pollution Meteorology with the Air and Waste Management Association,*

Lim, C. Y., Stein, M., Ching, J., & Tang, R. (2010). Statistical properties of differences between low and high resolution CMAQ runs with matched initial and boundary conditions. *Environmental Modelling and Software, 25*(1), 158-169. doi:10.1016/j.envsoft.2009.06.007

Lin, J., Youn, D., Liang, X., & Wuebbles, D. (2008). Global model simulation of summertime U.S. ozone diurnal cycle and its sensitivity to PBL mixing, spatial resolution, and emissions. *Atmos.Environ., 42*(36), 8470-8483. doi:10.1016/j.atmosenv.2008.08.012

Lin, C. J., Ho, T. C., Chu, H. w., Yang, H., Chandru, S., Krishnarajanagar, N., Chiou, P., & Hopper, J. R. (2005). Sensitivity analysis of ground-level ozone concentration to emission changes in two urban regions of southeast Texas. *Journal of Environmental Management, 75*(4), 315-323. doi:10.1016/j.jenvman.2004.09.012

Lin, M., Oki, T., Holloway, T., Streets, D. G., Bengtsson, M., & Kanae, S. (2008). Long-range transport of acidifying substances in east Asia—Part I. *Atmospheric Environment, 42*(24), 5939-5955. doi:10.1016/j.atmosenv.2008.04.008

Luecken, D. J., Phillips, S., Sarwar, G., & Jang, C. (2008). Effects of using the CB05 vs. SAPRC99 vs. CB4 chemical mechanism on model predictions: Ozone and gas-phase

photochemical precursor concentrations. *Atmospheric Environment, 42*(23), 5805-5820. doi:10.1016/j.atmosenv.2007.08.056

Luecken, D. J., Tonnesen, G. S., & Sickles II, J. E. (1999). Differences in NOy speciation predicted by three photochemical mechanisms. *Atmospheric Environment, 33*(7), 1073-1084. doi:10.1016/S1352-2310(98)00319-7

Martin, R. (2008). Satellite remote sensing of surface air quality. *Atmospheric Environment, 42*, 7823-7843. doi:10.1016/j.atmosenv.2008.07.018

Mazzeo, N. A., Venegas, L. E., & Choren, H. (2005). Analysis of NO, NO_2, O_3 and NOx concentrations measured at a green area of buenos aires city during wintertime. *Atmospheric Environment, 39*(17), 3055-3068. doi:10.1016/j.atmosenv.2005.01.029

McConnell, R., Berhane, K., Gilliland, F., London, S. J., Islam, T., Gauderman, W. J., Avol, E., Margolis, H. G., & Peters, J. M. (2002). Asthma in exercising children exposed to ozone: A cohort study. *The Lancet, 359*(9304), 386-391. doi:10.1016/S0140-6736(02)07597-9

McKendry, I. G. (1993). Ground-level ozone in Montreal, Canada. *Atmospheric Environment.Part B, Urban Atmosphere, 27*(1), 93-103. doi:10.1016/0957-1272(93)90049-C

Minoura, H., & Ito, A. (2010). Observation of the primary NO_2 and NO oxidation near the trunk road in Tokyo. *Atmospheric Environment, 44*(1), 23-29. doi:10.1016/j.atmosenv.2009.10.003

Misenis, C., Hu, X., Krishnan, S., Zhang, Y., & Fast, J. D. (2006). Sensitivity of WRF/Chem predictions to meteorological schemes. *86th Annual AMS Conference/the 14th Joint Conference on the Applications of Air Pollution Meteorology with the A&WMA*, Atlanta, Gorgia. 6.

Mohsenin, V. (1994). Human exposure to oxides of nitrogen at ambient and supra-ambient concentrations. *Toxicology, 89*(3), 301-312.

Monks, P. S., Granier, C., Fuzzi, S., Stohl, A., Williams, M. L., Akimoto, H., Amann, M., Baklanov, A., Baltensperger, U., Bey, I., Blake, N., Blake, R. S., Carslaw, K., Cooper, O. R., Dentener, F., Fowler, D., Fragkou, E., Frost, G. J., Generoso, S., Ginoux, P., Grewe, V., Guenther, A., Hansson, H. C., Henne, S., Hjorth, J., Hofzumahaus, A., Huntrieser, H., Isaksen, I. S. A., Jenkin, M. E., Kaiser, J., Kanakidou, M., Klimont, Z., Kulmala, M., Laj, P., Lawrence, M. G., Lee, J. D., Liousse, C., Maione, M., McFiggans, G., Metzger, A., Mieville, A., Moussiopoulos, N., Orlando, J. J., O'Dowd,

C. D., Palmer, P. I., Parrish, D. D., Petzold, A., Platt, U., Pöschl, U., Prévôt, A. S. H., Reeves, C. E., Reimann, S., Rudich, Y., Sellegri, K., Steinbrecher, R., Simpson, D., ten Brink, H., Theloke, J., van der Werf, G. R., Vautard, R., Vestreng, V., Vlachokostas, C., & von Glasow, R. (2009). Atmospheric composition change – global and regional air quality. *Atmospheric Environment, 43*(33), 5268-5350. doi:10.1016/j.atmosenv.2009.08.021

Morris, R. E., Koo, B., Guenther, A., Yarwood, G., McNally, D., Tesche, T. W., Tonnesen, G., Boylan, J., & Brewer, P. (2006). Model sensitivity evaluation for organic carbon using two multi-pollutant air quality models that simulate regional haze in the southeastern United States. *Atmospheric Environment, 40*(26), 4960-4972. doi:10.1016/j.atmosenv.2005.09.088

Moussiopoulos, N., Vlachokostas, C., Tsilingiridis, G., Douros, I., Hourdakis, E., Naneris, C., & Sidiropoulos, C. (2009). Air quality status in greater Thessaloniki area and the emission reductions needed for attaining the EU air quality legislation. *Science of the Total Environment, 407*(4), 1268-1285. doi:10.1016/j.scitotenv.2008.10.034

Mudway, I. S., & Kelly, F. J. (2000). Ozone and the lung: A sensitive issue. *Molecular Aspects of Medicine, 21*(1-2), 1-48. doi:10.1016/S0098-2997(00)00003-0

Mueller, S. F., Mao, Q., & Mallard, J. W. (2010). Modeling natrual emissions in the community multiscale air quality (CMAQ) model - part 2: Modifications for simulating natural emissions. *Atmospheric Chemistry and Physics Discussions, 10*, 15811-15884. doi:10.5194/acpd-10-15811-2010

Mukammal, E. I., Neumann, H. H., & Gillespie, T. J. (1982). Meteorological conditions associated with ozone in south western Ontario, Canada. *Atmospheric Environment (1967), 16*(9), 2095-2106. doi:10.1016/0004-6981(82)90281-5

Oğuz, Ö., Karman, D., & Tuncel, G. (2003). Measurement of traffic related toxic air pollutants in an urban atmosphere. *Water, Air and Soil Pollution: Focus, 3*(5-6), 181-198.

Oltmans, S. J., Lefohn, A. S., Harris, J. M., Galbally, I., Scheel, H. E., Bodeker, G., Brunke, E., Claude, H., Tarasick, D., Johnson, B. J., Simmonds, P., Shadwick, D., Anlauf, K., Hayden, K., Schmidlin, F., Fujimoto, T., Akagi, K., Meyer, C., Nichol, S., Davies, J., Redondas, A., & Cuevas, E. (2006). Long-term changes in tropospheric ozone. *Atmospheric Environment, 40*(17), 3156-3173. doi:10.1016/j.atmosenv.2006.01.029

Ontario Medical Association. (2007). *The illness costs of air pollution: 2005-2026 health and economic damage estimates.* (ICAP Summary Report Toronto: Ontario Medical Association.

Ontario Ministry of the Environment. (2010). *Ontario smog advisories for 2005*. Retrieved August 15, 2010, from http://www.airqualityontario.com/press/advisories_2005.cfm

Otte, T. L. (2009). In Rebello Z. (Ed.), *M3DRY dry deposition velocity*

Peel, J. L., Tolbert, P. E., Klein, M., Metzger, K. B., Flanders, W. D., Todd, K., Mulholland, J. A., Ryan, P. B., & Frumkin, H. (2005). Ambient air pollution and respiratory emergency department visits. *Epidemiology, 16*(2), 164-174. doi:10.1097/01.ede.0000152905.42113.db

Phillips, S. B., & Finkelstein, P. L. (2006). Comparison of spatial patterns of pollutant distribution with CMAQ predictions. *Atmospheric Environment, 40*(26), 4999-5009. doi:10.1016/j.atmosenv.2005.12.064

Pielke, R. (2002). *Mesoscale meteorological modeling*. San Diego, California: Academic Press.

Pleijel, H., Klingberg, J., & Bäck, E. (2009). Characteristics of NO_2 pollution in the city of gothenburg, south-west Sweden—Relation to NOx and O_3 levels, photochemistry and monitoring location. *Water, Air, & Soil Pollution: Focus, 9*(1-2), 15-25. doi:10.1007/s11267-008-9201-y

Quickert, N., & Dubois, L. (1973). Some factors affecting the ambient ozone concentrations measured at Ottawa. *Science of the Total Environment, 2*(1), 81-87.

Roselle, S. J., & Binkowski, F. S. (1999). Cloud dynamics and chemistry. In D. Byun, & J. K. S. Ching (Eds.), *Science algorithms of the EPA models-3 community multiscale air quality (CMAQ) modeling system* (pp. 1-10). Research Triangle Park, North Carolina: National Exposure Research Laboratory, U.S. EPA.

Russell, A., & Dennis, R. (2000). NARSTO critical review of photochemical models and modeling. *Atmospheric Environment, 34*(12-14), 2283-2324. doi:10.1016/S1352-2310(99)00468-9

San José, R., Pérez, J., Morant, J., & González Barras, R. (2009). The use of modern third-generation air quality models (MM5-EMIMO-CMAQ) for real-time operational air quality impact assessment of industrial plants. *Water, Air, & Soil Pollution: Focus, 9*(1-2), 27-37. doi:10.1007/s11267-008-9196-4

San José, R., Pérez, J. L., Morant, J. L., & González, R. M. (2008). European operational air quality forecasting system by using MM5–CMAQ–EMIMO tool. *Simulation Modelling Practice and Theory, 16*(10), 1534-1540. doi:10.1016/j.simpat.2007.11.021

Sarwar, G., Pinder, R. W., Appel, K. W., Mathur, R., & Carlton, A. G. (2009). Examination of the impact of photoexcited NO_2 chemistry on regional air quality. *Atmospheric Environment, 43*(40), 6383-6387. doi:10.1016/j.atmosenv.2009.09.012

Sawar, G., Luecken, D., Yarwood, G., Whitten, G., & Carter, W. (2008). Impact of an updated carbon bond mechanism on predictions from the CMAQ modeling system: Preliminary assessment. *Journal of Applied Meteorology and Climatology, 47*(1), 3-14. doi:10.1175/2007JAMC1393.1

Selin, N. E., Wu, S., Nam, K. M., Reilly, J. M., Paltsev, S., Prinn, R. G., & Webster, M. D. (2009). Global health and economic impacts of future ozone pollution. *Environmental Research Letters, 4*(4), 1-9. doi:10.1088/1748-9326/4/4/044014

Shi, C., Fernando, H. J. S., Wang, Z., An, X., & Wu, Q. (2008). Tropospheric NO_2 columns over east central china: Comparisons between SCIAMACHY measurements and nested CMAQ simulations. *Atmospheric Environment, 42*(30), 7165-7173. doi:10.1016/j.atmosenv.2008.05.046

Shi, C., & Zhang, B. (2008). Tropospheric NO_2 columns over northeastern North America: Comparison of CMAQ model simulations with GOME satellite measurements. *Advances in Atmospheric Sciences, 25*(1), 59-71. doi:10.1007/s00376-008-0059-8

Shrestha, K. L., Kondo, A., Kaga, A., & Inoue, Y. (2009). High-resolution modeling and evaluation of ozone air quality of Osaka using MM5-CMAQ system. *Journal of Environmental Sciences, 21*(6), 782-789. doi:10.1016/S1001-0742(08)62341-4

Sickles, J. E., & Shadwick, D. S. (2007). Seasonal and regional air quality and atmospheric deposition in the eastern United States. *Journal of Geophysical Research, 112*(D17), 1-19. doi:10.1029/2006JD008356

Sillman, S. (1993). Tropospheric ozone: The debate over control strategies. *Annual Review of Energy and the Environment, 18*, 31-56. doi:1056-3466/93/1022-0031$02.00

Skamarock, W. C., Klemp, J. B., Dudhia, J., Gill, D. O., Barker, D. M., Wang, W., & Powers, J. G. (2005). *A description of the advanced research WRF version 2.* (Technical Report No. NCAR/TN–468+STR). Boulder, Colorado: National Center for Atmospheric Research.

Smyth, S. C., Jiang, W., Yin, D., Roth, H., & Giroux, E. (2006). Evaluation of CMAQ O_3 and PM2.5 performance using pacific 2001 measurement data. *Atmospheric Environment, 40*(15), 2735-2749. doi:10.1016/j.atmosenv.2005.10.068

Smyth, S. C., Jiang, W., Roth, H., Moran, M. D., Makar, P. A., Yang, F., Bouchet, V. S., & Landry, H. (2009). A comparative performance evaluation of the AURAMS and CMAQ air-quality modelling systems. *Atmospheric Environment, 43*(5), 1059-1070. doi:10.1016/j.atmosenv.2008.11.027

Sofiev, M., Miranda, A. I., Sokhi, R., Camevale, C., Covre, M., Drobinski, P., Finardi, S., Finzi, G., Fisher, B., Ganev, K., Gariazzo, E., Gonzalez, R., Hellen, H., Jalkanen, L., Kaasik, M., Kaminski, J., Kangas, L., Karppinen, A., Karvosenoja, N., Kitwiroon, N., Kukkonen, J., Marins, H., Milan, M., & Miranda, A. (2009). *Review of the capabilities of meteorological and chemistry-transport models for describing and predicting air pollution episodes.* No. WMO/TD-No. 1502).European Science Foundation.

Sokhi, R. S., San Jose, R., Kitwiroon, N., Fragkou, E., Perez, J. L., & Middleton, D. R. (2006). Prediction of ozone levels in London using the MM5-CMAQ modelling system. *Environmental Modelling and Software, 21*(4), 566-576.

Spak, S. N. (2009). *Characterizing chemical transport of ozone and fine particles in the great lakes region.* (Unpublished Doctoral dissertation). University of Wisconsin-Madison, 2009, Ann Arbor, Michigan. (3367490)

Staniforth, A. (1997). Regional modeling: A theoretical discussion. *Meteorology and Atmospheric Physics, 63*(1-2), 15-29. doi:10.1007/BF01025361

Stockwell, W. R. (1999). *Review of the updated maximum incremental reactivity scale of Dr. William Carter.* Sacramento, California: California Air Resources Board.

Strand, A., & Hov, O. (1996). The impact of man-made and natural NO_x emissions on upper tropospheric ozone: A two-dimensional model study. *Atmospheric Environment, 30*(8), 1291-1303.

Stroud, C. A., Morneau, G., Makar, P. A., Moran, M. D., Gong, W., Pabla, B., Zhang, J., Bouchet, V. S., Fox, D., Venkatesh, S., Wang, D., & Dann, T. (2008). OH-reactivity of volatile organic compounds at urban and rural sites across canada: Evaluation of air quality model predictions using speciated VOC measurements. *Atmospheric Environment, 42*(33), 7746-7756. doi:10.1016/j.atmosenv.2008.05.054

Tang, Y., Lee, P., Tsidulko, M., Huang, H., McQueen, J., DiMego, G., Emmons, L., Pierce, R., Thompson, A., Lin, H., Kang, D., Tong, D., Yu, S., Mathur, R., Pleim, J., Otte, T.,

Pouliot, G., Young, J., Schere, K., Davidson, P., & Stajner, I. (2009). The impact of chemical lateral boundary conditions on CMAQ predictions of tropospheric ozone over the continental United States. *Environmental Fluid Mechanics, 9*(1), 43-58. doi:10.1007/s10652-008-9092-5

Tesche, T. W., Morris, R., Tonnesen, G., McNally, D., Boylan, J., & Brewer, P. (2006). CMAQ/CAMx annual 2002 performance evaluation over the eastern US. *Atmospheric Environment, 40*(26), 4906-4919. doi:10.1016/j.atmosenv.2005.08.046

Thornton, J. A., Wooldridge, P. J., Cohen, R. C., Martinez, M., Harder, H., Brune, W. H., Williams, E. J., Robers, J. M., Fehsenfeld, F. C., Hall, S. R., Shetter, R. E., Wert, B. P., & Fried, A. (2002). Ozone production rates as a function of NOx abundances and HOx production rates in the Nashville urban plume. *Journal of Geophysical Research, 107*(D12), 1-17. doi:10.1029/2001JD000932

Tkacz, B., Moody, B., Castillo, J. V., & Fenn, M. E. (2008). Forest health conditions in North Aamerica. *Environmental Pollution, 155*(3), 409-425. doi:10.1016/j.envpol.2008.03.003

Tong, D., & Mauzerall, D. (2005). *Numerical instability in the community multiscale air quality model and its impacts on aerosol and ozone simulations.* Unpublished manuscript.

Tong, D., & Mauzerall, D. L. (2006). Spatial variability of summertime tropospheric ozone over the continental United States: Implications of an evaluation of the CMAQ model. *Atmospheric Environment, 40*(17), 3041-3056. doi:10.1016/j.atmosenv.2005.11.058

Urquizo, N., Spitzer, D., Pugsley, W., & Robinson, M. (2009). *Mapping small scale pollution distribution using satellite observations in a large Canadian city.* Unpublished manuscript.

US EPA. (1991). *Guideline for regulatory application of the urban airshed model.* No. EPA-450/4-91-013). Research Triangle Park, North Carolina: Office of Air and Radiation, Office of Air Quality Planning.

US EPA. (2006). *CMAQ v4.6 operational guidance document.* Research Triangle Park, North Carolina: Atmospheric Science Modeling Division.

Valari, M., & Menut, L. (2010). Transferring the heterogeneity of surface emissions to variability in pollutant concentrations over urban areas through a chemistry-transport model. *Atmospheric Environment, 44*(27), 3229-3238. doi:10.1016/j.atmosenv.2010.06.001

Van Noije, T. P., Eskes, H. J., Dentener, F. J., Stevenson, D. S., Ellingsen, K., Schultz, M. G., Wild, O., Amann, M., Atherton, C. S., Bergmann, D. J., Bey, I., Boersma, K. F., Butler, T., Cofala, J., Drevet, J., Fiore, A. M., Gauss, M., Hauglustaine, D. A., Horowitz, L. W., Isaksen, I. S., Krol, M. C., Lamarque, J. F., Lawrence, M. G., Martin, R. V., Montanaro, V., Muller, J. F., Pitari, F., Prather, M. J., Pyle, J. A., Richter, A., Rodriquez, J. M., Savage, N. H., Strahan, S. E., Sudo, K., Szopa, S., & van Roozendael, M. (2006). Multi-model ensemble simulations of tropospheric NO_2 compared with GOME retrievals for the year 2000. *Atmospheric Chemistry and Physics, 6*(10), 2943-2979.

Vingarzan, R. (2004). A review of surface ozone background levels and trends. *Atmospheric Environment, 38*(21), 3431-3442. doi:10.1016/j.atmosenv.2004.03.030

Vlachokostas, C., Nastis, S. A., Achillas, C., Kalogeropoulos, K., Karmiris, I., Moussiopoulos, N., Chourdakis, E., Banias, G., & Limperi, N. (2010). Economic damages of ozone air pollution to crops using combined air quality and GIS modelling. *Atmospheric Environment, 44*(28), 3352-3361. doi:10.1016/j.atmosenv.2010.06.023

Wallace, J., & Hobbs, P. (2006). In Hele J. (Ed.), *Atmospoheric science: An introductory survey* (2nd ed.). Amsterdam: Elsevier Inc.

Wang, H., Jacob, D. J., Le Sager, P., Streets, D. G., Park, R. J., Gilliland, A. B., & van Donkelaar, A. (2009). Surface ozone background in the United States: Canadian and Mexican pollution influences. *Atmospheric Environment, 43*(6), 1310-1319. doi:10.1016/j.atmosenv.2008.11.036

Wang, W., Barker, D., Bruyere, C., Dudhia, J., Gill, D. & Michalakes, J. (2004). *WRF version 2 modeling system user's guide.* http://www.mmm.ucar.edu/wrf/users/docs/user_guide/.

Wayne, R. P. (1987). The photochemistry of ozone. *Atmospheric Environment, 21*(8), 1683-1694. doi:10.1016/0004-698(87)90107-7

Wen, D. (2006). *Modelling of atmospheric mercury emission, transport, trasnformation and deposition in North America.* (Unpublished Doctoral dissertation). University of Waterloo, 2006, Waterloo, Ontario.

White, M. C., Etzel, R. A., Wilcox, W. D., & Lloyd, C. (1994). Exacerbations of childhood asthma and ozone pollution in Atlanta. *Environmental Research, 65*(1), 56-68. doi:10.1006/enrs.1994.1021

Williams, D. J. (2007). *Ozone in the atmospheric boundary layer, transport mechanisms and predictive indicators at 36ºN.* (Unpublished Doctoral dissertation). Oklahoma State University, Ann Arbor, Michigan. (32630068)

Wilson, A. M., Wake, C. P., Kelly, T., & Salloway, J. C. (2005). Air pollution, weather, and respiratory emergency room visits in two northern New England cities: An ecological time-series study. *Environmental Research, 97*(3), 312-321. doi:10.1016/j.envres.2004.07.010

Wilson, A. M., Salloway, J. C., Wake, C. P., & Kelly, T. (2004). Air pollution and the demand for hospital services: A review. *Environment International, 30*(8), 1109-1118. doi:10.1016/j.envint.2004.01.004

Wong, S. (2010). In Rebello Z. (Ed.), *CAN emissions*

Xie, Y. (2008). *Testing ozone sensitivities using process analysis, chemical indicators, and very fine scale modeling with CMAQ in the pacific northwest.* (Unpublished doctoral dissertation). Washington State University, Ann Arbor, Michegan. (3381819)

Xie, X., Shao, M., Liu, Y., Lu, S., Chang, C., C.-C., & Chen, Z., Z.-M. (2008). Estimate of initial isoprene contribution to ozone formation potential in Beijing, China. *Atmospheric Environment, 42*(24), 6000-6010. doi:10.1016/j.atmosenv.2008.03.035

Yap, D., Ning, D. T., & Dong, W. (1988). An assessment of source contributions to the ozone concentrations in southern ontario, 1979-1985. *Atmospheric Environment (1967), 22*(6), 1161-1168. doi:10.1016/0004-6981(88)90346-0

Yarwood, G., Rao, S., Yocke, M., & Whitten, G. (2005). *Updates to the carbon bond chemical mechanism: CB05: Final report to the US EPA, RT-04-00675.* Retrieved from http://www.camx.com/publ/pdfs/CB05_Final_Report_120805.pdf

Yarwood, G., Stoeckenius, T. E., Heiken, J. G., & Dunker, A. M. (2003). Modeling Weekday/Weekend ozone differences in the Los Angeles region for 1997. *Journal of Air and Waste Management Association, 53*, 864-875.

Yu, Y., Sokhi, R. S., Kitwiroon, N., Middleton, D. R., & Fisher, B. (2008). Performance characteristics of MM5-SMOKE-CMAQ for a summer photochemical episode in southeast England, United Kingdom. *Atmospheric Environment, 42*(20), 4870-4883. doi:10.1016/j.atmosenv.2008.02.051

Zhang, B. N., & Oanh, N. T. (2002). Photochemical smog pollution in the Bangkok metropolitan region of Thailand in relation of O_3 precursor concentrations and meteorological conditions. *Atmospheric Environment, 36*(26), 4211-4222. doi:10.1016/S1352-23-10(02)00348-5

Zhang, L., Wiebe, A., Vet, R., Mihele, C., O'Brien, J. M., Iqbal, S., & Liang, Z. (2008). Measurements of reactive oxidized nitrogen at eight Canadian rural sites. *Atmospheric Environment, 42*(34), 8065-8078. doi:10.1016/j.atmosenv.2008.06.034

Zhang, M., Uno, I., Zhang, R., Han, Z., Wang, Z., & Pu, Y. (2006). Evaluation of the models-3 community multi-scale air quality (CMAQ) modeling system with observations obtained during the TRACE-P experiment: Comparison of ozone and its related species. *Atmospheric Environment, 40*(26), 4874-4882. doi:10.1016/j.atmosenv.2005.06.063

Zhang, Y., Liu, P., Pun, B., & Seigneur, C. (2006a). A comprehensive performance evaluation of MM5-CMAQ for the summer 1999 southern oxidants study episode, part III: Diagnostic and mechanistic evaluations. *Atmospheric Environment, 40*(26), 4856-4873. doi:10.1016/j.atmosenv.2005.12.046

Zhang, Y., Liu, P., Pun, B., & Seigneur, C. (2006b). A comprehensive performance evaluation of MM5-CMAQ for the summer 1999 southern oxidants study episode-part I: Evaluation protocols, databases, and meteorological predictions. *Atmospheric Environment, 40*(26), 4825-4838. doi:10.1016/j.atmosenv.2005.12.043

Zhang, Y., Liu, P., Queen, A., Misenis, C., Pun, B., Seigneur, C., & Wu, S. Y. (2006). A comprehensive performance evaluation of MM5-CMAQ for the summer 1999 southern oxidants study episode-part II: Gas and aerosol predictions. *Atmospheric Environment, 40*(26), 4839-4855. doi:10.1016/j.atmosenv.2005.12.048

Appendix A

To run CMAQ in parallel the following lines were added to the end of the run script:

```
ls -l $BASE/$EXEC; size $BASE/$EXEC
#> Executable call for multiple PE, set location of MPIRUN script
set MPIRUN = /share/apps/mpich-1.2.7p1-pgi/bin/mpirun
set TASKMAP = $BASE/machines8
cat $TASKMAP
time $MPIRUN -machinefile $TMPDIR/machines -np $NSLOTS $BASE/$EXEC
```

Appendix B

The following reactions were included in the SAPRC99_AE3_AQ chemical mechanism used in this study:

REACTIONS[CM] =

<1> NO2 = NO + O3P # 1.0/<NO2_SAPRC99>;

<2> O3P + O2 + M = O3 # 5.68e-34^-2.80;

<3> O3P + O3 = # 8.00e-12@2060;

<4> O3P + NO + M = NO2 # 1.00e-31^-1.60;

<5> O3P + NO2 = NO # 6.50e-12@-120;

<6> O3P + NO2 = NO3 # 9.00e-32^-2.00&2.20e-11&0.80&1.0;

<8> O3 + NO = NO2 # 1.80e-12@1370;

<9> O3 + NO2 = NO3 # 1.40e-13@2470;

<10> NO + NO3 = 2*NO2 # 1.80e-11@-110;

<11> NO + NO + O2 = 2*NO2 # 3.30e-39@-530;

<12> NO2 + NO3 = N2O5 # 2.80e-30^-3.50&2.00e-12^0.20&0.45&1.0;

<13> N2O5 = NO2 + NO3 # 1.00e-03^-3.50@11000&9.70e+14^0.10@11080&0.45&1.0;

<14> N2O5 + H2O = 2*HNO3 # 2.60e-22;

<17> NO2 + NO3 = NO + NO2 # 4.50e-14@1260;

<18> NO3 = NO # 1.0/<NO3NO_SAPRC99>;

<19> NO3 = NO2 + O3P # 1.0/<NO3NO2_SAPRC99>;

<20> O3 = O3P # 1.0/<O3O3P_SAPRC99>;

<21> O3 = O1D2 # 1.0/<O3O1D_SAPRC99>;

<22> O1D2 + H2O = 2*HO # 2.20e-10;

<23> O1D2 + M = O3P # 2.09e-11@-95;

<24> HO + NO = HONO # 7.00e-31^-2.60&3.60e-11^-0.10&0.60&1.0;

<25> HONO = HO + NO # 1.0/<HONO_NO_SAPRC99>;

<26> HONO = HO2 + NO2 # 1.0/<HONO_NO2_SAPRC99>;

<27> HO + HONO = NO2 # 2.70e-12@-260;

<28> HO + NO2 = HNO3 # 2.43e-30^-3.10&1.67e-11^-2.10&0.60&1.0;

<29> HO + NO3 = HO2 + NO2 # 2.00e-11;

<30> HO + HNO3 = NO3 %2 # 7.20e-15@-785&4.10e-16@-1440&1.90e-33@-725;

<31> HNO3 = HO + NO2 # 1.0/<HNO3_SAPRC99>;

<32> HO + CO = HO2 %3 # 1.30e-13@0.0&3.19e-33@0.0;

<33> HO + O3 = HO2 # 1.90e-12@1000;

<34> HO2 + NO = HO + NO2 # 3.40e-12@-270;

<35> HO2 + NO2 = HNO4 # 1.80e-31^-3.20&4.70e-12&0.60&1.0;

<36> HNO4 = HO2 + NO2 # 4.10e-05@10650&5.70e+15@11170&0.50&1.0;

<37> HNO4 = 0.61*HO2 + 0.61*NO2 + 0.39*HO + 0.39*NO3 # 1.0/<HO2NO2_SAPRC99>;

<38> HNO4 + HO = NO2 # 1.50e-12@-360;

<39> HO2 + O3 = HO # 1.40e-14@600;

<40A> HO2 + HO2 = HO2H %3 # 2.20e-13@-600&1.85e-33@-980;

<40B> HO2 + HO2 + H2O = HO2H %3 # 3.08e-34@-2800&2.59e-54@-3180;

<41> NO3 + HO2 = 0.8*HO + 0.8*NO2 + 0.2*HNO3 # 4.00e-12;

<42> NO3 + NO3 = 2*NO2 # 8.50e-13@2450;

<43> HO2H = 2*HO # 1.0/<H2O2_SAPRC99>;

<44> HO2H + HO = HO2 # 2.90e-12@160;

<45> HO + HO2 = # 4.80e-11@-250;

<S2OH> HO + SO2 = HO2 + SULF + SULAER # 4.00e-31^-3.30&2.00e-12&0.45&1.0;

<H2OH> HO + H2 = HO2 # 7.70e-12@2100;

<MER1> C_O2 + NO = NO2 + HCHO + HO2 # 2.80e-12@-285;

<MER4> C_O2 + HO2 = COOH # 3.80e-13@-780;

<MEN3> C_O2 + NO3 = HCHO + HO2 + NO2 # 1.30e-12;

<MER5> C_O2 + C_O2 = MEOH + HCHO # 2.45e-14@-710;

<MER6> C_O2 + C_O2 = 2*HCHO + 2*HO2 # 5.90e-13@509;

<RRNO> RO2_R + NO = NO2 + HO2 # 2.70e-12@-360;

<RRH2> RO2_R + HO2 = ROOH # 1.90e-13@-1300;

<RRN3> RO2_R + NO3 = NO2 + HO2 # 2.30e-12;

<RRME> RO2_R + C_O2 = HO2 + 0.75*HCHO + 0.25*MEOH # 2.00e-13;

<RRR2> RO2_R + RO2_R = HO2 # 3.50e-14;

<R2NO> R2O2 + NO = NO2 # 1.0*K<RRNO>;

<R2H2> R2O2 + HO2 = HO2 # 1.0*K<RRH2>;

<R2N3> R2O2 + NO3 = NO2 # 1.0*K<RRN3>;

<R2ME> R2O2 + C_O2 = C_O2 # 1.0*K<RRME>;

<R2RR> R2O2 + RO2_R = RO2_R # 1.0*K<RRR2>;

<R2R3> R2O2 + R2O2 = # 1.0*K<RRR2>;

<RNNO> RO2_N + NO = RNO3 # 1.0*K<RRNO>;

<RNH2> RO2_N + HO2 = ROOH # 1.0*K<RRH2>;

<RNME> RO2_N + C_O2 = HO2 + 0.25*MEOH + 0.5*MEK + 0.5*PROD2 + 0.75*HCHO
1.0*K<RRME>;

<RNN3> RO2_N + NO3 = NO2 + HO2 + MEK # 1.0*K<RRN3>;

<RNRR> RO2_N + RO2_R = HO2 + 0.5*MEK + 0.5*PROD2 # 1.0*K<RRR2>;

<RNR2> RO2_N + R2O2 = RO2_N # 1.0*K<RRR2>;

<RNRN> RO2_N + RO2_N = MEK + HO2 + PROD2 # 1.0*K<RRR2>;

<APN2> CCO_O2 + NO2 = PAN # 2.70e-28^-7.10&1.20e-11^-0.90&0.30&1.0;

<DPAN> PAN = CCO_O2 + NO2 # 4.90e-03@12100&4.00e+16@13600&0.30&1.0;

<APNO> CCO_O2 + NO = C_O2 + NO2 # 7.80e-12@-300;

<APH2> CCO_O2 + HO2 = 0.75*CCO_OOH + 0.25*CCO_OH + 0.25*O3 # 4.30e-13@-1040;

<APN3> CCO_O2 + NO3 = C_O2 + NO2 # 4.00e-12;

<APME> CCO_O2 + C_O2 = CCO_OH + HCHO # 1.80e-12@-500;

<APRR> CCO_O2 + RO2_R = CCO_OH # 7.50e-12;

<APR2> CCO_O2 + R2O2 = CCO_O2 # 1.0*K<APRR>;

<APRN> CCO_O2 + RO2_N = CCO_OH + PROD2 # 1.0*K<APRR>;

<APAP> CCO_O2 + CCO_O2 = 2*C_O2 # 2.90e-12@-500;

<PPN2> RCO_O2 + NO2 = PAN2 # 1.20e-11^-0.90;

<PAN2> PAN2 = RCO_O2 + NO2 # 2.00e+15@12800;

<PPNO> RCO_O2 + NO = NO2 + CCHO + RO2_R # 1.25e-11@-240;

<PPH2> RCO_O2 + HO2 = 0.75*RCO_OOH + 0.25*RCO_OH + 0.25*O3 # 1.0*K<APH2>;

<PPN3> RCO_O2 + NO3 = NO2 + CCHO + RO2_R # 1.0*K<APN3>;

<PPME> RCO_O2 + C_O2 = RCO_OH + HCHO # 1.0*K<APME>;

<PPRR> RCO_O2 + RO2_R = RCO_OH # 1.0*K<APRR>;

<PPR2> RCO_O2 + R2O2 = RCO_O2 # 1.0*K<APRR>;

<PPRN> RCO_O2 + RO2_N = RCO_OH + PROD2 # 1.0*K<APRR>;

<PPAP> RCO_O2 + CCO_O2 = C_O2 + CCHO + RO2_R # 1.0*K<APAP>;

<PPPP> RCO_O2 + RCO_O2 = 2*CCHO + 2*RO2_R # 1.0*K<APAP>;

<BPN2> BZCO_O2 + NO2 = PBZN # 1.37e-11;

<BPAN> PBZN = BZCO_O2 + NO2 # 7.90e+16@14000;

<BPNO> BZCO_O2 + NO = NO2 + BZ_O + R2O2 # 1.0*K<PPNO>;

<BPH2> BZCO_O2 + HO2 = 0.75*RCO_OOH + 0.25*RCO_OH + 0.25*O3 # 1.0*K<APH2>;

<BPN3> BZCO_O2 + NO3 = NO2 + BZ_O + R2O2 # 1.0*K<APN3>;

<BPME> BZCO_O2 + C_O2 = RCO_OH + HCHO # 1.0*K<APME>;

<BPRR> BZCO_O2 + RO2_R = RCO_OH # 1.0*K<APRR>;

<BPR2> BZCO_O2 + R2O2 = BZCO_O2 # 1.0*K<APRR>;

<BPRN> BZCO_O2 + RO2_N = RCO_OH + PROD2 # 1.0*K<APRR>;

<BPAP> BZCO_O2 + CCO_O2 = C_O2 + BZ_O + R2O2 # 1.0*K<APAP>;

<BPPP> BZCO_O2 + RCO_O2 = CCHO + RO2_R + BZ_O + R2O2 # 1.0*K<APAP>;

<BPBP> BZCO_O2 + BZCO_O2 = 2*BZ_O + 2*R2O2 # 1.0*K<APAP>;

<MPN2> MA_RCO3 + NO2 = MA_PAN # 1.0*K<PPN2>;

<MPPN> MA_PAN = MA_RCO3 + NO2 # 1.60e+16@13486;

<MPNO> MA_RCO3 + NO = NO2 + HCHO + CCO_O2 # 1.0*K<PPNO>;

<MPH2> MA_RCO3 + HO2 = 0.75*RCO_OOH + 0.25*RCO_OH + 0.25*O3 # 1.0*K<APH2>;

<MPN3> MA_RCO3 + NO3 = NO2 + HCHO + CCO_O2 # 1.0*K<APN3>;

<MPME> MA_RCO3 + C_O2 = RCO_OH + HCHO # 1.0*K<APME>;

<MPRR> MA_RCO3 + RO2_R = RCO_OH # 1.0*K<APRR>;

<MPR2> MA_RCO3 + R2O2 = MA_RCO3 # 1.0*K<APRR>;

<MPRN> MA_RCO3 + RO2_N = 2*RCO_OH # 1.0*K<APRR>;

<MPAP> MA_RCO3 + CCO_O2 = C_O2 + HCHO + CCO_O2 # 1.0*K<APAP>;

<MPPP> MA_RCO3 + RCO_O2 = HCHO + CCO_O2 + CCHO + RO2_R # 1.0*K<APAP>;

<MPBP> MA_RCO3 + BZCO_O2 = HCHO + CCO_O2 + BZ_O + R2O2 # 1.0*K<APAP>;

<MPMP> MA_RCO3 + MA_RCO3 = 2*HCHO + 2*CCO_O2 # 1.0*K<APAP>;

<TBON> TBU_O + NO2 = RNO3 # 2.40e-11;

<TBOD> TBU_O = ACET + C_O2 # 7.50e+14@8152;

<BRN2> BZ_O + NO2 = NPHE # 2.30e-11@-150;

<BRH2> BZ_O + HO2 = PHEN # 1.0*K<RRH2>;

<BRXX> BZ_O = PHEN # 1.00e-03;

<BNN2> BZNO2_O + NO2 = # 1.0*K<BRN2>;

<BNH2> BZNO2_O + HO2 = NPHE # 1.0*K<RRH2>;

<BNXX> BZNO2_O = NPHE # 1.0*K<BRXX>;

<FAHV> HCHO = 2*HO2 + CO # 1.0/<HCHO_R_SAPRC99>;

<FAVS> HCHO = CO # 1.0/<HCHO_M_SAPRC99>;

<FAOH> HCHO + HO = HO2 + CO # 8.60e-12@-20;

<FAH2> HCHO + HO2 = HOCOO # 9.70e-15@-625;

<FAHR> HOCOO = HO2 + HCHO # 2.40e+12@7000;

<FAHN> HOCOO + NO = HCOOH + NO2 + HO2 # 1.0*K<MER1>;

<FAN3> HCHO + NO3 = HNO3 + HO2 + CO # 2.00e-12@2431;

<AAOH> CCHO + HO = CCO_O2 # 5.60e-12@-310;

<AAHV> CCHO = CO + HO2 + C_O2 # 1.0/<CCHO_R_SAPRC99>;

<AAN3> CCHO + NO3 = HNO3 + CCO_O2 # 1.40e-12@1860;

<PAOH> RCHO + HO = 0.034*RO2_R + 0.001*RO2_N + 0.965*RCO_O2 + 0.034*CO +
0.034*CCHO # 2.00e-11;

<PAHV> RCHO = CCHO + RO2_R + CO + HO2 # 1.0/<C2CHO_SAPRC99>;

<PAN3> RCHO + NO3 = HNO3 + RCO_O2 # 1.40e-12@1771;

<K3OH> ACET + HO = HCHO + CCO_O2 + R2O2 # 1.10e-12@520;

<K3HV> ACET = CCO_O2 + C_O2 # 1.0/<ACETONE_SAPRC99>;

<K4OH> MEK + HO = 0.37*RO2_R + 0.042*RO2_N + 0.616*R2O2 + 0.492*CCO_O2 +
0.096*RCO_O2 + 0.115*HCHO + 0.482*CCHO + 0.37*RCHO # 1.30e-12^2.00@25;

<K4HV> MEK = CCO_O2 + CCHO + RO2_R # 1.50e-1/<KETONE_SAPRC99>;

<MeOH> MEOH + HO = HCHO + HO2 # 3.10e-12^2.00@360;

<MER9> COOH + HO = 0.35*HCHO + 0.35*HO + 0.65*C_O2 # 2.90e-12@-190;

<MERA> COOH = HCHO + HO2 + HO # 1.0/<COOH_SAPRC99>;

<LPR9> ROOH + HO = RCHO + 0.34*RO2_R + 0.66*HO # 1.10e-11;

<LPRA> ROOH = RCHO + HO2 + HO # 1.0/<COOH_SAPRC99>;

<GLHV> GLY = 2*CO + 2*HO2 # 1.0/<GLY_R_SAPRC99>;

<GLVM> GLY = HCHO + CO # 6.00e-3/<GLY_ABS_SAPRC99>;

<GLOH> GLY + HO = 0.63*HO2 + 1.26*CO + 0.37*RCO_O2 # 1.10e-11;

<GLN3> GLY + NO3 = HNO3 + 0.63*HO2 + 1.26*CO + 0.37*RCO_O2 # 2.80e-12@2376;

<MGHV> MGLY = HO2 + CO + CCO_O2 # 1.0/<MGLY_ADJ_SAPRC99>;

<MGOH> MGLY + HO = CO + CCO_O2 # 1.50e-11;

<MGN3> MGLY + NO3 = HNO3 + CO + CCO_O2 # 1.40e-12@1895;

<BAHV> BACL = 2*CCO_O2 # 1.0/<BACL_ADJ_SAPRC99>;

<PHOH> PHEN + HO = 0.24*BZ_O + 0.76*RO2_R + 0.23*GLY # 2.63e-11;

<PHN3> PHEN + NO3 = HNO3 + BZ_O # 3.78e-12;

<CROH> CRES + HO = 0.24*BZ_O + 0.76*RO2_R + 0.23*MGLY + CRESAER # 4.20e-11;

<CRN3> CRES + NO3 = HNO3 + BZ_O + CRESAER # 1.37e-11;

<NPN3> NPHE + NO3 = HNO3 + BZNO2_O # 1.0*K<PHN3>;

<BZOH> BALD + HO = BZCO_O2 # 1.29e-11;

<BZHV> BALD = # 5.00e-2/<BZCHO_SAPRC99>;

<BZNT> BALD + NO3 = HNO3 + BZCO_O2 # 1.40e-12@1872;

<MAOH> METHACRO + HO = 0.5*RO2_R + 0.416*CO + 0.084*HCHO + 0.416*MEK +

0.084*MGLY + 0.5*MA_RCO3 # 1.86e-11@-176;

<MAO3> METHACRO + O3 = 0.008*HO2 + 0.1*RO2_R + 0.208*HO + 0.1*RCO_O2 +
0.45*CO +

0.2*HCHO + 0.9*MGLY + 0.333*HCOOH # 1.36e-15@2114;

<MAN3> METHACRO + NO3 = 0.5*HNO3 + 0.5*RO2_R + 0.5*CO + 0.5*MA_RCO3

1.50e-12@1726;

<MAOP> METHACRO + O3P = RCHO # 6.34e-12;

<MAHV> METHACRO = 0.34*HO2 + 0.33*RO2_R + 0.33*HO + 0.67*CCO_O2 +
0.67*CO +

0.67*HCHO + 0.33*MA_RCO3 # 4.10e-3/<ACROLEIN_SAPRC99>;

<MVOH> MVK + HO = 0.3*RO2_R + 0.025*RO2_N + 0.675*R2O2 + 0.675*CCO_O2 +

0.3*HCHO + 0.675*RCHO + 0.3*MGLY # 4.14e-12@-453;

<MVO3> MVK + O3 = 0.064*HO2 + 0.05*RO2_R + 0.164*HO + 0.05*RCO_O2 +
0.475*CO +

0.1*HCHO + 0.95*MGLY + 0.351*HCOOH # 7.51e-16@1520;

<MVOP> MVK + O3P = 0.45*RCHO + 0.55*MEK # 4.32e-12;

<MVHV> MVK = 0.3*C_O2 + 0.7*CO + 0.7*PROD2 + 0.3*MA_RCO3

2.10e-3/<ACROLEIN_SAPRC99>;

<IPOH> ISOPROD + HO = 0.67*RO2_R + 0.041*RO2_N + 0.289*MA_RCO3 + 0.336*CO
+

0.055*HCHO + 0.129*CCHO + 0.013*RCHO + 0.15*MEK + 0.332*PROD2 +

0.15*GLY + 0.174*MGLY # 6.19e-11;

<IPO3> ISOPROD + O3 = 0.4*HO2 + 0.048*RO2_R + 0.048*RCO_O2 + 0.285*HO +
0.498*CO + 0.125*HCHO + 0.047*CCHO + 0.21*MEK + 0.023*GLY +
0.742*MGLY + 0.1*HCOOH + 0.372*RCO_OH # 4.18e-18;

<IPN3> ISOPROD + NO3 = 0.799*RO2_R + 0.051*RO2_N + 0.15*MA_RCO3 +
0.572*CO +
0.15*HNO3 + 0.227*HCHO + 0.218*RCHO + 0.008*MGLY + 0.572*RNO3
1.00e-13;

<IPHV> ISOPROD = 1.233*HO2 + 0.467*CCO_O2 + 0.3*RCO_O2 + 1.233*CO +
0.3*HCHO +
0.467*CCHO + 0.233*MEK # 4.10e-3/<ACROLEIN_SAPRC99>;

<K6OH> PROD2 + HO = 0.379*HO2 + 0.473*RO2_R + 0.07*RO2_N + 0.029*CCO_O2 +
0.049*RCO_O2 + 0.213*HCHO + 0.084*CCHO + 0.558*RCHO + 0.115*MEK +
0.329*PROD2 # 1.50e-11;

<K6HV> PROD2 = 0.96*RO2_R + 0.04*RO2_N + 0.515*R2O2 + 0.667*CCO_O2 +
0.333*RCO_O2 + 0.506*HCHO + 0.246*CCHO + 0.71*RCHO
2.00e-2/<KETONE_SAPRC99>;

<RNOH> RNO3 + HO = 0.338*NO2 + 0.113*HO2 + 0.376*RO2_R + 0.173*RO2_N +
0.596*R2O2 + 0.01*HCHO + 0.439*CCHO + 0.213*RCHO + 0.006*ACET +
0.177*MEK + 0.048*PROD2 + 0.31*RNO3 # 7.80e-12;

<RNHV> RNO3 = NO2 + 0.341*HO2 + 0.564*RO2_R + 0.095*RO2_N + 0.152*R2O2 +
0.134*HCHO + 0.431*CCHO + 0.147*RCHO + 0.02*ACET + 0.243*MEK +
0.435*PROD2 # 1.0/<IC3ONO2_SAPRC99>;

<D1OH> DCB1 + HO = RCHO + RO2_R + CO # 5.00e-11;

<D1O3> DCB1 + O3 = 1.5*HO2 + 0.5*HO + 1.5*CO + GLY # 2.00e-18;

<D2OH> DCB2 + HO = R2O2 + RCHO + CCO_O2 # 5.00e-11;

<D2HV> DCB2 = RO2_R + 0.5*CCO_O2 + 0.5*HO2 + CO + R2O2 + 0.5*GLY + 0.5*MGLY

3.65e-1/<MGLY_ABS_SAPRC99>;

<D3OH> DCB3 + HO = R2O2 + RCHO + CCO_O2 # 5.00e-11;

<D3HV> DCB3 = RO2_R + 0.5*CCO_O2 + 0.5*HO2 + CO + R2O2 + 0.5*GLY + 0.5*MGLY

7.28e+0/<ACROLEIN_SAPRC99>;

<c1OH> CH4 + HO = C_O2 # 2.15e-12@1735;

<etOH> ETHENE + HO = RO2_R + 1.61*HCHO + 0.195*CCHO # 1.96e-12@-438;

<etO3> ETHENE + O3 = 0.12*HO + 0.12*HO2 + 0.5*CO + HCHO + 0.37*HCOOH

9.14e-15@2580;

<etN3> ETHENE + NO3 = RO2_R + RCHO # 4.39e-13^2.00@2282;

<etOA> ETHENE + O3P = 0.5*HO2 + 0.2*RO2_R + 0.3*C_O2 + 0.491*CO + 0.191*HCHO +

0.25*CCHO + 0.009*GLY # 1.04e-11@792;

<isOH> ISOPRENE + HO = 0.907*RO2_R + 0.093*RO2_N + 0.079*R2O2 + 0.624*HCHO +

0.23*METHACRO + 0.32*MVK + 0.357*ISOPROD # 2.50e-11@-408;

<isO3> ISOPRENE + O3 = 0.266*HO + 0.066*RO2_R + 0.008*RO2_N + 0.126*R2O2 +

0.192*MA_RCO3 + 0.275*CO + 0.592*HCHO + 0.1*PROD2 + 0.39*METHACRO
+

0.16*MVK + 0.204*HCOOH + 0.15*RCO_OH # 7.86e-15@1912;

<isN3> ISOPRENE + NO3 = 0.187*NO2 + 0.749*RO2_R + 0.064*RO2_N +
0.187*R2O2 +

0.936*ISOPROD # 3.03e-12@448;

<isOP> ISOPRENE + O3P = 0.01*RO2_N + 0.24*R2O2 + 0.25*C_O2 +
0.24*MA_RCO3 +

0.24*HCHO + 0.75*PROD2 # 3.60e-11;

<t1OH> TRP1 + HO = 0.75*RO2_R + 0.25*RO2_N + 0.5*R2O2 + 0.276*HCHO +

0.474*RCHO + 0.276*PROD2 + TRP1AER # 1.83e-11@-449;

<t1O3> TRP1 + O3 = 0.567*HO + 0.033*HO2 + 0.031*RO2_R + 0.18*RO2_N +

0.729*R2O2 + 0.123*CCO_O2 + 0.201*RCO_O2 + 0.157*CO + 0.235*HCHO +

0.205*RCHO + 0.13*ACET + 0.276*PROD2 + 0.001*GLY + 0.031*BACL +

0.103*HCOOH + 0.189*RCO_OH + TRP1AER # 1.08e-15@821;

<t1N3> TRP1 + NO3 = 0.474*NO2 + 0.276*RO2_R + 0.25*RO2_N + 0.75*R2O2 +

0.474*RCHO + 0.276*RNO3 + TRP1AER # 3.66e-12@-175;

<t1OP> TRP1 + O3P = 0.147*RCHO + 0.853*PROD2 + TRP1AER # 3.27e-11;

<a1OH> ALK1 + HO = RO2_R + CCHO # 1.37e-12^2.00@498;

<a2OH> ALK2 + HO = 0.246*HO + 0.121*HO2 + 0.612*RO2_R + 0.021*RO2_N +
0.16*CO +

0.039*HCHO + 0.155*RCHO + 0.417*ACET + 0.248*GLY + 0.121*HCOOH

9.87e-12@671;

<a3OH> ALK3 + HO = 0.695*RO2_R + 0.07*RO2_N + 0.559*R2O2 + 0.236*TBU_O +
0.026*HCHO + 0.445*CCHO + 0.122*RCHO + 0.024*ACET + 0.332*MEK
1.02e-11@434;

<a4OH> ALK4 + HO = 0.835*RO2_R + 0.143*RO2_N + 0.936*R2O2 + 0.011*C_O2 +
0.011*CCO_O2 + 0.002*CO + 0.024*HCHO + 0.455*CCHO + 0.244*RCHO +
0.452*ACET + 0.11*MEK + 0.125*PROD2 # 5.95e-12@91;

<a5OH> ALK5 + HO = 0.653*RO2_R + 0.347*RO2_N + 0.948*R2O2 + 0.026*HCHO +
0.099*CCHO + 0.204*RCHO + 0.072*ACET + 0.089*MEK + 0.417*PROD2 +
ALK5AER # 1.11e-11@52;

<b1OH> ARO1 + HO = 0.224*HO2 + 0.765*RO2_R + 0.011*RO2_N + 0.055*PROD2 +
0.118*GLY + 0.119*MGLY + 0.017*PHEN + 0.207*CRES + 0.059*BALD +
0.491*DCB1 + 0.108*DCB2 + 0.051*DCB3 + ARO1AER # 1.81e-12@-355;

<b2OH> ARO2 + HO = 0.187*HO2 + 0.804*RO2_R + 0.009*RO2_N + 0.097*GLY +
0.287*MGLY + 0.087*BACL + 0.187*CRES + 0.05*BALD + 0.561*DCB1 +
0.099*DCB2 + 0.093*DCB3 + ARO2AER # 2.64e-11;

<o1OH> OLE1 + HO = 0.91*RO2_R + 0.09*RO2_N + 0.205*R2O2 + 0.732*HCHO +
0.294*CCHO + 0.497*RCHO + 0.005*ACET + 0.119*PROD2 # 7.10e-12@-451;

<o1O3> OLE1 + O3 = 0.155*HO + 0.056*HO2 + 0.022*RO2_R + 0.001*RO2_N +
0.076*C_O2 + 0.345*CO + 0.5*HCHO + 0.154*CCHO + 0.363*RCHO +
0.001*ACET + 0.215*PROD2 + 0.185*HCOOH + 0.05*CCO_OH +
0.119*RCO_OH
2.62e-15@1640;

<o1N3> OLE1 + NO3 = 0.824*RO2_R + 0.176*RO2_N + 0.488*R2O2 + 0.009*CCHO +
0.037*RCHO + 0.024*ACET + 0.511*RNO3 # 4.45e-14@376;

<o1OP> OLE1 + O3P = 0.45*RCHO + 0.437*MEK + 0.113*PROD2 # 1.07e-11@234;

<o2OH> OLE2 + HO = 0.918*RO2_R + 0.082*RO2_N + 0.001*R2O2 + 0.244*HCHO +
0.732*CCHO + 0.511*RCHO + 0.127*ACET + 0.072*MEK + 0.061*BALD +
0.025*METHACRO + 0.025*ISOPROD + OLE2AER # 1.74e-11@-384;

<o2O3> OLE2 + O3 = 0.378*HO + 0.003*HO2 + 0.033*RO2_R + 0.002*RO2_N +
0.137*R2O2 + 0.197*C_O2 + 0.137*CCO_O2 + 0.006*RCO_O2 + 0.265*CO +
0.269*HCHO + 0.456*CCHO + 0.305*RCHO + 0.045*ACET + 0.026*MEK +
0.006*PROD2 + 0.042*BALD + 0.026*METHACRO + 0.073*HCOOH +
0.129*CCO_OH + 0.303*RCO_OH + OLE2AER # 5.02e-16@461;

<o2N3> OLE2 + NO3 = 0.391*NO2 + 0.442*RO2_R + 0.136*RO2_N + 0.711*R2O2 +
0.03*C_O2 + 0.079*HCHO + 0.507*CCHO + 0.151*RCHO + 0.102*ACET +
0.001*MEK + 0.015*BALD + 0.048*MVK + 0.321*RNO3 + OLE2AER
7.26e-13;

<o2OP> OLE2 + O3P = 0.013*HO2 + 0.012*RO2_R + 0.001*RO2_N + 0.012*CO +
0.069*RCHO + 0.659*MEK + 0.259*PROD2 + 0.012*METHACRO # 2.09e-11;

<c1OH> HCOOH + HO = HO2 # 4.5E-13;

<c2OH> CCO_OH + HO = 0.13*RO2_R + 0.87*C_O2 + 0.13*MGLY # 8.00E-13;

<c3OH> RCO_OH + HO = RO2_R + 0.605*CCHO + 0.21*RCHO + 0.185*BACL #
1.16E-12;